# Search for charged Higgs bosons decaying via $H^\pm \to \tau^\pm \nu_\tau$ in the $\tau$+jets and $\tau$+lepton final states with 36 fb$^{-1}$ of $pp$ collision data recorded at $\sqrt{s} = 13$ TeV with the ATLAS experiment

## The ATLAS collaboration

*E-mail:* atlas.publications@cern.ch

ABSTRACT: Charged Higgs bosons produced either in top-quark decays or in association with a top-quark, subsequently decaying via $H^\pm \to \tau^\pm \nu_\tau$, are searched for in 36.1 fb$^{-1}$ of proton-proton collision data at $\sqrt{s} = 13$ TeV recorded with the ATLAS detector. Depending on whether the top-quark produced together with $H^\pm$ decays hadronically or leptonically, the search targets $\tau$+jets and $\tau$+lepton final states, in both cases with a hadronically decaying $\tau$-lepton. No evidence of a charged Higgs boson is found. For the mass range of $m_{H^\pm} = 90$–2000 GeV, upper limits at the 95% confidence level are set on the production cross-section of the charged Higgs boson times the branching fraction $\mathcal{B}(H^\pm \to \tau^\pm \nu_\tau)$ in the range 4.2–0.0025 pb. In the mass range 90–160 GeV, assuming the Standard Model cross-section for $t\bar{t}$ production, this corresponds to upper limits between 0.25% and 0.031% for the branching fraction $\mathcal{B}(t \to bH^\pm) \times \mathcal{B}(H^\pm \to \tau^\pm \nu_\tau)$.

# Contents

## 1 Introduction

The discovery of a new particle at the Large Hadron Collider (LHC) [1] in 2012 [2, 3], with a measured mass close to 125 GeV [4], opens the question of whether this is the Higgs boson of the Standard Model (SM), or part of an extended scalar sector. Charged Higgs bosons[1] are predicted in several extensions of the SM that add a second doublet [5, 6] or triplets [7–10] to its scalar sector. In CP-conserving Two-Higgs-Doublet Models (2HDMs), the properties of the charged Higgs boson depend on its mass, the mixing angle $\alpha$ of the neutral CP-even Higgs bosons and the ratio of the vacuum expectation values of the two Higgs doublets ($\tan \beta$). Although the search for charged Higgs bosons presented in this paper is performed in a model-independent manner, results are interpreted in the framework of the hMSSM benchmark scenario [11, 12], which is a type-II 2HDM, where down-type quarks and charged leptons couple to one Higgs doublet, while up-type quarks couple to the other. For $H^+$ masses below the top-quark mass ($m_{H^+} < m_{\text{top}}$), the main production mechanism is through the decay of a top-quark, $t \to bH^+$, in a double-resonant top-quark production. In this mass range, the decay $H^+ \to \tau \nu$ usually dominates in a type-II 2HDM, although $H^+ \to cs$ and $cb$ may also become sizeable at low $\tan \beta$. For $H^+$ masses above the top-quark mass ($m_{H^+} > m_{\text{top}}$), the leading production mode is

---

[1]In the following, charged Higgs bosons are denoted $H^+$, with the charge-conjugate $H^-$ always implied. Generic symbols are also used for particles produced in association with charged Higgs bosons and in their decays.
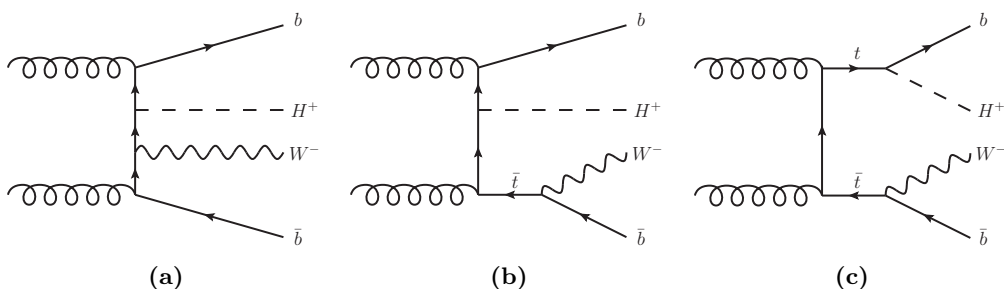
**Figure 1.** Examples of leading-order Feynman diagrams contributing to the production of charged Higgs bosons in $pp$ collisions: (a) non-resonant top-quark production, (b) single-resonant top-quark production that dominates at large $H^+$ masses, (c) double-resonant top-quark production that dominates at low $H^+$ masses. The interference between these three main diagrams becomes most relevant in the intermediate-mass region.

$gg \to tbH^+$ (single-resonant top-quark production). Close to the alignment limit, i.e. at $\cos(\beta-\alpha) \simeq 0$, the dominant decay is $H^+ \to tb$; however the branching fraction of $H^+ \to \tau\nu$ can reach 10–15% at large values of $\tan\beta$ in a type-II 2HDM. In the intermediate-mass region ($m_{H^+} \simeq m_{\text{top}}$), accurate theoretical predictions recently became available for the non-resonant top-quark production [13], which now allows a dedicated comparison of the $H^+$ models with data near the top-quark mass. Figure 1 illustrates the main production modes for charged Higgs bosons in proton-proton ($pp$) collisions.

The ATLAS and CMS Collaborations searched for charged Higgs bosons in $pp$ collisions at $\sqrt{s} = 7$–8 TeV, probing the mass range below the top-quark mass with the $\tau\nu$ [14–18] and $cs$ [19, 20] decay modes, as well as the mass range above the top-quark mass with the $\tau\nu$ and $tb$ decay modes [16, 18, 21]. More recently, using $3.2\,\text{fb}^{-1}$ of data collected at $\sqrt{s} = 13$ TeV, searches for charged Higgs bosons heavier than $m_{\text{top}}$ were performed by ATLAS in the $\tau\nu$ decay mode [22]. In addition, $H^+ \to WZ$ was searched for in the vector-boson-fusion production mode at 8 TeV by the ATLAS Collaboration [23] and at 13 TeV by the CMS Collaboration [24]. No evidence of charged Higgs bosons was found in any of these searches. The ATLAS and CMS Collaborations also searched for neutral scalar resonances decaying to a $\tau\tau$ pair [25, 26], to which the hMSSM is also sensitive in some regions of its parameter space.

This paper describes a search for charged Higgs bosons using the $H^+ \to \tau\nu$ decay, with a subsequent hadronic decay of the $\tau$-lepton (referred to as $\tau_{\text{had}}$), in the mass range 90–2000 GeV, including the intermediate-mass region. Depending on the assumption made for the decay mode of the $W$ boson originating from the top-quark produced together with $H^+$, two channels are targeted: $\tau_{\text{had}}$+jets if the $W$ boson decays into a $q\bar{q}'$ pair, or $\tau_{\text{had}}$+lepton if the $W$ boson decays into an electron or muon and at least one neutrino (directly or via a leptonically decaying $\tau$-lepton). The data used for this analysis are from $pp$ collisions at $\sqrt{s} = 13$ TeV, collected with the ATLAS experiment at the LHC in 2015 and 2016, corresponding to integrated luminosities of $3.2\,\text{fb}^{-1}$ and $32.9\,\text{fb}^{-1}$, respectively. In section 2, the data and simulated samples are summarised. In section 3, the reconstruction of physics

objects is described. The analysis strategy and event selection are discussed in section 4. Section 5 describes the data-driven estimation of backgrounds with misidentified $\tau$ objects. A discussion of the systematic uncertainties and a description of the statistical analysis used to derive exclusion limits on the production of a charged Higgs boson decaying via $H^+ \to \tau\nu$ are presented in sections 6 and 7, respectively. Finally, a summary is given in section 8.

## 2 Data and samples of simulated events

The ATLAS experiment [27] is a multipurpose detector with a forward-backward symmetric cylindrical geometry with respect to the LHC beam-axis.[2] The innermost layers of ATLAS consist of tracking detectors in the pseudorapidity range $|\eta| < 2.5$, including the insertable B-layer [28, 29] installed for Run-2. This inner detector is surrounded by a thin superconducting solenoid that provides a 2 T axial magnetic field. It is enclosed by the electromagnetic and hadronic calorimeters which cover $|\eta| < 4.9$. The outermost layers consist of an external muon spectrometer within $|\eta| < 2.7$, incorporating three large toroidal magnet assemblies. A two-level trigger [30, 31] reduces the event rate to a maximum of 1 kHz for offline data storage.

The dataset used in this analysis, collected during stable beam conditions and with all ATLAS subsystems fully operational, corresponds to an integrated luminosity of $36.1 \pm 0.8$ fb$^{-1}$, derived following a methodology similar to that detailed in ref. [32]. Data-quality criteria are applied in order to remove events where reconstructed jets are consistent with noise in the calorimeter or non-collision backgrounds [33].

Signal events with $H^+ \to \tau\nu$ were generated with MADGRAPH5_AMC@NLO [34] in three distinct mass regions:

- In the mass range below the top-quark mass (90–150 GeV), $t\bar{t}$ events with one top-quark decaying into a charged Higgs boson and a $b$-quark were generated at leading order (LO). Contributions from events in which both top-quarks decay via $t \to bH^+$ and from single-top-quark events with a subsequent decay $t \to bH^+$ are negligible, hence not simulated.

- In the intermediate-mass region (160–180 GeV), the full process $pp \to H^+Wbb$ was generated at LO.

- In the mass range above the top-quark mass (200–2000 GeV), $H^+$ production in association with a top-quark was simulated at next-to-leading order (NLO).

The interference between the Feynman diagrams of figure 1 is taken into account in the intermediate-mass region, where it is most relevant. In all cases, the matrix-element generator was interfaced to PYTHIA v8.186 [35] for the simulation of the parton shower and the

---

[2]The ATLAS experiment uses a right-handed coordinate system with its origin at the nominal interaction point (IP) in the centre of the detector and the $z$-axis along the beam pipe. The $x$-axis points from the IP to the centre of the LHC ring, and the $y$-axis points upward. Cylindrical coordinates $(r, \phi)$ are used in the transverse plane, $\phi$ being the azimuthal angle around the $z$-axis. The pseudorapidity is defined in terms of the polar angle $\theta$ as $\eta = -\ln[\tan(\theta/2)]$. Transverse momenta are computed from the three-momenta $\vec{p}$ as $p_{\mathrm{T}} = |\vec{p}| \sin\theta$. The distance in the $\eta$-$\phi$ space is commonly referred to as $\Delta R = \sqrt{(\Delta\eta)^2 + (\Delta\phi)^2}$.

underlying event, with the A14 [36] set of tuned parameters (tune). The NNPDF2.3 [37] parton distribution function (PDF) sets were used for the matrix-element generation and the parton shower.

The SM background processes include the production of $t\bar{t}$ pairs, single top-quarks, $W$+jets, $Z/\gamma^*$+jets and electroweak gauge-boson pairs ($WW/WZ/ZZ$), as well as multi-jet events. The $t\bar{t}$ events constitute the main background in the low- and intermediate-mass $H^+$ searches, while multi-jet events dominate for large charged Higgs boson masses. All backgrounds arising from a quark- or gluon-initiated jet misidentified as a hadronically decaying $\tau$-lepton are estimated with a data-driven method, described in section 5.

The generation of $t\bar{t}$ events used the Powheg-Box v2 [38–40] generator, with the CT10 [41] PDF set in the matrix-element calculations. Single-top-quark events were generated in the $Wt$-, $t$- and $s$-channels using the Powheg-Box v1 generator, with the CT10 PDF set in the $Wt$- and $s$-channels or the fixed 4-flavour CT10f4 [42] PDF set in the $t$-channel. For all processes above, top-quark spin correlations are preserved (MadSpin [43] was used for top-quark decays in the $t$-channel). The parton shower and the underlying event were simulated using Pythia v6.428 [44] with the CTEQ6L1 [45] PDF set and the corresponding Perugia 2012 [46] tune. The top-quark mass was set to 172.5 GeV. The sample of $t\bar{t}$ events is normalised to the next-to-next-to-leading-order (NNLO) cross-section, including soft-gluon resummation to next-to-next-to-leading-logarithm (NNLL) order [47]. The normalisation of the sample of single-top-quark events uses an approximate calculation at NLO in QCD for the $s$- and $t$-channels [48, 49] and an NLO+NNLL calculation for the $Wt$-channel [50, 51].

Events containing a $W$ or $Z$ boson with associated jets were simulated using Sherpa v2.2.1 [52] together with the NNPDF3.0NNLO [53] PDF set. Matrix elements were calculated for up to two partons at NLO and four partons at LO using Comix [54] and OpenLoops [55], and they were merged with the Sherpa parton shower [56] according to the ME+PS@NLO prescription [57]. The $W/Z$+jets events are normalised to the NNLO cross-sections calculated using FEWZ [58–60]. Diboson processes ($WW$, $WZ$ and $ZZ$) were simulated at NLO using the Powheg-Box v2 generator, interfaced to the Pythia v8.186 parton shower model. The CT10nlo PDF set was used for the hard-scatter process, while the CTEQL1 PDF set was used for the parton shower. The non-perturbative effects were modelled using the AZNLO [61] tune. EvtGen v1.2.0 [62] was used for the properties of bottom- and charm-hadron decays, except in samples generated with Sherpa. All simulated events were overlaid with additional minimum-bias events generated with Pythia v8.186 using the A2 [63] tune and the MSTW2008LO [64] PDF set to simulate the effect of multiple $pp$ collisions per bunch crossing (pile-up). Simulated events were then weighted to have the same distribution of the number of collisions per bunch crossing as the data. All signal and background events were processed through a simulation [65] of the detector geometry and response based on Geant4 [66] and they are reconstructed using the same algorithms as the data.

## 3 Physics object reconstruction

The search reported in this paper makes use of most of the physics objects reconstructed in ATLAS: charged leptons (electrons and muons), jets (including those compatible with the hadronisation of $b$-quarks or hadronic decays of $\tau$-leptons) and missing transverse momentum. These physics objects are detailed below.

Electrons are reconstructed by matching clustered energy deposits in the electromagnetic calorimeter to a track reconstructed in the inner detector [67]. They are required to have $p_{\mathrm{T}} > 20$ GeV and $|\eta| < 2.47$ (the transition region between the barrel and end-cap calorimeters, $1.37 < |\eta| < 1.52$, is excluded). In the $\tau_{\mathrm{had}}$+jets ($\tau_{\mathrm{had}}$+lepton) channel, electrons must satisfy a loose (tight) identification criterion based on a likelihood discriminant.

Muon candidates are required to contain matching inner-detector and muon-spectrometer tracks [68], as well as to have $p_{\mathrm{T}} > 20$ GeV and $|\eta| < 2.5$. The final muon tracks are re-fitted using the complete track information from both detector systems. In the $\tau_{\mathrm{had}}$+jets ($\tau_{\mathrm{had}}$+lepton) channel, muons must satisfy a loose (tight) identification criterion.

In order to ensure that electrons (muons) originate from the primary vertex, defined as the vertex with the highest sum of the $p_{\mathrm{T}}^2$ of its associated tracks, the track associated with the lepton is required to have a longitudinal impact parameter and a transverse impact parameter significance that fulfil, respectively, $|z_0 \sin\theta| < 0.5$ mm and $|d_0/\sigma(d_0)| < 5$ (3). In order to reduce contamination by leptons from hadron decays or photon conversion, isolation requirements are applied. The calorimeter-based isolation relies on energy deposits within a cone of size $\Delta R = 0.2$ around the electron or muon, while the track-based isolation uses a variable cone size starting at $\Delta R = 0.2$ for electrons or $\Delta R = 0.3$ for muons, and then decreasing as $p_{\mathrm{T}}$ increases. The efficiency of the calorimeter- and track-based isolation requirements are, respectively, 96% and 99% in the $\tau_{\mathrm{had}}$+lepton channel (looser isolation requirements are applied in the $\tau_{\mathrm{had}}$+jets channel, with efficiencies of 99%).

Jets are reconstructed from energy deposits in the calorimeters using the anti-$k_t$ algorithm [69] implemented in the FASTJET package [70] with a radius parameter value of $R = 0.4$. Jets are corrected for pile-up energy and calibrated using energy- and $\eta$-dependent corrections [33]. Only jets with a transverse momentum $p_{\mathrm{T}} > 25$ GeV and within $|\eta| < 2.5$ are considered in the following. A multivariate technique (jet vertex tagger) that allows identification and selection of jets originating from the hard-scatter interaction through the use of tracking and vertexing information is applied to jets with $p_{\mathrm{T}} < 60$ GeV and $|\eta| < 2.4$ [71]. In order to identify jets containing $b$-hadrons (referred to as $b$-jets in the following), an algorithm is used, which combines impact parameter information with the explicit identification of secondary and tertiary vertices within the jet into a multivariate discriminant [72, 73]. Operating points are defined by a single threshold in the range of discriminant output values and are chosen to provide a specific $b$-jet efficiency in simulated $t\bar{t}$ events. The 70% working point is used in this analysis. It has rejection factors of 13, 56 and 380 against $c$-jets, hadronic $\tau$ decays and jets from light quarks or gluons, respectively.

The detection and reconstruction of hadronically decaying $\tau$-leptons is seeded by anti-$k_t$ jets depositing a transverse energy $E_{\mathrm{T}} > 10$ GeV in the calorimeter [74] and with one

or three associated tracks reconstructed in the inner detector within a cone of $\Delta R = 0.2$ around the axis of the object associated with the visible decay products of the hadronically decaying $\tau$-leptons. Referred to as $\tau_{\text{had-vis}}$ in the following, these objects are required to have a visible transverse momentum ($p_T^\tau$) of at least 30 GeV and to be within $|\eta| < 2.3$ (the transition region between the barrel and end-cap calorimeters, $1.37 < |\eta| < 1.52$, is excluded). In order to distinguish $\tau_{\text{had-vis}}$ candidates from quark- or gluon-initiated jets, a boosted decision tree (BDT) is used, separately for candidates with one and three charged-particle tracks [75, 76]. For the nominal definition of $\tau_{\text{had-vis}}$ candidates, a working point with an identification efficiency of 75% (60%) for 1-prong (3-prong) hadronic $\tau$ decays in $Z \to \tau\tau$ events is chosen, corresponding to rejection factors of 30–80 (200–1000) against quark- and gluon-initiated jets in multi-jet events. An additional likelihood-based veto is used to reduce the number of electrons misidentified as $\tau_{\text{had-vis}}$ candidates, providing a constant 95% efficiency as a function of $\tau_{\text{had-vis}}$ $p_T$ and $\eta$, as well as a background rejection of 20–200, depending on $\eta$.

When several objects overlap geometrically, the following procedure is applied. First, any $\tau_{\text{had-vis}}$ object is removed if found within $\Delta R = 0.2$ of either an electron or a muon with loose identification criteria and with a transverse momentum above 20 GeV or 7 GeV, respectively. Then, any electron sharing an inner-detector track with a muon is discarded. Next, jets within $\Delta R = 0.2$ of an electron or muon are removed, unless they are $b$-tagged, have a large $p_T$ relative to that of the lepton and, in the case of an overlap with a muon, a high track multiplicity. Then, electrons and muons are removed if found within $\Delta R = 0.4$ of a remaining jet. Finally, jets are discarded if they are within $\Delta R = 0.2$ of the highest-$p_T$ $\tau_{\text{had-vis}}$ candidate.

The magnitude of the missing transverse momentum, $E_T^{\text{miss}}$ [77], is reconstructed from the negative vector sum of transverse momenta of reconstructed and fully calibrated objects, with an additional term that is calculated from inner-detector tracks that are matched to the primary vertex and not associated with any of the selected objects.

## 4 Analysis strategy

This paper describes a search for a charged Higgs boson decaying via $H^+ \to \tau\nu$ in topologies where it is produced either in top-quark decays or in association with a top-quark. Depending on whether the top-quark produced with the $H^+$ decays hadronically or semileptonically, two channels are targeted: $\tau_{\text{had-vis}}$+jets or $\tau_{\text{had-vis}}$+lepton, respectively. The corresponding signal regions are described below.

**Event selection in the $\tau_{\text{had-vis}}$+jets channel.** The analysis of the $\tau_{\text{had-vis}}$+jets channel is based on events accepted by an $E_T^{\text{miss}}$ trigger with a threshold at 70, 90 or 110 GeV, depending on the data-taking period and thereby accounting for different pile-up conditions. The efficiency of these triggers is measured in data and used to reweight the simulated events, with the same method as in ref. [22]. At least one vertex with two or more associated tracks with $p_T > 400$ MeV is required, and the following event selection criteria are applied:

- at least one $\tau_\text{had-vis}$ candidate with $p_\text{T}^\tau > 40$ GeV;

- no loose leptons (electron or muon) with $p_\text{T} > 20$ GeV;

- at least three jets with $p_\text{T} > 25$ GeV, of which at least one is $b$-tagged;

- $E_\text{T}^\text{miss} > 150$ GeV;

- $m_\text{T} > 50$ GeV.

Here, the transverse mass $m_\text{T}$ of the highest-$p_\text{T}$ $\tau_\text{had-vis}$ candidate and $E_\text{T}^\text{miss}$ is defined as,

$$m_\text{T} = \sqrt{2p_\text{T}^\tau E_\text{T}^\text{miss}(1 - \cos \Delta\phi_{\tau,\text{miss}})}, \tag{4.1}$$

where $\Delta\phi_{\tau,\text{miss}}$ is the azimuthal angle between the $\tau_\text{had-vis}$ candidate and the direction of the missing transverse momentum.

**Event selection in the $\tau_\text{had-vis}$+lepton channel.** The $\tau_\text{had-vis}$+electron and $\tau_\text{had-vis}$+muon sub-channels are based on events accepted by single-lepton triggers. Triggers for electrons or muons with low $E_\text{T}$ or $p_\text{T}$ thresholds respectively (24–26 GeV depending on the data-taking period, for both the electrons and muons) and isolation requirements are combined in a logical OR with triggers having higher $(E_\text{T}, p_\text{T})$ thresholds (60–140 GeV for electrons, 50 GeV for muons) and looser isolation or identification requirements in order to maximise the efficiency. Following the same vertex requirement as in the $\tau_\text{had-vis}$+jets channel, events are selected as follows:

- exactly one lepton matched to the single-lepton trigger object, with $p_\text{T} > 30$ GeV. Depending on whether the lepton is an electron or a muon, two sub-channels, $\tau_\text{had-vis}$+electron and $\tau_\text{had-vis}$+muon, are considered;

- exactly one $\tau_\text{had-vis}$ candidate with $p_\text{T}^\tau > 30$ GeV and an electric charge opposite to that of the lepton;

- at least one $b$-tagged jet with $p_\text{T} > 25$ GeV;

- $E_\text{T}^\text{miss} > 50$ GeV.

**Multivariate discriminant.** Following the event selections above, kinematic variables that differentiate between the signal and backgrounds are identified and combined into a multivariate discriminant. The output score of BDTs is then used in order to separate the $H^+$ signal from the SM background processes. The training of the BDTs is performed using the FastBDT [78] library via the TMVA toolkit [79].

The simulated signal samples are divided into five $H^+$ mass bins chosen to ensure that within each bin both the kinematic distributions of the input variables and the event topology are similar. The mass bins used in both channels are 90–120 GeV, 130–160 GeV (in that case, an additional signal sample with a 160 GeV $H^+$ arising solely from top-quark decays is used), 160–180 GeV, 200–400 GeV and 500–2000 GeV. All available $H^+$ signal samples corresponding to a given mass bin are normalised to the same event yield

and combined into one inclusive signal sample. The BDTs are trained separately for $\tau_{\text{had-vis}}$+jets and $\tau_{\text{had-vis}}$+lepton events, and depending on whether the leading $\tau_{\text{had-vis}}$ candidate has one or three associated tracks. The variables entering the BDT training differ for the two types of final states considered in this search, and they are summarised in table 1. If there is more than one $\tau_{\text{had-vis}}$ candidate or more than one $b$-tagged jet, the object that has the largest $p_{\text{T}}$ is considered in the BDT input variables.

At low $H^+$ masses, the kinematics of the $t \to bH^+$ and $t \to bW$ decay products are similar. In that case, the polarisation of the $\tau$-lepton is employed as a discriminating variable: in the main SM background processes, the $\tau_{\text{had-vis}}$ object originates from a vector-boson decay, whereas it is generated in the decay of a scalar particle in the case of $H^+$ signal [80]. The polarisation of the $\tau_{\text{had-vis}}$ candidates can be measured by the asymmetry of energies carried by the charged and neutral pions from the 1-prong $\tau$-lepton decay, measured in the laboratory frame. For this purpose, the variable $\Upsilon$ is introduced [81]:

$$\Upsilon = \frac{E_{\text{T}}^{\pi^\pm} - E_{\text{T}}^{\pi^0}}{E_{\text{T}}^\tau} \approx 2\frac{p_{\text{T}}^{\tau\text{-track}}}{p_{\text{T}}^\tau} - 1.$$

It is defined for all $\tau_{\text{had-vis}}$ candidates with only one associated track, and $p_{\text{T}}^{\tau\text{-track}}$ is the transverse momentum of that track. For $H^+$ masses in the range 90–400 GeV, the BDT training is performed separately for events with a selected 1- or 3-prong $\tau_{\text{had-vis}}$ object, and $\Upsilon$ is included in the BDT discriminant for events where $\tau_{\text{had-vis}}$ has only one associated track. While $\Upsilon$ is one of the most discriminating input variables of the BDT at low $H^+$ masses, the importance of other kinematic variables in the BDT training becomes much greater at large $H^+$ masses, in particular the three variables entering the computation of the tranvserse mass, i.e. $E_{\text{T}}^{\text{miss}}$, $p_{\text{T}}^\tau$ and $\Delta\phi_{\tau,\text{miss}}$. Hence, for the mass range 500–2000 GeV, the BDT discriminant does not contain the variable $\Upsilon$ and is thus inclusive in the number of tracks associated with the $\tau_{\text{had-vis}}$ candidate.

## 5 Background modelling

The dominant background processes are categorised according to the object that gives rise to the identified $\tau_{\text{had-vis}}$ candidate. Simulation is used to estimate backgrounds in which $\tau_{\text{had-vis}}$ arises from a hadronically decaying $\tau$-lepton, electron or muon at the event-generator level; however, in the case of $t\bar{t}$ events, the normalisation is obtained from a fit to the data. If $\tau_{\text{had-vis}}$ arises from a quark- or gluon-initiated jet, a data-driven method is employed to estimate the corresponding background.

**Data-driven fake-factor method.** Background processes where a quark- or gluon-initiated jet is reconstructed and selected as a $\tau_{\text{had-vis}}$ candidate are estimated from data. For this purpose, an anti-$\tau_{\text{had-vis}}$ selection is defined by requiring that the $\tau_{\text{had-vis}}$ candidate does not satisfy the BDT-based identification criteria of the nominal selection. Meanwhile, a loose requirement on the $\tau_{\text{had-vis}}$ BDT output score is maintained in order to ensure that the relative fractions of gluon- and quark-initiated jets mimicking $\tau_{\text{had-vis}}$ candidates are similar in the signal region and the corresponding anti-$\tau_{\text{had-vis}}$ region. Then, a fake factor

| BDT input variable | $\tau_{\text{had-vis}}$+jets | $\tau_{\text{had-vis}}$+lepton |
|---|:---:|:---:|
| $E_{\text{T}}^{\text{miss}}$ | ✓ | ✓ |
| $p_{\text{T}}^{\tau}$ | ✓ | ✓ |
| $p_{\text{T}}^{b\text{-jet}}$ | ✓ | ✓ |
| $p_{\text{T}}^{\ell}$ | | ✓ |
| $\Delta\phi_{\tau_{\text{had-vis}},\,\text{miss}}$ | ✓ | ✓ |
| $\Delta\phi_{b\text{-jet},\,\text{miss}}$ | ✓ | ✓ |
| $\Delta\phi_{\ell,\,\text{miss}}$ | | ✓ |
| $\Delta R_{\tau_{\text{had-vis}},\,\ell}$ | | ✓ |
| $\Delta R_{b\text{-jet},\,\ell}$ | | ✓ |
| $\Delta R_{b\text{-jet},\,\tau_{\text{had-vis}}}$ | ✓ | |
| $\Upsilon$ | ✓ | ✓ |

**Table 1.** List of kinematic variables used as input to the BDT in the $\tau_{\text{had-vis}}$+jets and $\tau_{\text{had-vis}}$+lepton channels. Here, $\ell$ refers to the selected lepton (electron or muon). $\Delta\phi_{X,\,\text{miss}}$ denotes the difference in azimuthal angle between a reconstructed object $X$ ($X = \tau_{\text{had-vis}}$, $b$-jet, $\ell$) and the direction of the missing transverse momentum. The variable $\Upsilon$ is related to the polarisation of the $\tau$-lepton and is only defined for 1-prong $\tau_{\text{had-vis}}$ candidates. Hence, for $H^+$ masses in the range 90–400 GeV, where the variable $\Upsilon$ is used, the BDT training is performed separately for events with a selected 1- or 3-prong $\tau_{\text{had-vis}}$ candidate. In the mass range 500–2000 GeV, $\Upsilon$ is not used, hence the BDT training is inclusive in number of tracks associated with $\tau_{\text{had-vis}}$ candidates.

(FF) is defined as the ratio of the number of jets reconstructed as $\tau_{\text{had-vis}}$ candidates that pass the nominal $\tau_{\text{had-vis}}$ selection to the number that pass the anti-$\tau_{\text{had-vis}}$ selection in a given control region (CR):

$$\text{FF} = \frac{N_{\tau_{\text{had-vis}}}^{\text{CR}}}{N_{\text{anti-}\tau_{\text{had-vis}}}^{\text{CR}}}.$$

The actual computation of FFs is described later in the text. Events are selected with the nominal criteria described in section 4, except that an inverted identification criterion for the $\tau_{\text{had-vis}}$ candidate is required. In this sample, the $\tau_{\text{had}}$ contribution is subtracted using simulated events in which a $\tau_{\text{had}}$ at generator level fulfils the anti-$\tau_{\text{had-vis}}$ criterion. The resulting number of events is $N_{\text{anti-}\tau_{\text{had-vis}}}$. Then, the number of events with a misidentified $\tau_{\text{had-vis}}$ candidate ($N_{\text{fakes}}^{\tau_{\text{had-vis}}}$) is derived from the subset of anti-$\tau_{\text{had-vis}}$ candidates as follows:

$$N_{\text{fakes}}^{\tau_{\text{had-vis}}} = \sum_i N_{\text{anti-}\tau_{\text{had-vis}}}(i) \times \text{FF}(i),$$

where the index $i$ refers to each bin in the parameterisation of the FF, in terms of $p_{\text{T}}^{\tau}$ and number of associated tracks.

In order to account for different sources of misidentified $\tau_{\text{had-vis}}$ candidates in the signal region and the corresponding anti-$\tau_{\text{had-vis}}$ region, FFs are measured in two control regions of the data with different fractions of quark- and gluon-initiated jets, and then combined.

A first control region with a significant fraction of gluon-initiated jets (referred to as the multi-jet CR) is defined by applying the same event selection as for the $\tau_{\text{had-vis}}$+jets channel, but with a $b$-jet veto and $E_{\text{T}}^{\text{miss}} < 80$ GeV. Such events are collected using a combination of multi-jet triggers instead of the $E_{\text{T}}^{\text{miss}}$ trigger. A second control region enriched in quark-initiated jets (referred to as the $W$+jets CR) is defined by applying the same event selection as for the combined $\tau_{\text{had-vis}}$+lepton channel, but with a $b$-jet veto, no requirement on $E_{\text{T}}^{\text{miss}}$ and the requirement 60 GeV $< m_{\text{T}}(\ell, E_{\text{T}}^{\text{miss}}) < 160$ GeV, where the transverse mass of the lepton and the missing transverse momentum is computed by replacing the $\tau_{\text{had-vis}}$ candidate by a lepton in eq. (4.1). The FFs measured in these two control regions are shown in figure 2a.

In the anti-$\tau_{\text{had-vis}}$ regions corresponding to the nominal event selections of section 4, the fractions of $\tau_{\text{had-vis}}$ candidates arising from quark- and gluon-initiated jets are then measured using a template-fit approach, based on variables that are sensitive to the differences in quark- and gluon-fractions between these two types of jets. For 3-prong $\tau_{\text{had-vis}}$ candidates, the $\tau_{\text{had-vis}}$ BDT output score is used as a template. For 1-prong $\tau_{\text{had-vis}}$ candidates, the so-called $\tau_{\text{had-vis}}$ width is used, defined as:

$$w_\tau = \frac{\sum \left[ p_{\text{T}}^{\text{track}} \times \Delta R \left( \tau_{\text{had-vis}}, \text{track} \right) \right]}{\sum p_{\text{T}}^{\text{track}}},$$

for tracks satisfying $\Delta R \left( \tau_{\text{had-vis}}, \text{track} \right) < 0.4$. Two binned templates, denoted $f_{\text{multi-jet}}$ and $f_{W+\text{jets}}$, are obtained in the multi-jet and $W$+jets control regions defined above, respectively. Each corresponds to a linear combination of templates of gluon- and quark-initiated jets, where the fraction of gluon-initiated jets is by construction larger in the multi-jet control region. Then, a linear combination of the two templates is defined as $f(x|\alpha_{\text{MJ}}) = \alpha_{\text{MJ}} \times f_{\text{multi-jet}}(x) + (1 - \alpha_{\text{MJ}}) \times f_{W+\text{jets}}(x)$ with a free parameter $\alpha_{\text{MJ}}$ (here, $f(x)$ is the $\tau_{\text{had-vis}}$ width or BDT score). This linear combination is fitted to the normalised distribution of the $\tau_{\text{had-vis}}$ width or BDT score measured in the anti-$\tau_{\text{had-vis}}$ regions corresponding to the nominal event selections, by varying $\alpha_{\text{MJ}}$ and separately minimising a $\chi^2$-function in every bin of the fake factors, separately in the $\tau_{\text{had-vis}}$+jets and $\tau_{\text{had-vis}}$+lepton channels. From the best-fit values of $\alpha_{\text{MJ}}$, combined fake factors are then given by:

$$\text{FF}^{\text{comb}}(i) = \alpha_{\text{MJ}}(i) \times \text{FF}^{\text{multi-jet}}(i) + [1 - \alpha_{\text{MJ}}(i)] \times \text{FF}^{W+\text{jets}}(i),$$

where the index $i$ refers to each bin in the parameterisation of the FF, and where $\text{FF}^{\text{multi-jet}}$ and $\text{FF}^{W+\text{jets}}$ indicate the FF calculated in the two respective control regions. The combined FFs, used in the $\tau_{\text{had-vis}}$+jets and $\tau_{\text{had-vis}}$+lepton channels, are shown in figure 2b.

The data-driven method as described does not correctly predict the shape of $\Upsilon$ measured in the signal region. Indeed, the distribution of $\Upsilon$ is found to be different for $\tau_{\text{had-vis}}$ and anti-$\tau_{\text{had-vis}}$ candidates, because this variable is strongly correlated with the leading-track momentum fraction, which is one of the input variables used for the identification of $\tau_{\text{had-vis}}$ candidates. On the other hand, $\Upsilon$ shows no correlation with any of the other variables used as input to the final BDT discriminant. Hence, an inverse transform sampling method [82] can be employed in order to model the shape of $\Upsilon$ for misidentified $\tau_{\text{had-vis}}$
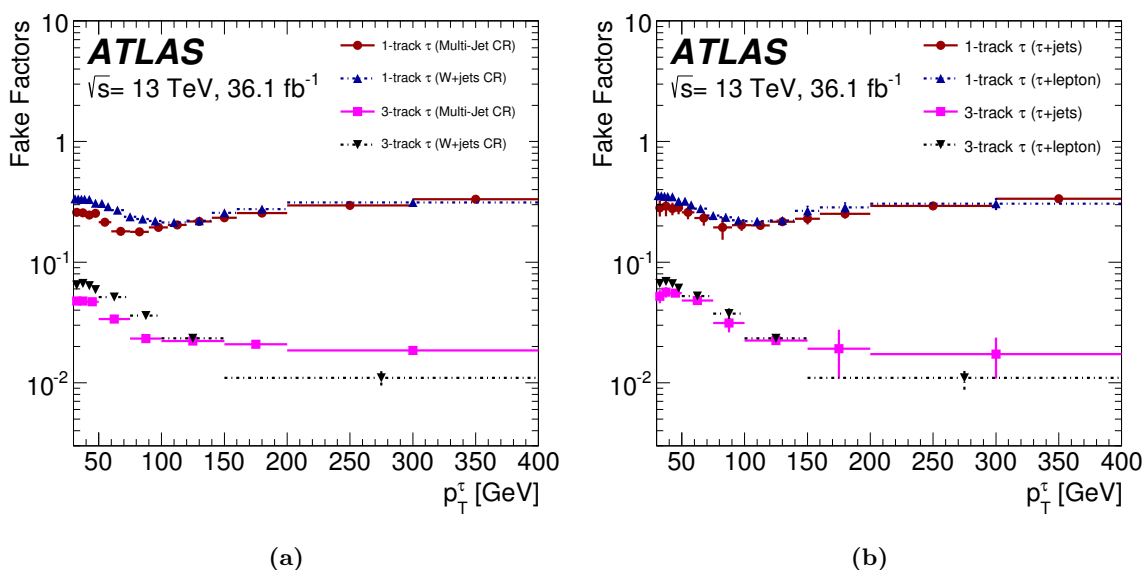
**Figure 2.** Fake factors parameterised as a function of $p_T^\tau$ and the number of charged $\tau$ decay products (two categories: 1-prong and 3-prong), as obtained (a) in the multi-jet and $W$+jets CRs, (b) after reweighting by $\alpha_{MJ}$ in the $\tau_{had\text{-}vis}$+jets and $\tau_{had\text{-}vis}$+lepton channels. Details about the computation of fake factors in the different control regions are given in the text. The errors shown represent the statistical uncertainty in a given $p_T^\tau$ bin (a) and with additional systematic uncertainties obtained from the combination in a given $p_T^\tau$ bin (b).

candidates in the signal regions. In the control regions where FFs are measured, cumulative distribution functions $F(\Upsilon)$ are calculated from the shapes of $\Upsilon$, obtained separately for $\tau_{had\text{-}vis}$ and anti-$\tau_{had\text{-}vis}$ candidates. Then, in the signal regions, the shape of $\Upsilon$ predicted for $\tau_{had\text{-}vis}$ candidates is derived from that measured for anti-$\tau_{had\text{-}vis}$ candidates, as follows:

$$\Upsilon_{\tau_{had\text{-}vis}} = F^{-1}_{\tau_{had\text{-}vis}}(F_{anti\text{-}\tau_{had\text{-}vis}}(\Upsilon)),$$

where $F^{-1}$ stands for the inverse of the cumulative distribution function. This procedure is only applied to 1-prong objects, since $\Upsilon$ is not used in the training of the final BDT discriminant for 3-prong $\tau_{had\text{-}vis}$ candidates.

**Validation of the background modelling.** The modelling of the backgrounds, especially $t\bar{t}$ and events with a misidentified $\tau_{had\text{-}vis}$ candidate, is validated in signal-depleted regions. A region enriched in $t\bar{t}$ events is defined with the same event selection as the $\tau_{had\text{-}vis}$+lepton channel, but with the requirement of having an $e\mu$ pair (with $p_T$ above 30 GeV for both the electron and muon) instead of the $e/\mu + \tau_{had\text{-}vis}$ pair. This control region is included as a single-bin distribution in the statistical analysis described in section 7. The modelling of the background with misidentified $\tau_{had\text{-}vis}$ objects is validated in a region that is defined with the same selection criteria as the $\tau_{had\text{-}vis}$+lepton channel, but with a veto on $b$-tagged jets. Predicted and measured BDT score distributions are compared in the two regions discussed above, and they are found to be in good agreement prior to any fit to the data, as shown in figures 3 and 4. This procedure validates the modelling of the two main SM background processes.
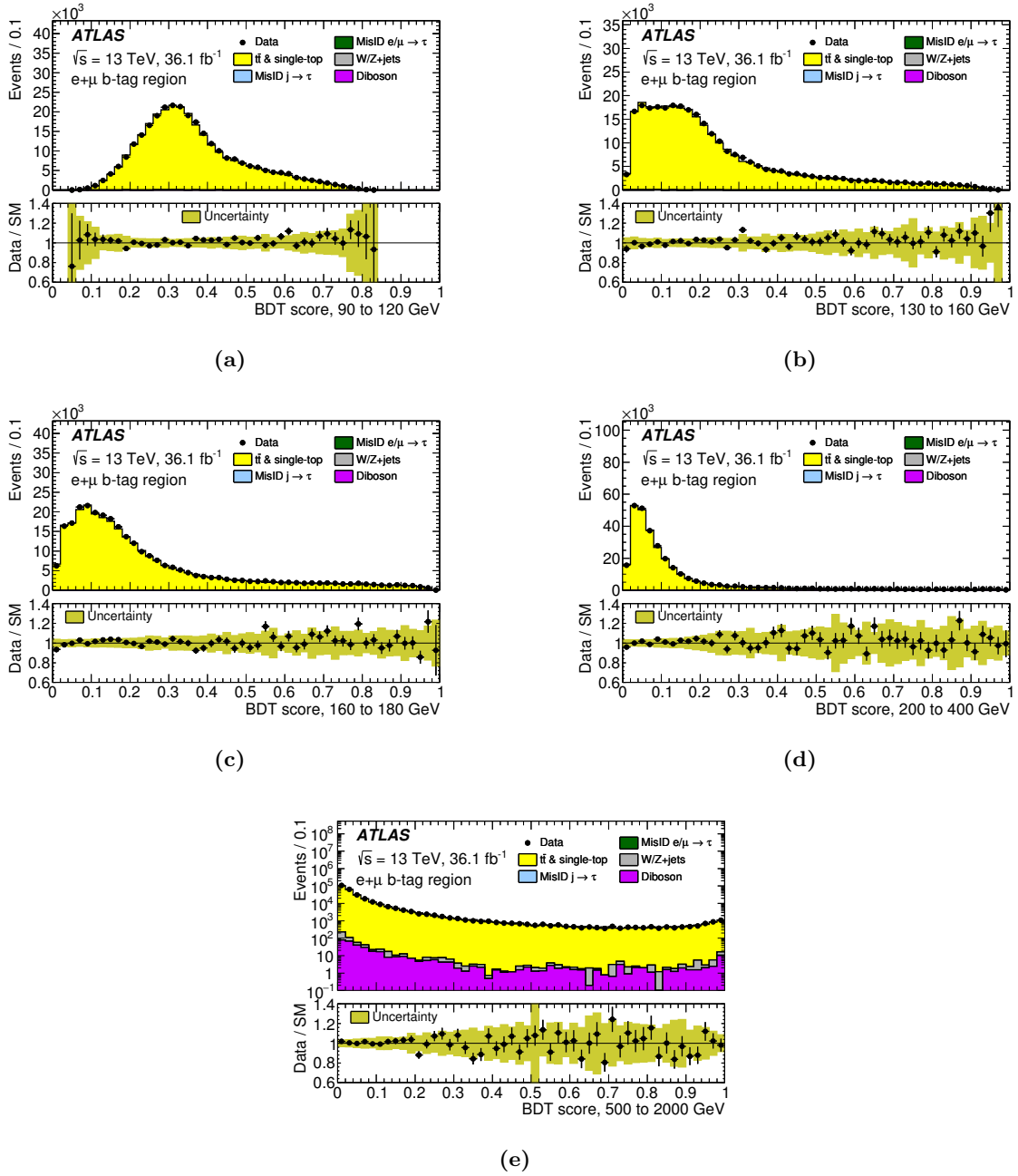
**Figure 3.** BDT score distribution for the predicted backgrounds and data in a region with the same event selection as for the $\tau_{\text{had-vis}}$+lepton channel, except for the requirement of an $e\mu$ pair instead of the $e/\mu + \tau_{\text{had-vis}}$ pair (as described in the text). The five $H^+$ mass range trainings are shown. The lower panel of each plot shows the ratio of data to the SM background prediction. The uncertainty bands include all statistical and systematic uncertainties.

**Figure 4.** BDT score distribution for the predicted backgrounds and data in a region with the same event selection as for the $\tau_{\text{had-vis}}$+lepton channel, except that it has exactly zero $b$-tagged jet (as described in the text). The five $H^+$ mass range trainings are shown. The lower panel of each plot shows the ratio of data to the SM background prediction. The uncertainty bands include all statistical and systematic uncertainties.
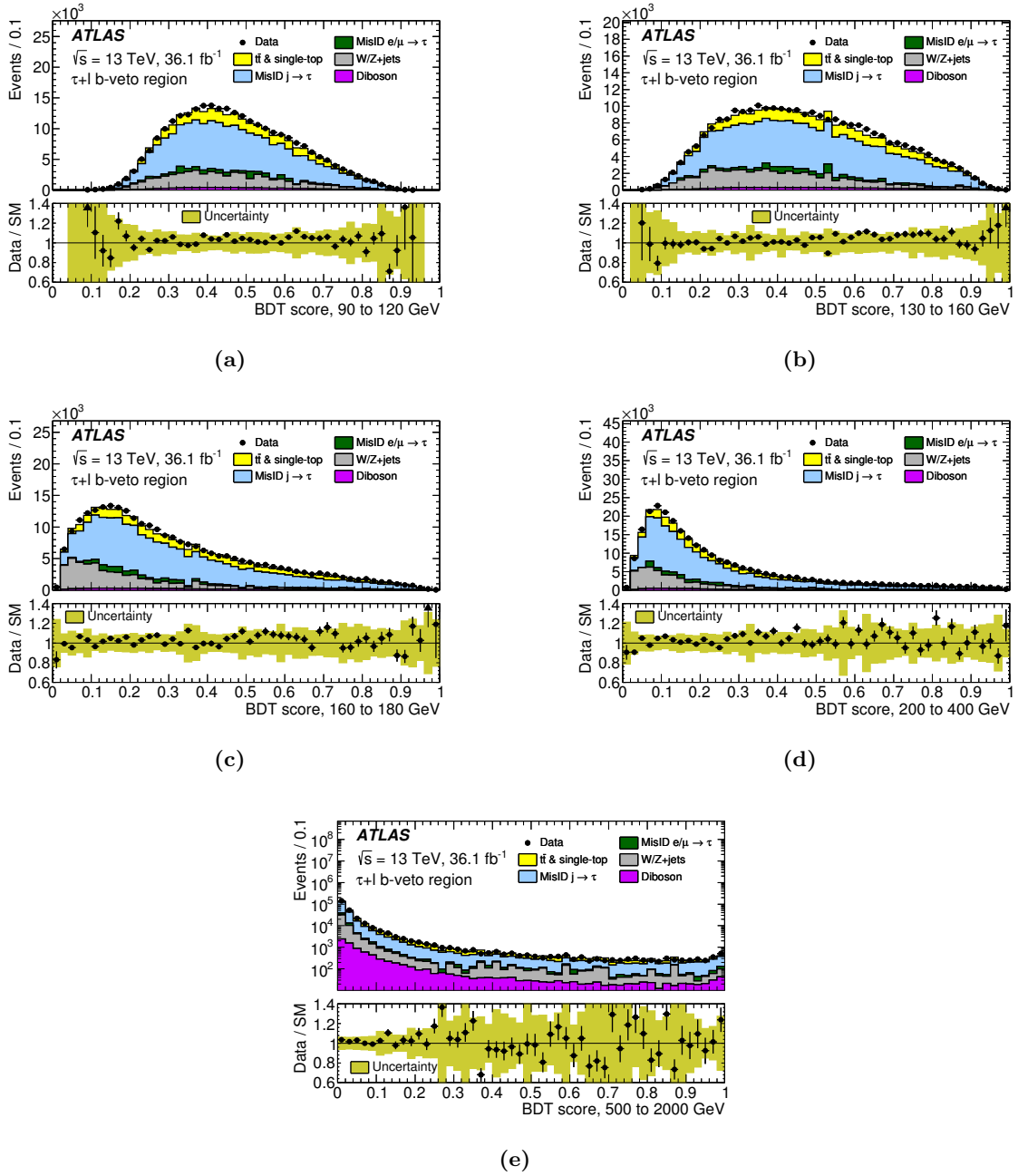
# 6 Systematic uncertainties

Several sources of systematic uncertainty affect the normalisation of the signal and background processes, as well as the shape of the BDT score distribution used as the final discriminant. Individual sources of systematic uncertainty are assumed to be uncorrelated. However, when the systematic variations are applied to different samples of simulated events, correlations of a given systematic uncertainty are taken into account across processes.

All instrumental sources of systematic uncertainty, i.e. the reconstruction and identification efficiencies, as well as the energy scales and resolutions of electrons, muons, ($b$-tagged) jets and $\tau_{\text{had-vis}}$ candidates, are considered, including their impact on the reconstructed $E_{\text{T}}^{\text{miss}}$. In both the $\tau_{\text{had-vis}}$+jets and $\tau_{\text{had-vis}}$+lepton channels, the dominant systematic uncertainties come from the jet energy scale [33] (between 1% and 4.5% depending on the jet $p_{\text{T}}$), the $b$-tagging efficiency [83] (ranging from 2% to 10% depending on the jet $p_{\text{T}}$), the reconstruction and identification efficiencies of $\tau_{\text{had-vis}}$ candidates (3% and 6%, respectively), and their energy scale (2–3%) [76]. Additional uncertainties based on multi-jet data and single-particle response are added for the identification efficiency and the energy scale of $\tau_{\text{had-vis}}$ objects at high $p_{\text{T}}$, respectively. The probability for electrons to be misidentified as $\tau_{\text{had-vis}}$ is measured with a precision of 3–14%. The uncertainty of 2.1% in the integrated luminosity is applied directly to the event yields of all simulated events. In the $\tau_{\text{had-vis}}$+lepton channel, the impact of the systematic uncertainty in the single-lepton trigger efficiency is at most 1%. In the $\tau_{\text{had-vis}}$+jets channel, the efficiency of the $E_{\text{T}}^{\text{miss}}$ trigger is measured in a control region of the data, as described in ref. [22]. The associated systematic uncertainty in the event yield of the signal region is 1.4%.

In the estimation of backgrounds with jets misidentified as $\tau_{\text{had-vis}}$ candidates, the sources of systematic uncertainty are:

- the loose requirement on the $\tau_{\text{had-vis}}$ BDT output score used in the definition of the anti-$\tau_{\text{had-vis}}$ sample, which modifies the corresponding fractions of quark- and gluon-initiated jets, as well as the event topology (assessed by considering the shape of the final discriminant obtained for two alternative thresholds for the BDT output score that are symmetric around the nominal threshold);

- the level of contamination of true $\tau_{\text{had-vis}}$ candidates fulfilling the anti-$\tau_{\text{had-vis}}$ selection (varied by 50%);

- the statistical uncertainties in the event yields entering the computation of FFs, in each bin of their parameterisation and for each control region;

- the statistical uncertainty of the best-fit value of $\alpha_{\text{MJ}}$;

- the modelling of heavy-flavour jets mimicking $\tau_{\text{had-vis}}$ candidates, obtained by computing the fake factors separately for light- and heavy-quark-initiated jets, as in ref. [22], and comparing those with the nominal predictions, then using the difference as a systematic uncertainty;

- for the $\Upsilon$ distribution only, the uncertainty in the inverse transform sampling method, taken as the difference between the computations obtained in the two control regions where the FFs are measured.

The dominant background with a true $\tau_{\text{had-vis}}$ candidate is from $t\bar{t}$ pairs and single-top-quark events. A normalisation factor is computed for this background by including the control region of the $\tau_{\text{had-vis}}$+lepton channel with an $e\mu$ pair and at least one $b$-jet as a single-bin distribution in the statistical analysis. Systematic uncertainties in the modelling of the $t\bar{t}$ background are included. Those due to the choice of parton shower and hadronisation models are derived by comparing $t\bar{t}$ events generated with POWHEG-BOX v2 interfaced to either PYTHIA6 or Herwig++ [84]. The systematic uncertainties arising from additional radiation, which modify the jet production rate, are computed with the same packages as for the baseline $t\bar{t}$ event generation, by varying the shower radiation, the factorisation and renormalisation scales, as well as the NLO radiation. The uncertainty due to the choice of matrix-element generator is evaluated by comparing $t\bar{t}$ samples generated with MADGRAPH5_AMC@NLO or POWHEG-BOX, both using the CT10 PDF set and interfaced to Herwig++. The impacts of the three systematic uncertainties listed above on the event yield of the $t\bar{t}$ background are, respectively, 14%, 4%, 13% in the $\tau_{\text{had-vis}}$+jets channel and 13%, 8%, 9% in the $\tau_{\text{had-vis}}$+lepton channel. For the $W$+jets and $Z$+jets backgrounds, uncertainties of 35% and 40% based on variations of the scales in SHERPA are considered, respectively. An additional uncertainty in the heavy-flavour jet modelling is derived by comparing the predictions of SHERPA and MADGRAPH5_AMC@NLO interfaced to PYTHIA6: it is about 6% in the $\tau_{\text{had-vis}}$+jets channel and 14% in the $\tau_{\text{had-vis}}$+lepton channel. For the small diboson backgrounds, an uncertainty of 50%, arising from the inclusive cross-section and additional jet production, is used [85].

Systematic uncertainties in the $H^+$ signal generation are estimated as follows. The uncertainty arising from the missing higher-order corrections is assessed by varying the factorisation and renormalisation scales up and down by a factor of two. The largest variation of the signal acceptance is then symmetrised and taken as the scale uncertainty, 4–8% depending on the $H^+$ mass hypothesis. The signal acceptances are computed with various PDF sets, following the PDF4LHC prescriptions [86], and their envelope is taken as a systematic uncertainty. The impact of A14 tune variations on the signal acceptance is estimated by adding in quadrature the excursions from a subset of tune variations that cover underlying-event and jet-structure effects, as well as different aspects of extra jet production. This uncertainty amounts to 8–10%.

In the low- and intermediate-mass $H^+$ search, the main systematic uncertainties arise from the estimation of the background with misidentified $\tau_{\text{had-vis}}$ candidates, as well as the reconstruction and identification of $\tau_{\text{had-vis}}$ candidates. For large $H^+$ masses, systematic uncertainties from the signal modelling and the estimation of the background with misidentified $\tau_{\text{had-vis}}$ candidates dominate, but the search is also limited by the number of selected events. The impact of the systematic uncertainties on the sensitivity of the analysis is discussed in section 7.

## 7 Results

The statistical interpretation is based on a simultaneous fit of the parameter of interest, e.g. $\mu \equiv \sigma(pp \to tbH^+) \times \mathcal{B}(H^+ \to \tau\nu)$, and the nuisance parameters $\theta$ that encode statistical and systematic uncertainties, by means of a negative log-likelihood minimisation. The test statistic $\tilde{q}_\mu$ [87] used to test the compatibility of the data with the background-only and signal+background hypotheses is computed from the profile likelihood ratio, and the asymptotic approximation is used throughout the statistical analysis. Three signal regions and one control region enriched in $t\bar{t}$ events are considered in the simultaneous fit:

- Binned likelihood functions are used for the BDT score distributions in the three signal regions ($\tau_{\text{had-vis}}$+jets, $\tau_{\text{had-vis}}$+electron and $\tau_{\text{had-vis}}$+muon). The binning of the discriminating variable is optimised to maximise the sensitivity of the analysis prior to looking at the data in the signal regions.

- A single-bin likelihood is used in the control region enriched in $t\bar{t}$ events, defined with the same event selection as the $\tau_{\text{had-vis}}$+lepton channel, but with the requirement of an $e\mu$ pair instead of the $e/\mu + \tau_{\text{had-vis}}$ pair.

The expected number of events for all SM processes and the measured event yields in the signal regions are shown in tables 2 and 3, prior to using the multivariate discriminant and applying the statistical fitting procedure. The contributions from hypothetical charged Higgs bosons are also shown, assuming a mass of 170 GeV or 1000 GeV, and with $\sigma(pp \to tbH^+) \times \mathcal{B}(H^+ \to \tau\nu)$ set to the prediction from the hMSSM scenario for $\tan\beta = 40$, as computed using refs. [13] and [88–92] for the production cross-section and HDECAY [93] for the branching fraction. The signal acceptances for a charged Higgs boson mass hypothesis of 170 GeV, as evaluated in a sample of simulated events where both the $\tau$-lepton and the top-quark decay inclusively, are 0.9%, 0.6% and 0.5% in the $\tau_{\text{had-vis}}$+jets, $\tau_{\text{had-vis}}$+electron and $\tau_{\text{had-vis}}$+muon signal regions, respectively. They become 11.6%, 0.9% and 1.2% for a charged Higgs boson mass of 1 TeV. The event yields observed in 36.1 fb$^{-1}$ of data collected at 13 TeV are consistent with the expected SM backgrounds, but very little sensitivity to $H^+$ signals can be obtained from the comparison of event yields only.

The BDT score distributions in the five charged Higgs boson mass ranges considered in the analysis are shown in figure 5 for the signal region of the $\tau_{\text{had-vis}}$+jets channel, as well as in figures 6 and 7 for the $\tau_{\text{had-vis}}$+electron and $\tau_{\text{had-vis}}$+muon sub-channels, respectively. All plots are obtained after the statistical fitting procedure with the background-only hypothesis. The binning shown in the figures is also used in the statistical analysis.

The data are found to be consistent with the background-only hypothesis (the smallest $p_0$-value is 0.3 around 350 GeV). Exclusion limits are set at the 95% confidence level (CL), by using the CL$_\text{s}$ procedure [94], on $\sigma(pp \to tbH^+) \times \mathcal{B}(H^+ \to \tau\nu)$ for the full mass range investigated, as well as on $\mathcal{B}(t \to bH^+) \times \mathcal{B}(H^+ \to \tau\nu)$ in the low $H^+$ mass range. Figure 8 shows the expected and observed exclusion limits as a function of the $H^+$ mass hypothesis. The observed limits range from 4.2 pb to 2.5 fb over the mass range considered

| Sample | Event yields $\tau_{\text{had-vis}}$+jets | | |
|---|---|---|---|
| True $\tau_{\text{had}}$ | | | |
| $\quad t\bar{t}$ | 6900 | $\pm$ 60 | $\pm$ 1800 |
| $\quad$ Single-top-quark | 750 | $\pm$ 20 | $\pm$ 100 |
| $\quad W \to \tau\nu$ | 1050 | $\pm$ 30 | $\pm$ 180 |
| $\quad Z \to \tau\tau$ | 84 | $\pm$ 42 | $\pm$ 28 |
| $\quad$ Diboson ($WW, WZ, ZZ$) | 63.2 | $\pm$ 4.6 | $\pm$ 7.2 |
| Misidentified $e, \mu \to \tau_{\text{had-vis}}$ | 265 | $\pm$ 12 | $\pm$ 35 |
| Misidentified jet $\to \tau_{\text{had-vis}}$ | 2370 | $\pm$ 20 | $\pm$ 260 |
| All backgrounds | 11500 | $\pm$ 80 | $\pm$ 1800 |
| $H^+$ (170 GeV), hMSSM $\tan\beta = 40$ | 1400 | $\pm$ 10 | $\pm$ 170 |
| $H^+$ (1000 GeV), hMSSM $\tan\beta = 40$ | 10.33 | $\pm$ 0.06 | $\pm$ 0.78 |
| Data | 11021 | | |

**Table 2.** Expected event yields for the backgrounds and a hypothetical $H^+$ signal after applying all $\tau_{\text{had-vis}}$+jets selection criteria, and comparison with $36.1\,\text{fb}^{-1}$ of data. All yields are evaluated prior to using the multivariate discriminant and applying the statistical fitting procedure. The values shown for the signal assume a charged Higgs boson mass of 170 GeV and 1000 GeV, with a cross-section times branching fraction $\sigma(pp \to tbH^+) \times \mathcal{B}(H^+ \to \tau\nu)$ corresponding to $\tan\beta = 40$ in the hMSSM benchmark scenario. Statistical and systematic uncertainties are quoted, respectively.

in this search. The limits are interpolated between the $H^+$ mass regions which are tested explicitly. The bias in the expected limits from this interpolation is found to be smaller than the statistical uncertainty. For the mass range between 90 and 160 GeV, the limits on $\sigma(pp \to tbH^+) \times \mathcal{B}(H^+ \to \tau\nu)$ translate into observed limits between 0.25% and 0.031% for the branching fraction $\mathcal{B}(t \to bH^+) \times \mathcal{B}(H^+ \to \tau\nu)$ if one assumes that the production cross-section is equal to that of $t\bar{t}$ pairs.

The impact from the various sources of systematic uncertainty is estimated by comparing the expected 95% CL limits on $\sigma(pp \to tbH^+) \times \mathcal{B}(H^+ \to \tau\nu)$ when taking only statistical uncertainties into account and those obtained when a certain set of systematic uncertainties is added in the limit-setting procedure, as summarised in table 4 for $H^+$ masses of 170 GeV and 1000 GeV.

Figure 9 shows the 95% CL exclusion limits on $\tan\beta$ as a function of the charged Higgs boson mass in the context of the hMSSM scenario. All $\tan\beta$ values are excluded for $m_{H^+} \lesssim 160$ GeV. At $\tan\beta = 60$, above which no reliable theoretical calculations exist, the charged Higgs boson mass range up to 1100 GeV is excluded, hence significantly improving on the limits based on the dataset collected in 2015, which corresponds to an integrated luminosity of $3.2\,\text{fb}^{-1}$.
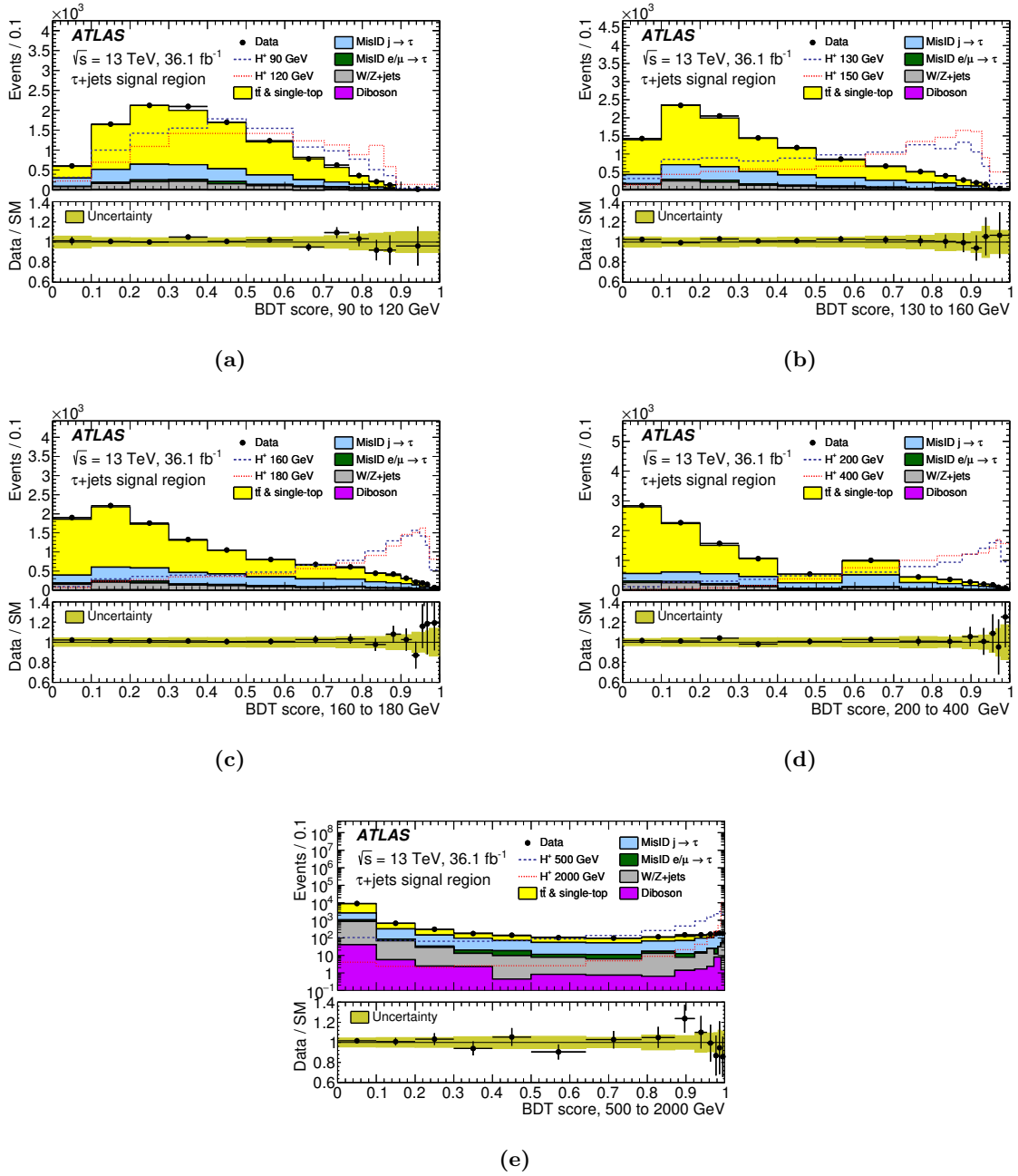
**Figure 5.** BDT score distributions in the signal region of the $\tau_{\text{had-vis}}$+jets channel, in the five mass ranges used for the BDT trainings, after a fit to the data with the background-only hypothesis. The lower panel of each plot shows the ratio of data to the SM background prediction. The uncertainty bands include all statistical and systematic uncertainties. The normalisation of the signal (shown for illustration) corresponds to the integral of the background.

**Figure 6.** BDT score distributions in the signal region of the $\tau_{\mathrm{had\text{-}vis}}$+electron sub-channel, in the five mass ranges used for the BDT trainings, after a fit to the data with the background-only hypothesis. The lower panel of each plot shows the ratio of data to the SM background prediction. The uncertainty bands include all statistical and systematic uncertainties. The normalisation of the signal (shown for illustration) corresponds to the integral of the background.
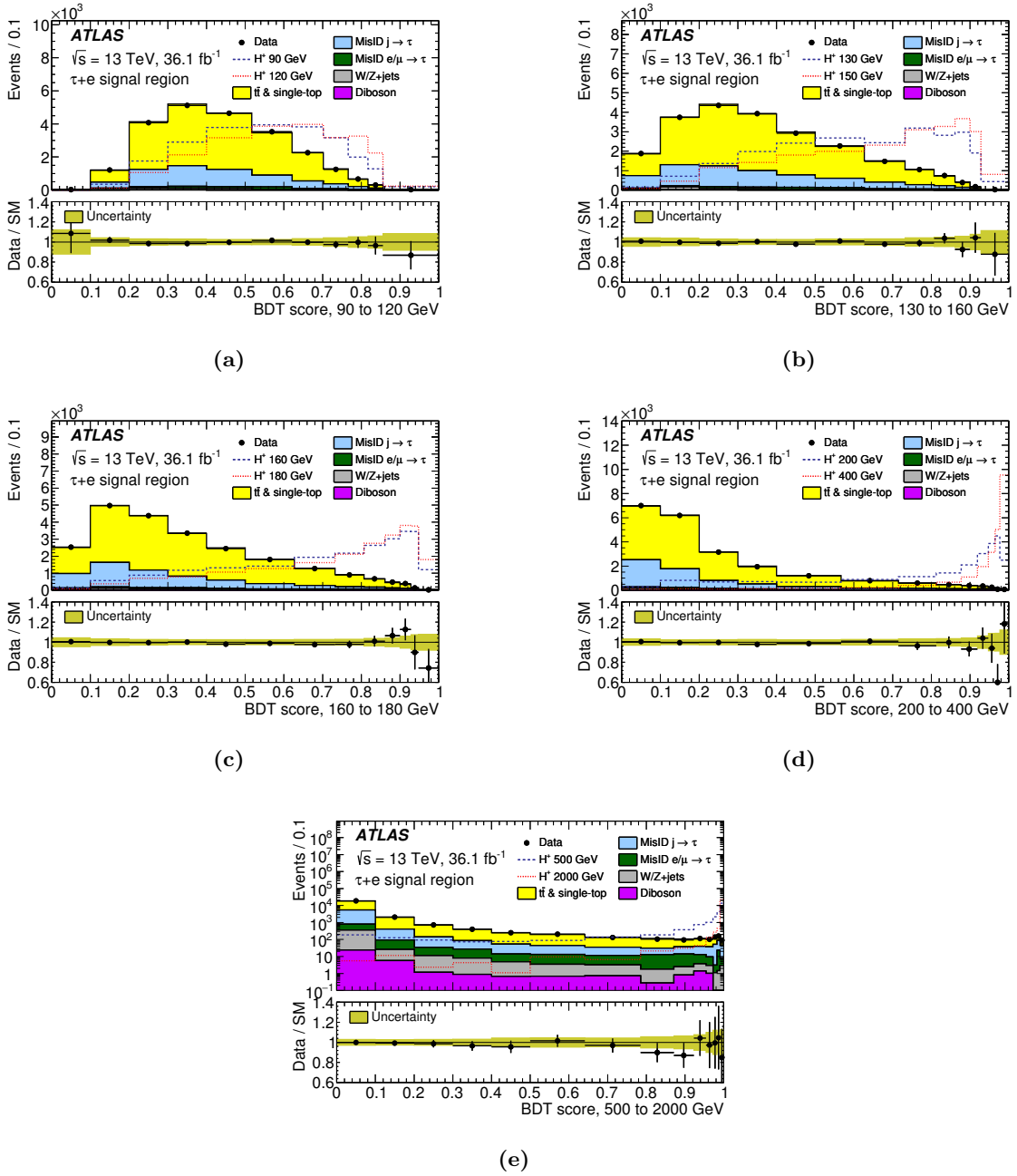
**Figure 7.** BDT score distributions in the signal region of the $\tau_{\text{had-vis}}$+muon sub-channel, in the five mass ranges used for the BDT trainings, after a fit to the data with the background-only hypothesis. The lower panel of each plot shows the ratio of data to the SM background prediction. The uncertainty bands include all statistical and systematic uncertainties. The normalisation of the signal (shown for illustration) corresponds to the integral of the background.
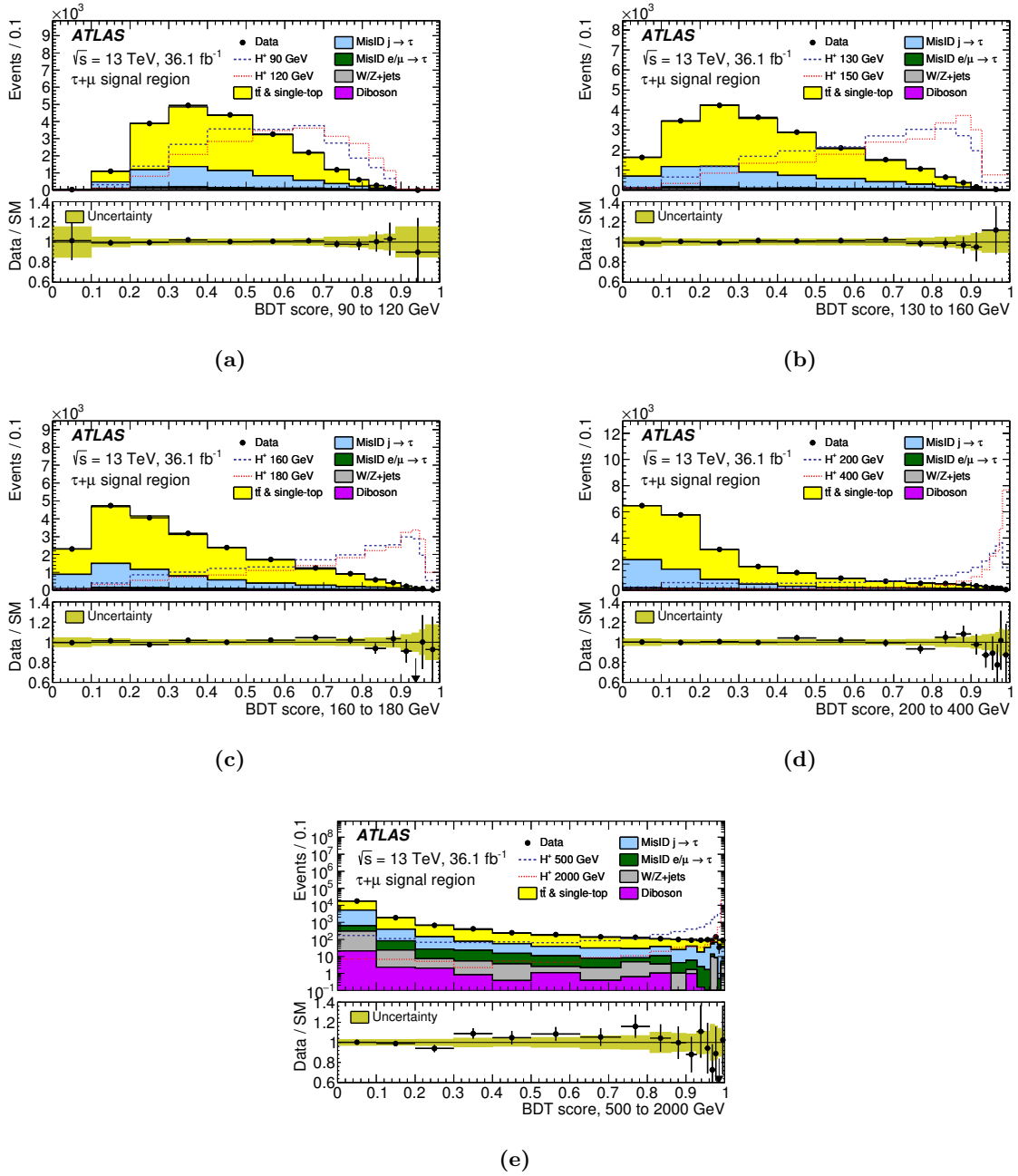
| Sample | Event yields $\tau_{\text{had-vis}}$+electron | | | Event yields $\tau_{\text{had-vis}}$+muon | | |
|---|---|---|---|---|---|---|
| True $\tau_{\text{had}}$ | | | | | | |
| $\quad t\bar{t}$ | 16000 | $\pm$ 80 | $\pm$ 2500 | 14600 | $\pm$ 80 | $\pm$ 2400 |
| $\quad$ Single-top-quark | 1260 | $\pm$ 20 | $\pm$ 110 | 1260 | $\pm$ 20 | $\pm$ 110 |
| $\quad Z \to \tau\tau$ | 433 | $\pm$ 27 | $\pm$ 80 | 352 | $\pm$ 48 | $\pm$ 43 |
| $\quad$ Diboson ($WW, WZ, ZZ$) | 39.3 | $\pm$ 2.1 | $\pm$ 4.5 | 32.3 | $\pm$ 1.7 | $\pm$ 3.6 |
| Misidentified $e, \mu \to \tau_{\text{had-vis}}$ | 626 | $\pm$ 27 | $\pm$ 59 | 454 | $\pm$ 16 | $\pm$ 27 |
| Misidentified jet $\to \tau_{\text{had-vis}}$ | 5640 | $\pm$ 40 | $\pm$ 450 | 5460 | $\pm$ 40 | $\pm$ 410 |
| All backgrounds | 24000 | $\pm$ 100 | $\pm$ 2600 | 22200 | $\pm$ 100 | $\pm$ 2500 |
| $H^+$ (170 GeV), hMSSM $\tan\beta = 40$ | 850 | $\pm$ 12 | $\pm$ 65 | 852 | $\pm$ 11 | $\pm$ 66 |
| $H^+$ (1000 GeV), hMSSM $\tan\beta = 40$ | 0.82 $\pm$ | 0.02 $\pm$ | 0.07 | 1.05 $\pm$ | 0.02 $\pm$ | 0.09 |
| Data | 22645 | | | 21419 | | |

**Table 3.** Expected event yields for the backgrounds and a hypothetical $H^+$ signal after applying all $\tau_{\text{had-vis}}$+lepton selection criteria, and comparison with $36.1\,\text{fb}^{-1}$ of data. All yields are evaluated prior to using the multivariate discriminant and applying the statistical fitting procedure. The values shown for the signal assume a charged Higgs boson mass of 170 GeV and 1000 GeV, with a cross-section times branching fraction $\sigma(pp \to tbH^+) \times \mathcal{B}(H^+ \to \tau\nu)$ corresponding to $\tan\beta = 40$ in the hMSSM benchmark scenario. Statistical and systematic uncertainties are quoted, respectively.
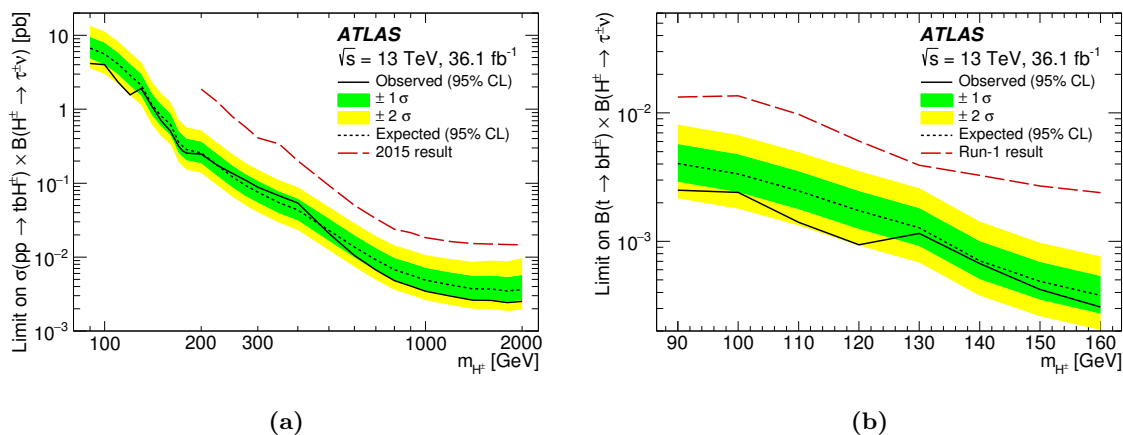


(a)                    (b)

**Figure 8.** Observed and expected 95% CL exclusion limits on (a) $\sigma(pp \to tbH^+) \times \mathcal{B}(H^+ \to \tau\nu)$ and (b) $\mathcal{B}(t \to bH^+) \times \mathcal{B}(H^+ \to \tau\nu)$ as a function of the charged Higgs boson mass in $36.1\,\text{fb}^{-1}$ of $pp$ collision data at $\sqrt{s} = 13$ TeV, after combination of the $\tau_{\text{had-vis}}$+jets and $\tau_{\text{had-vis}}$+lepton channels. In the case of the expected limits, one- and two-standard-deviation uncertainty bands are also shown. As a comparison, the observed exclusion limits on $\mathcal{B}(t \to bH^+) \times \mathcal{B}(H^+ \to \tau\nu)$ obtained with the Run-1 data at $\sqrt{s} = 8$ TeV [16] and on $\sigma(pp \to tbH^+) \times \mathcal{B}(H^+ \to \tau\nu)$ obtained with the dataset collected in 2015 at $\sqrt{s} = 13$ TeV [22] are also shown.

| Source of systematic | Impact on the expected limit (stat. only) in % | |
| --- | --- | --- |
| uncertainty | $m_{H^+} = 170$ GeV | $m_{H^+} = 1000$ GeV |
| Experimental | | |
|     luminosity | 2.9 | 0.2 |
|     trigger | 1.3 | <0.1 |
|     $\tau_{\text{had-vis}}$ | 14.6 | 0.3 |
|     jet | 16.9 | 0.2 |
|     electron | 10.1 | 0.1 |
|     muon | 1.1 | <0.1 |
|     $E_{\text{T}}^{\text{miss}}$ | 9.9 | <0.1 |
| Fake-factor method | 20.3 | 2.7 |
| $\Upsilon$ modelling | 0.8 | – |
| Signal and background models | | |
|     $t\bar{t}$ modelling | 6.3 | 0.1 |
|     $W/Z$+jets modelling | 1.1 | <0.1 |
|     cross-sections $(W/Z/VV/t)$ | 9.6 | 0.4 |
|     $H^+$ signal modelling | 2.5 | 6.4 |
| All | 52.1 | 13.8 |

**Table 4.** Impact of systematic uncertainties on the expected 95% CL limit on $\sigma(pp \to tbH^+) \times \mathcal{B}(H^+ \to \tau\nu)$, for two $H^+$ mass hypotheses: 170 GeV and 1000 GeV. The impact is obtained by comparing the expected limit considering only statistical uncertainties (stat. only) with the expected limit when a certain set of systematic uncertainties is added in the limit-setting procedure. In the absence of correlations and assuming Gaussian uncertainties, the row "All" would be obtained by summing in quadrature (linearly) the individual contributions of the systematic uncertainties if these were much larger (smaller) than the statistical uncertainties.
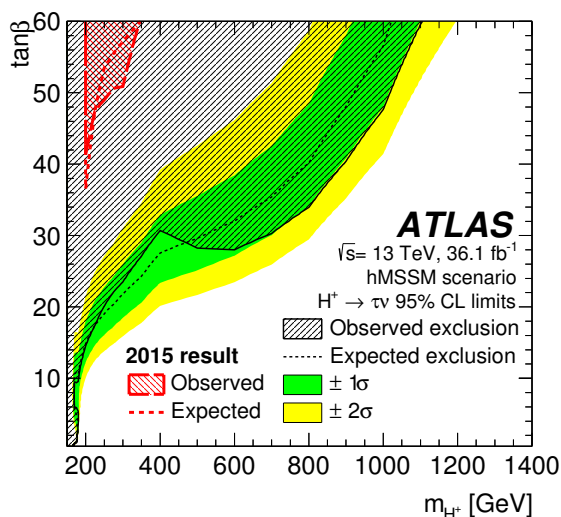
**Figure 9.** 95% CL exclusion limits on $\tan\beta$ as a function of $m_{H^+}$, shown in the context of the hMSSM, for the regions in which theoretical predictions are available ($0.5 \le \tan\beta \le 60$). In the case of the expected limits, one- and two-standard-deviation uncertainty bands are also shown. As a comparison, the red curves near the upper-left corner show the observed and expected exclusion limits based on the dataset of 3.2 fb$^{-1}$ collected in 2015 at $\sqrt{s} = 13$ TeV [22].

## 8 Conclusion

A search for charged Higgs bosons produced either in top-quark decays or in association with a top-quark, and subsequently decaying via $H^+ \to \tau\nu$, is performed in the $\tau$+jets and $\tau$+lepton channels, according to the hadronic or semileptonic decay of the top quark produced together with $H^+$. The dataset contains 36.1 fb$^{-1}$ of $pp$ collisions at $\sqrt{s} = 13$ TeV, recorded with the ATLAS detector at the LHC. The data are found to be in agreement with the background-only hypothesis. Upper limits at the 95% confidence level are set on the $H^+$ production cross-section times the branching fraction $\mathcal{B}(H^+ \to \tau\nu)$ between 4.2 pb and 2.5 fb for a charged Higgs boson mass range of 90–2000 GeV, corresponding to upper limits between 0.25% and 0.031% for the branching fraction $\mathcal{B}(t \to bH^+) \times \mathcal{B}(H^+ \to \tau\nu)$ in the mass range 90–160 GeV. These exclusion limits are about 5–7 times more stringent than those obtained by ATLAS with 3.2 fb$^{-1}$ of 13 TeV data for $H^+$ masses above 200 GeV [22] and with Run-1 data in the $H^+$ mass range 90–160 GeV [16]. In the intermediate-mass region where $m_{H^+} \simeq m_{\text{top}}$, accurate theoretical predictions recently became available, allowing a dedicated comparison of the $H^+$ models with data near the top-quark mass. In the context of the hMSSM scenario, all $\tan\beta$ values are excluded for $m_{H^+} \lesssim 160$ GeV. The $H^+$ mass range up to 1100 GeV is excluded at $\tan\beta = 60$.

## Acknowledgments

# References

[1] L. Evans and P. Bryant, *LHC machine*, 2008 *JINST* **3** S08001 [inSPIRE].

[2] ATLAS collaboration, *Observation of a new particle in the search for the Standard Model Higgs boson with the ATLAS detector at the LHC*, *Phys. Lett.* **B 716** (2012) 1 [arXiv:1207.7214] [inSPIRE].

[3] CMS collaboration, *Observation of a new boson at a mass of 125 GeV with the CMS experiment at the LHC*, *Phys. Lett.* **B 716** (2012) 30 [arXiv:1207.7235] [inSPIRE].

[4] ATLAS and CMS collaborations, *Combined measurement of the Higgs boson mass in pp collisions at $\sqrt{s} = 7$ and 8 TeV with the ATLAS and CMS experiments*, *Phys. Rev. Lett.* **114** (2015) 191803 [arXiv:1503.07589] [inSPIRE].

[5] A. Djouadi, *The anatomy of electro-weak symmetry breaking. II. The Higgs bosons in the minimal supersymmetric model*, *Phys. Rept.* **459** (2008) 1 [hep-ph/0503173] [INSPIRE].

[6] G.C. Branco, P.M. Ferreira, L. Lavoura, M.N. Rebelo, M. Sher and J.P. Silva, *Theory and phenomenology of two-Higgs-doublet models*, *Phys. Rept.* **516** (2012) 1 [arXiv:1106.0034] [INSPIRE].

[7] G. Senjanović and R.N. Mohapatra, *Exact left-right symmetry and spontaneous violation of parity*, *Phys. Rev.* **D 12** (1975) 1502 [INSPIRE].

[8] J.E. Cieza Montalvo, N.V. Cortez, J. Sa Borges and M.D. Tonasse, *Searching for doubly charged Higgs bosons at the LHC in a 3-3-1 model*, *Nucl. Phys.* **B 756** (2006) 1 [*Erratum ibid.* **B 796** (2008) 422] [hep-ph/0606243] [INSPIRE].

[9] J.F. Gunion, R. Vega and J. Wudka, *Higgs triplets in the Standard Model*, *Phys. Rev.* **D 42** (1990) 1673 [INSPIRE].

[10] H. Georgi and M. Machacek, *Doubly charged Higgs bosons*, *Nucl. Phys.* **B 262** (1985) 463 [INSPIRE].

[11] A. Djouadi, L. Maiani, G. Moreau, A. Polosa, J. Quevillon and V. Riquer, *The post-Higgs MSSM scenario: habemus MSSM?*, *Eur. Phys. J.* **C 73** (2013) 2650 [arXiv:1307.5205] [INSPIRE].

[12] A. Djouadi, L. Maiani, A. Polosa, J. Quevillon and V. Riquer, *Fully covering the MSSM Higgs sector at the LHC*, *JHEP* **06** (2015) 168 [arXiv:1502.05653] [INSPIRE].

[13] C. Degrande, R. Frederix, V. Hirschi, M. Ubiali, M. Wiesemann and M. Zaro, *Accurate predictions for charged Higgs production: closing the $m_{H^\pm} \sim m_t$ window*, *Phys. Lett.* **B 772** (2017) 87 [arXiv:1607.05291] [INSPIRE].

[14] ATLAS collaboration, *Search for charged Higgs bosons decaying via $H^+ \to \tau\nu$ in top quark pair events using pp collision data at $\sqrt{s} = 7$ TeV with the ATLAS detector*, *JHEP* **06** (2012) 039 [arXiv:1204.2760] [INSPIRE].

[15] ATLAS collaboration, *Search for charged Higgs bosons through the violation of lepton universality in $t\bar{t}$ events using pp collision data at $\sqrt{s} = 7$ TeV with the ATLAS experiment*, *JHEP* **03** (2013) 076 [arXiv:1212.3572] [INSPIRE].

[16] ATLAS collaboration, *Search for charged Higgs bosons decaying via $H^\pm \to \tau^\pm\nu$ in fully hadronic final states using pp collision data at $\sqrt{s} = 8$ TeV with the ATLAS detector*, *JHEP* **03** (2015) 088 [arXiv:1412.6663] [INSPIRE].

[17] CMS collaboration, *Search for a light charged Higgs boson in top quark decays in pp collisions at $\sqrt{s} = 7$ TeV*, *JHEP* **07** (2012) 143 [arXiv:1205.5736] [INSPIRE].

[18] CMS collaboration, *Search for a charged Higgs boson in pp collisions at $\sqrt{s} = 8$ TeV*, *JHEP* **11** (2015) 018 [arXiv:1508.07774] [INSPIRE].

[19] ATLAS collaboration, *Search for a light charged Higgs boson in the decay channel $H^+ \to c\bar{s}$ in $t\bar{t}$ events using pp collisions at $\sqrt{s} = 7$ TeV with the ATLAS detector*, *Eur. Phys. J.* **C 73** (2013) 2465 [arXiv:1302.3694] [INSPIRE].

[20] CMS collaboration, *Search for a light charged Higgs boson decaying to $c\bar{s}$ in pp collisions at $\sqrt{s} = 8$ TeV*, *JHEP* **12** (2015) 178 [arXiv:1510.04252] [INSPIRE].

[21] ATLAS collaboration, *Search for charged Higgs bosons in the $H^{\pm} \to tb$ decay channel in pp collisions at $\sqrt{s} = 8\,TeV$ using the ATLAS detector*, *JHEP* **03** (2016) 127 [arXiv:1512.03704] [INSPIRE].

[22] ATLAS collaboration, *Search for charged Higgs bosons produced in association with a top quark and decaying via $H^{\pm} \to \tau\nu$ using pp collision data recorded at $\sqrt{s} = 13\,TeV$ by the ATLAS detector*, *Phys. Lett.* **B 759** (2016) 555 [arXiv:1603.09203] [INSPIRE].

[23] ATLAS collaboration, *Search for a charged Higgs boson produced in the vector-boson fusion mode with decay $H^{\pm} \to W^{\pm}Z$ using pp collisions at $\sqrt{s} = 8\,TeV$ with the ATLAS experiment*, *Phys. Rev. Lett.* **114** (2015) 231801 [arXiv:1503.04233] [INSPIRE].

[24] CMS collaboration, *Search for charged Higgs bosons produced via vector boson fusion and decaying into a pair of $W$ and $Z$ bosons using pp collisions at $\sqrt{s} = 13\,TeV$*, *Phys. Rev. Lett.* **119** (2017) 141802 [arXiv:1705.02942] [INSPIRE].

[25] ATLAS collaboration, *Search for additional heavy neutral Higgs and gauge bosons in the ditau final state produced in $36\,fb^{-1}$ of pp collisions at $\sqrt{s} = 13\,TeV$ with the ATLAS detector*, *JHEP* **01** (2018) 055 [arXiv:1709.07242] [INSPIRE].

[26] CMS collaboration, *Search for additional neutral MSSM Higgs bosons in the $\tau\tau$ final state in proton-proton collisions at $\sqrt{s} = 13\,TeV$*, *JHEP* **09** (2018) 007 [arXiv:1803.06553] [INSPIRE].

[27] ATLAS collaboration, *The ATLAS experiment at the CERN Large Hadron Collider*, 2008 *JINST* **3** S08003 [INSPIRE].

[28] ATLAS collaboration, *ATLAS insertable B-layer technical design report*, ATLAS-TDR-19, CERN, Geneva, Switzerland, (2010) [CERN-LHCC-2010-013].

[29] ATLAS collaboration, *ATLAS insertable B-layer technical design report addendum*, ATLAS-TDR-19-ADD-1, CERN, Geneva, Switzerland, (2012) [CERN-LHCC-2012-009].

[30] ATLAS collaboration, *Performance of the ATLAS trigger system in* 2015, *Eur. Phys. J.* **C 77** (2017) 317 [arXiv:1611.09661] [INSPIRE].

[31] ATLAS collaboration, *Trigger menu in* 2016, ATL-DAQ-PUB-2017-001, CERN, Geneva, Switzerland, (2017).

[32] ATLAS collaboration, *Luminosity determination in pp collisions at $\sqrt{s} = 8\,TeV$ using the ATLAS detector at the LHC*, *Eur. Phys. J.* **C 76** (2016) 653 [arXiv:1608.03953] [INSPIRE].

[33] ATLAS collaboration, *Jet energy scale measurements and their systematic uncertainties in proton-proton collisions at $\sqrt{s} = 13\,TeV$ with the ATLAS detector*, *Phys. Rev.* **D 96** (2017) 072002 [arXiv:1703.09665] [INSPIRE].

[34] J. Alwall et al., *The automated computation of tree-level and next-to-leading order differential cross sections and their matching to parton shower simulations*, *JHEP* **07** (2014) 079 [arXiv:1405.0301] [INSPIRE].

[35] T. Sjöstrand, S. Mrenna and P.Z. Skands, *A brief introduction to PYTHIA 8.1*, *Comput. Phys. Commun.* **178** (2008) 852 [arXiv:0710.3820] [INSPIRE].

[36] ATLAS collaboration, *ATLAS run 1 PYTHIA8 tunes*, ATL-PHYS-PUB-2014-021, CERN, Geneva, Switzerland, (2014).

[37] R.D. Ball et al., *Parton distributions with LHC data*, *Nucl. Phys.* **B 867** (2013) 244 [arXiv:1207.1303] [INSPIRE].

[38] P. Nason, *A new method for combining NLO QCD with shower Monte Carlo algorithms*, *JHEP* **11** (2004) 040 [hep-ph/0409146] [INSPIRE].

[39] S. Frixione, P. Nason and C. Oleari, *Matching NLO QCD computations with parton shower simulations: the POWHEG method*, *JHEP* **11** (2007) 070 [arXiv:0709.2092] [INSPIRE].

[40] S. Alioli, P. Nason, C. Oleari and E. Re, *A general framework for implementing NLO calculations in shower Monte Carlo programs: the POWHEG BOX*, *JHEP* **06** (2010) 043 [arXiv:1002.2581] [INSPIRE].

[41] H.-L. Lai et al., *New parton distributions for collider physics*, *Phys. Rev.* **D 82** (2010) 074024 [arXiv:1007.2241] [INSPIRE].

[42] S. Dulat et al., *New parton distribution functions from a global analysis of quantum chromodynamics*, *Phys. Rev.* **D 93** (2016) 033006 [arXiv:1506.07443] [INSPIRE].

[43] P. Artoisenet, R. Frederix, O. Mattelaer and R. Rietkerk, *Automatic spin-entangled decays of heavy resonances in Monte Carlo simulations*, *JHEP* **03** (2013) 015 [arXiv:1212.3460] [INSPIRE].

[44] T. Sjöstrand, S. Mrenna and P.Z. Skands, *PYTHIA 6.4 physics and manual*, *JHEP* **05** (2006) 026 [hep-ph/0603175] [INSPIRE].

[45] J. Pumplin, D.R. Stump, J. Huston, H.L. Lai, P.M. Nadolsky and W.K. Tung, *New generation of parton distributions with uncertainties from global QCD analysis*, *JHEP* **07** (2002) 012 [hep-ph/0201195] [INSPIRE].

[46] P.Z. Skands, *Tuning Monte Carlo generators: the Perugia tunes*, *Phys. Rev.* **D 82** (2010) 074018 [arXiv:1005.3457] [INSPIRE].

[47] M. Czakon and A. Mitov, *Top++: a program for the calculation of the top-pair cross-section at hadron colliders*, *Comput. Phys. Commun.* **185** (2014) 2930 [arXiv:1112.5675] [INSPIRE].

[48] P. Kant et al., *HatHor for single top-quark production: updated predictions and uncertainty estimates for single top-quark production in hadronic collisions*, *Comput. Phys. Commun.* **191** (2015) 74 [arXiv:1406.4403] [INSPIRE].

[49] M. Aliev, H. Lacker, U. Langenfeld, S. Moch, P. Uwer and M. Wiedermann, *HATHOR: HAdronic Top and Heavy quarks crOss section calculatoR*, *Comput. Phys. Commun.* **182** (2011) 1034 [arXiv:1007.1327] [INSPIRE].

[50] N. Kidonakis, *Two-loop soft anomalous dimensions for single top quark associated production with a $W^-$ or $H^-$*, *Phys. Rev.* **D 82** (2010) 054018 [arXiv:1005.4451] [INSPIRE].

[51] N. Kidonakis, *Top quark production*, in *Proceedings of the Helmholtz International Summer School on Physics of Heavy Quarks and Hadrons (HQ 2013)*, JINR, Dubna, Russia, 15–28 July 2013, DESY-PROC-2013-03, (2014), pg. 139 [arXiv:1311.0283] [INSPIRE].

[52] T. Gleisberg et al., *Event generation with SHERPA 1.1*, *JHEP* **02** (2009) 007 [arXiv:0811.4622] [INSPIRE].

[53] NNPDF collaboration, R.D. Ball et al., *Parton distributions for the LHC run II*, *JHEP* **04** (2015) 040 [arXiv:1410.8849] [INSPIRE].

[54] T. Gleisberg and S. Höche, *Comix, a new matrix element generator*, *JHEP* **12** (2008) 039 [arXiv:0808.3674] [INSPIRE].

[55] F. Cascioli, P. Maierhofer and S. Pozzorini, *Scattering amplitudes with open loops*, *Phys. Rev. Lett.* **108** (2012) 111601 [arXiv:1111.5206] [INSPIRE].

[56] S. Schumann and F. Krauss, *A parton shower algorithm based on Catani-Seymour dipole factorisation*, *JHEP* **03** (2008) 038 [arXiv:0709.1027] [INSPIRE].

[57] S. Höche, F. Krauss, M. Schonherr and F. Siegert, *QCD matrix elements + parton showers: the NLO case*, *JHEP* **04** (2013) 027 [arXiv:1207.5030] [INSPIRE].

[58] C. Anastasiou, L.J. Dixon, K. Melnikov and F. Petriello, *High precision QCD at hadron colliders: electroweak gauge boson rapidity distributions at NNLO*, *Phys. Rev.* **D 69** (2004) 094008 [hep-ph/0312266] [INSPIRE].

[59] K. Melnikov and F. Petriello, *Electroweak gauge boson production at hadron colliders through* $O(\alpha_s^2)$, *Phys. Rev.* **D 74** (2006) 114017 [hep-ph/0609070] [INSPIRE].

[60] R. Gavin, Y. Li, F. Petriello and S. Quackenbush, *FEWZ 2.0: a code for hadronic Z production at next-to-next-to-leading order*, *Comput. Phys. Commun.* **182** (2011) 2388 [arXiv:1011.3540] [INSPIRE].

[61] ATLAS collaboration, *Measurement of the* $Z/\gamma^*$ *boson transverse momentum distribution in* pp *collisions at* $\sqrt{s} = 7$ *TeV with the ATLAS detector*, *JHEP* **09** (2014) 145 [arXiv:1406.3660] [INSPIRE].

[62] D.J. Lange, *The EvtGen particle decay simulation package*, *Nucl. Instrum. Meth.* **A 462** (2001) 152 [INSPIRE].

[63] ATLAS collaboration, *Summary of ATLAS PYTHIA 8 tunes*, ATL-PHYS-PUB-2012-003, CERN, Geneva, Switzerland, (2012).

[64] A.D. Martin, W.J. Stirling, R.S. Thorne and G. Watt, *Parton distributions for the LHC*, *Eur. Phys. J.* **C 63** (2009) 189 [arXiv:0901.0002] [INSPIRE].

[65] ATLAS collaboration, *The ATLAS simulation infrastructure*, *Eur. Phys. J.* **C 70** (2010) 823 [arXiv:1005.4568] [INSPIRE].

[66] GEANT4 collaboration, S. Agostinelli et al., *GEANT4: a simulation toolkit*, *Nucl. Instrum. Meth.* **A 506** (2003) 250 [INSPIRE].

[67] ATLAS collaboration, *Electron efficiency measurements with the ATLAS detector using the* 2015 *LHC proton-proton collision data*, ATLAS-CONF-2016-024, CERN, Geneva, Switzerland, (2016).

[68] ATLAS collaboration, *Muon reconstruction performance of the ATLAS detector in proton-proton collision data at* $\sqrt{s} = 13$ *TeV*, *Eur. Phys. J.* **C 76** (2016) 292 [arXiv:1603.05598] [INSPIRE].

[69] M. Cacciari, G.P. Salam and G. Soyez, *The anti-$k_t$ jet clustering algorithm*, *JHEP* **04** (2008) 063 [arXiv:0802.1189] [INSPIRE].

[70] M. Cacciari, G.P. Salam and G. Soyez, *FastJet user manual*, *Eur. Phys. J.* **C 72** (2012) 1896 [arXiv:1111.6097] [INSPIRE].

[71] ATLAS collaboration, *Tagging and suppression of pileup jets with the ATLAS detector*, ATLAS-CONF-2014-018, CERN, Geneva, Switzerland, (2014).

[72] ATLAS collaboration, *Performance of b-jet identification in the ATLAS experiment*, 2016 *JINST* **11** P04008 [arXiv:1512.01094] [INSPIRE].

[73] ATLAS collaboration, *Optimisation of the ATLAS b-tagging performance for the* 2016 *LHC run*, ATL-PHYS-PUB-2016-012, CERN, Geneva, Switzerland, (2016).

[74] ATLAS collaboration, *Identification and energy calibration of hadronically decaying tau leptons with the ATLAS experiment in pp collisions at $\sqrt{s} = 8\,TeV$*, *Eur. Phys. J.* **C 75** (2015) 303 [arXiv:1412.7086] [INSPIRE].

[75] ATLAS collaboration, *Reconstruction, energy calibration and identification of hadronically decaying tau leptons in the ATLAS experiment for run-2 of the LHC*, ATL-PHYS-PUB-2015-045, CERN, Geneva, Switzerland, (2015).

[76] ATLAS collaboration, *Measurement of the tau lepton reconstruction and identification performance in the ATLAS experiment using pp collisions at $\sqrt{s} = 13\,TeV$*, ATLAS-CONF-2017-029, CERN, Geneva, Switzerland, (2017).

[77] ATLAS collaboration, *Performance of missing transverse momentum reconstruction with the ATLAS detector using proton-proton collisions at $\sqrt{s} = 13\,TeV$*, arXiv:1802.08168 [INSPIRE].

[78] T. Keck, *FastBDT: a speed-optimized multivariate classification algorithm for the Belle II experiment*, *Comput. Softw. Big Sci.* **1** (2017) 2 [INSPIRE].

[79] A. Hocker et al., *TMVA — toolkit for multivariate data analysis*, PoS(ACAT)040 [physics/0703039] [INSPIRE].

[80] D.P. Roy, *The hadronic $\tau$ decay signature of a heavy charged Higgs boson at LHC*, *Phys. Lett.* **B 459** (1999) 607 [hep-ph/9905542] [INSPIRE].

[81] ATLAS collaboration, *Measurement of $\tau$ polarization in $W \to \tau\nu$ decays with the ATLAS detector in pp collisions at $\sqrt{s} = 7\,TeV$*, *Eur. Phys. J.* **C 72** (2012) 2062 [arXiv:1204.6720] [INSPIRE].

[82] L. Devroye, *Non-uniform random variate generation*, Springer, New York, U.S.A., (1986).

[83] ATLAS collaboration, *Calibration of b-tagging using dileptonic top pair events in a combinatorial likelihood approach with the ATLAS experiment*, ATLAS-CONF-2014-004, CERN, Geneva, Switzerland, (2014).

[84] M. Bahr et al., *HERWIG++ physics and manual*, *Eur. Phys. J.* **C 58** (2008) 639 [arXiv:0803.0883] [INSPIRE].

[85] ATLAS collaboration, *Multi-boson simulation for 13 TeV ATLAS analyses*, ATL-PHYS-PUB-2016-002, CERN, Geneva, Switzerland, (2016).

[86] J. Butterworth et al., *PDF4LHC recommendations for LHC run II*, *J. Phys.* **G 43** (2016) 023001 [arXiv:1510.03865] [INSPIRE].

[87] G. Cowan, K. Cranmer, E. Gross and O. Vitells, *Asymptotic formulae for likelihood-based tests of new physics*, *Eur. Phys. J.* **C 71** (2011) 1554 [*Erratum ibid.* **C 73** (2013) 2501] [arXiv:1007.1727] [INSPIRE].

[88] LHC HIGGS CROSS SECTION WORKING GROUP collaboration, J.R. Andersen et al., *Handbook of LHC Higgs cross sections: 3. Higgs properties*, arXiv:1307.1347 [INSPIRE].

[89] C. Degrande, M. Ubiali, M. Wiesemann and M. Zaro, *Heavy charged Higgs boson production at the LHC*, *JHEP* **10** (2015) 145 [arXiv:1507.02549] [INSPIRE].

[90] M. Flechl, R. Klees, M. Krämer, M. Spira and M. Ubiali, *Improved cross-section predictions for heavy charged Higgs boson production at the LHC*, *Phys. Rev.* **D 91** (2015) 075015 [arXiv:1409.5615] [INSPIRE].

[91] S. Dittmaier, M. Krämer, M. Spira and M. Walser, *Charged-Higgs-boson production at the LHC: NLO supersymmetric QCD corrections*, *Phys. Rev.* **D 83** (2011) 055005 [arXiv:0906.2648] [INSPIRE].

[92] E.L. Berger, T. Han, J. Jiang and T. Plehn, *Associated production of a top quark and a charged Higgs boson*, *Phys. Rev.* **D 71** (2005) 115012 [hep-ph/0312286] [INSPIRE].

[93] A. Djouadi, J. Kalinowski and M. Spira, *HDECAY: a program for Higgs boson decays in the Standard Model and its supersymmetric extension*, *Comput. Phys. Commun.* **108** (1998) 56 [hep-ph/9704448] [INSPIRE].

[94] A.L. Read, *Presentation of search results: the $CL_s$ technique*, *J. Phys.* **G 28** (2002) 2693 [INSPIRE].

[95] ATLAS collaboration, *ATLAS computing acknowledgements*, ATL-GEN-PUB-2016-002, CERN, Geneva, Switzerland, (2016).

## The ATLAS collaboration

M. Aaboud[34d], G. Aad[99], B. Abbott[124], O. Abdinov[13,*], B. Abeloos[128], D.K. Abhayasinghe[91], S.H. Abidi[164], O.S. AbouZeid[39], N.L. Abraham[153], H. Abramowicz[158], H. Abreu[157], Y. Abulaiti[6], B.S. Acharya[64a,64b,n], S. Adachi[160], L. Adamczyk[81a], J. Adelman[119], M. Adersberger[112], A. Adiguzel[12c], T. Adye[141], A.A. Affolder[143], Y. Afik[157], C. Agheorghiesei[27c], J.A. Aguilar-Saavedra[136f,136a], F. Ahmadov[77,ad], G. Aielli[71a,71b], S. Akatsuka[83], T.P.A. Åkesson[94], E. Akilli[52], A.V. Akimov[108], G.L. Alberghi[23b,23a], J. Albert[173], P. Albicocco[49], M.J. Alconada Verzini[86], S. Alderweireldt[117], M. Aleksa[35], I.N. Aleksandrov[77], C. Alexa[27b], T. Alexopoulos[10], M. Alhroob[124], B. Ali[138], G. Alimonti[66a], J. Alison[36], S.P. Alkire[145], C. Allaire[128], B.M.M. Allbrooke[153], B.W. Allen[127], P.P. Allport[21], A. Aloisio[67a,67b], A. Alonso[39], F. Alonso[86], C. Alpigiani[145], A.A. Alshehri[55], M.I. Alstaty[99], B. Alvarez Gonzalez[35], D. Álvarez Piqueras[171], M.G. Alviggi[67a,67b], B.T. Amadio[18], Y. Amaral Coutinho[78b], L. Ambroz[131], C. Amelung[26], D. Amidei[103], S.P. Amor Dos Santos[136a,136c], S. Amoroso[44], C.S. Amrouche[52], C. Anastopoulos[146], L.S. Ancu[52], N. Andari[142], T. Andeen[11], C.F. Anders[59b], J.K. Anders[20], K.J. Anderson[36], A. Andreazza[66a,66b], V. Andrei[59a], C.R. Anelli[173], S. Angelidakis[37], I. Angelozzi[118], A. Angerami[38], A.V. Anisenkov[120b,120a], A. Annovi[69a], C. Antel[59a], M.T. Anthony[146], M. Antonelli[49], D.J.A. Antrim[168], F. Anulli[70a], M. Aoki[79], J.A. Aparisi Pozo[171], L. Aperio Bella[35], G. Arabidze[104], J.P. Araque[136a], V. Araujo Ferraz[78b], R. Araujo Pereira[78b], A.T.H. Arce[47], R.E. Ardell[91], F.A. Arduh[86], J-F. Arguin[107], S. Argyropoulos[75], A.J. Armbruster[35], L.J. Armitage[90], A Armstrong[168], O. Arnaez[164], H. Arnold[118], M. Arratia[31], O. Arslan[24], A. Artamonov[109,*], G. Artoni[131], S. Artz[97], S. Asai[160], N. Asbah[57], A. Ashkenazi[158], E.M. Asimakopoulou[169], L. Asquith[153], K. Assamagan[29], R. Astalos[28a], R.J. Atkin[32a], M. Atkinson[170], N.B. Atlay[148], K. Augsten[138], G. Avolio[35], R. Avramidou[58a], M.K. Ayoub[15a], G. Azuelos[107,aq], A.E. Baas[59a], M.J. Baca[21], H. Bachacou[142], K. Bachas[65a,65b], M. Backes[131], P. Bagnaia[70a,70b], M. Bahmani[82], H. Bahrasemani[149], A.J. Bailey[171], J.T. Baines[141], M. Bajic[39], C. Bakalis[10], O.K. Baker[180], P.J. Bakker[118], D. Bakshi Gupta[93], E.M. Baldin[120b,120a], P. Balek[177], F. Balli[142], W.K. Balunas[133], J. Balz[97], E. Banas[82], A. Bandyopadhyay[24], S. Banerjee[178,j], A.A.E. Bannoura[179], L. Barak[158], W.M. Barbe[37], E.L. Barberio[102], D. Barberis[53b,53a], M. Barbero[99], T. Barillari[113], M-S. Barisits[35], J. Barkeloo[127], T. Barklow[150], N. Barlow[31], R. Barnea[157], S.L. Barnes[58c], B.M. Barnett[141], R.M. Barnett[18], Z. Barnovska-Blenessy[58a], A. Baroncelli[72a], G. Barone[26], A.J. Barr[131], L. Barranco Navarro[171], F. Barreiro[96], J. Barreiro Guimarães da Costa[15a], R. Bartoldus[150], A.E. Barton[87], P. Bartos[28a], A. Basalaev[134], A. Bassalat[128], R.L. Bates[55], S.J. Batista[164], S. Batlamous[34e], J.R. Batley[31], M. Battaglia[143], M. Bauce[70a,70b], F. Bauer[142], K.T. Bauer[168], H.S. Bawa[150,l], J.B. Beacham[122], T. Beau[132], P.H. Beauchemin[167], P. Bechtle[24], H.C. Beck[51], H.P. Beck[20,p], K. Becker[50], M. Becker[97], C. Becot[44], A. Beddall[12d], A.J. Beddall[12a], V.A. Bednyakov[77], M. Bedognetti[118], C.P. Bee[152], T.A. Beermann[35], M. Begalli[78b], M. Begel[29], A. Behera[152], J.K. Behr[44], A.S. Bell[92], G. Bella[158], L. Bellagamba[23b], A. Bellerive[33], M. Bellomo[157], P. Bellos[9], K. Belotskiy[110], N.L. Belyaev[110], O. Benary[158,*], D. Benchekroun[34a], M. Bender[112], N. Benekos[10], Y. Benhammou[158], E. Benhar Noccioli[180], J. Benitez[75], D.P. Benjamin[47], M. Benoit[52], J.R. Bensinger[26], S. Bentvelsen[118], L. Beresford[131], M. Beretta[49], D. Berge[44], E. Bergeaas Kuutmann[169], N. Berger[5], L.J. Bergsten[26], J. Beringer[18], S. Berlendis[7], N.R. Bernard[100], G. Bernardi[132], C. Bernius[150], F.U. Bernlochner[24], T. Berry[91], P. Berta[97], C. Bertella[15a], G. Bertoli[43a,43b], I.A. Bertram[87], G.J. Besjes[39], O. Bessidskaia Bylund[179], M. Bessner[44], N. Besson[142], A. Bethani[98], S. Bethke[113], A. Betti[24], A.J. Bevan[90], J. Beyer[113], R.M.B. Bianchi[135], O. Biebel[112], D. Biedermann[19], R. Bielski[35], K. Bierwagen[97], N.V. Biesuz[69a,69b], M. Biglietti[72a], T.R.V. Billoud[107], M. Bindi[51], A. Bingul[12d], C. Bini[70a,70b],

S. Biondi[23b,23a], M. Birman[177], T. Bisanz[51], J.P. Biswal[158], C. Bittrich[46], D.M. Bjergaard[47],
J.E. Black[150], K.M. Black[25], T. Blazek[28a], I. Bloch[44], C. Blocker[26], A. Blue[55], U. Blumenschein[90],
Dr. Blunier[144a], G.J. Bobbink[118], V.S. Bobrovnikov[120b,120a], S.S. Bocchetta[94], A. Bocci[47],
D. Boerner[179], D. Bogavac[112], A.G. Bogdanchikov[120b,120a], C. Bohm[43a], V. Boisvert[91],
P. Bokan[169,w], T. Bold[81a], A.S. Boldyrev[111], A.E. Bolz[59b], M. Bomben[132], M. Bona[90],
J.S. Bonilla[127], M. Boonekamp[142], A. Borisov[140], G. Borissov[87], J. Bortfeldt[35], D. Bortoletto[131],
V. Bortolotto[71a,71b], D. Boscherini[23b], M. Bosman[14], J.D. Bossio Sola[30], K. Bouaouda[34a],
J. Boudreau[135], E.V. Bouhova-Thacker[87], D. Boumediene[37], C. Bourdarios[128], S.K. Boutle[55],
A. Boveia[122], J. Boyd[35], D. Boye[32b], I.R. Boyko[77], A.J. Bozson[91], J. Bracinik[21], N. Brahimi[99],
A. Brandt[8], G. Brandt[179], O. Brandt[59a], F. Braren[44], U. Bratzler[161], B. Brau[100], J.E. Brau[127],
W.D. Breaden Madden[55], K. Brendlinger[44], A.J. Brennan[102], L. Brenner[44], R. Brenner[169],
S. Bressler[177], B. Brickwedde[97], D.L. Briglin[21], D. Britton[55], D. Britzger[59b], I. Brock[24],
R. Brock[104], G. Brooijmans[38], T. Brooks[91], W.K. Brooks[144b], E. Brost[119], J.H Broughton[21],
P.A. Bruckman de Renstrom[82], D. Bruncko[28b], A. Bruni[23b], G. Bruni[23b], L.S. Bruni[118],
S. Bruno[71a,71b], B.H. Brunt[31], M. Bruschi[23b], N. Bruscino[135], P. Bryant[36], L. Bryngemark[44],
T. Buanes[17], Q. Buat[35], P. Buchholz[148], A.G. Buckley[55], I.A. Budagov[77], F. Buehrer[50],
M.K. Bugge[130], O. Bulekov[110], D. Bullock[8], T.J. Burch[119], S. Burdin[88], C.D. Burgard[118],
A.M. Burger[5], B. Burghgrave[119], K. Burka[82], S. Burke[141], I. Burmeister[45], J.T.P. Burr[131],
D. Büscher[50], V. Büscher[97], E. Buschmann[51], P. Bussey[55], J.M. Butler[25], C.M. Buttar[55],
J.M. Butterworth[92], P. Butti[35], W. Buttinger[35], A. Buzatu[155], A.R. Buzykaev[120b,120a],
G. Cabras[23b,23a], S. Cabrera Urbán[171], D. Caforio[138], H. Cai[170], V.M.M. Cairo[2], O. Cakir[4a],
N. Calace[52], P. Calafiura[18], A. Calandri[99], G. Calderini[132], P. Calfayan[63], G. Callea[40b,40a],
L.P. Caloba[78b], S. Calvente Lopez[96], D. Calvet[37], S. Calvet[37], T.P. Calvet[152], M. Calvetti[69a,69b],
R. Camacho Toro[132], S. Camarda[35], P. Camarri[71a,71b], D. Cameron[130], R. Caminal Armadans[100],
C. Camincher[35], S. Campana[35], M. Campanelli[92], A. Camplani[39], A. Campoverde[148],
V. Canale[67a,67b], M. Cano Bret[58c], J. Cantero[125], T. Cao[158], Y. Cao[170],
M.D.M. Capeans Garrido[35], I. Caprini[27b], M. Caprini[27b], M. Capua[40b,40a], R.M. Carbone[38],
R. Cardarelli[71a], F.C. Cardillo[146], I. Carli[139], T. Carli[35], G. Carlino[67a], B.T. Carlson[135],
L. Carminati[66a,66b], R.M.D. Carney[43a,43b], S. Caron[117], E. Carquin[144b], S. Carrá[66a,66b],
G.D. Carrillo-Montoya[35], D. Casadei[32b], M.P. Casado[14,f], A.F. Casha[164], D.W. Casper[168],
R. Castelijn[118], F.L. Castillo[171], V. Castillo Gimenez[171], N.F. Castro[136a,136e], A. Catinaccio[35],
J.R. Catmore[130], A. Cattai[35], J. Caudron[24], V. Cavaliere[29], E. Cavallaro[14], D. Cavalli[66a],
M. Cavalli-Sforza[14], V. Cavasinni[69a,69b], E. Celebi[12b], F. Ceradini[72a,72b], L. Cerda Alberich[171],
A.S. Cerqueira[78a], A. Cerri[153], L. Cerrito[71a,71b], F. Cerutti[18], A. Cervelli[23b,23a], S.A. Cetin[12b],
A. Chafaq[34a], D Chakraborty[119], S.K. Chan[57], W.S. Chan[118], Y.L. Chan[61a], J.D. Chapman[31],
B. Chargeishvili[156b], D.G. Charlton[21], C.C. Chau[33], C.A. Chavez Barajas[153], S. Che[122],
A. Chegwidden[104], S. Chekanov[6], S.V. Chekulaev[165a], G.A. Chelkov[77,ap], M.A. Chelstowska[35],
C. Chen[58a], C.H. Chen[76], H. Chen[29], J. Chen[58a], J. Chen[38], S. Chen[133], S.J. Chen[15c],
X. Chen[15b,ao], Y. Chen[80], Y-H. Chen[44], H.C. Cheng[103], H.J. Cheng[15d], A. Cheplakov[77],
E. Cheremushkina[140], R. Cherkaoui El Moursli[34e], E. Cheu[7], K. Cheung[62], L. Chevalier[142],
V. Chiarella[49], G. Chiarelli[69a], G. Chiodini[65a], A.S. Chisholm[35], A. Chitan[27b], I. Chiu[160],
Y.H. Chiu[173], M.V. Chizhov[77], K. Choi[63], A.R. Chomont[128], S. Chouridou[159], Y.S. Chow[118],
V. Christodoulou[92], M.C. Chu[61a], J. Chudoba[137], A.J. Chuinard[101], J.J. Chwastowski[82],
L. Chytka[126], D. Cinca[45], V. Cindro[89], I.A. Cioară[24], A. Ciocio[18], F. Cirotto[67a,67b],
Z.H. Citron[177], M. Citterio[66a], A. Clark[52], M.R. Clark[38], P.J. Clark[48], C. Clement[43a,43b],
Y. Coadou[99], M. Cobal[64a,64c], A. Coccaro[53b,53a], J. Cochran[76], H. Cohen[158], A.E.C. Coimbra[177],
L. Colasurdo[117], B. Cole[38], A.P. Colijn[118], J. Collot[56], P. Conde Muiño[136a,136b], E. Coniavitis[50],
S.H. Connell[32b], I.A. Connelly[98], S. Constantinescu[27b], F. Conventi[67a,ar], A.M. Cooper-Sarkar[131],

F. Cormier[172], K.J.R. Cormier[164], M. Corradi[70a,70b], E.E. Corrigan[94], F. Corriveau[101,ab],
A. Cortes-Gonzalez[35], M.J. Costa[171], D. Costanzo[146], G. Cottin[31], G. Cowan[91], B.E. Cox[98],
J. Crane[98], K. Cranmer[121], S.J. Crawley[55], R.A. Creager[133], G. Cree[33], S. Crépé-Renaudin[56],
F. Crescioli[132], M. Cristinziani[24], V. Croft[121], G. Crosetti[40b,40a], A. Cueto[96],
T. Cuhadar Donszelmann[146], A.R. Cukierman[150], J. Cúth[97], S. Czekierda[82], P. Czodrowski[35],
M.J. Da Cunha Sargedas De Sousa[58b,136b], C. Da Via[98], W. Dabrowski[81a], T. Dado[28a,w],
S. Dahbi[34e], T. Dai[103], F. Dallaire[107], C. Dallapiccola[100], M. Dam[39], G. D'amen[23b,23a],
J. Damp[97], J.R. Dandoy[133], M.F. Daneri[30], N.P. Dang[178,j], N.D Dann[98], M. Danninger[172],
V. Dao[35], G. Darbo[53b], S. Darmora[8], O. Dartsi[5], A. Dattagupta[127], T. Daubney[44], S. D'Auria[55],
W. Davey[24], C. David[44], T. Davidek[139], D.R. Davis[47], E. Dawe[102], I. Dawson[146], K. De[8],
R. De Asmundis[67a], A. De Benedetti[124], M. De Beurs[118], S. De Castro[23b,23a], S. De Cecco[70a,70b],
N. De Groot[117], P. de Jong[118], H. De la Torre[104], F. De Lorenzi[76], A. De Maria[51,r],
D. De Pedis[70a], A. De Salvo[70a], U. De Sanctis[71a,71b], M. De Santis[71a,71b], A. De Santo[153],
K. De Vasconcelos Corga[99], J.B. De Vivie De Regie[128], C. Debenedetti[143], D.V. Dedovich[77],
N. Dehghanian[3], M. Del Gaudio[40b,40a], J. Del Peso[96], Y. Delabat Diaz[44], D. Delgove[128],
F. Deliot[142], C.M. Delitzsch[7], M. Della Pietra[67a,67b], D. Della Volpe[52], A. Dell'Acqua[35],
L. Dell'Asta[25], M. Delmastro[5], C. Delporte[128], P.A. Delsart[56], D.A. DeMarco[164], S. Demers[180],
M. Demichev[77], S.P. Denisov[140], D. Denysiuk[118], L. D'Eramo[132], D. Derendarz[82],
J.E. Derkaoui[34d], F. Derue[132], P. Dervan[88], K. Desch[24], C. Deterre[44], K. Dette[164],
M.R. Devesa[30], P.O. Deviveiros[35], A. Dewhurst[141], S. Dhaliwal[26], F.A. Di Bello[52],
A. Di Ciaccio[71a,71b], L. Di Ciaccio[5], W.K. Di Clemente[133], C. Di Donato[67a,67b], A. Di Girolamo[35],
B. Di Micco[72a,72b], R. Di Nardo[100], K.F. Di Petrillo[57], R. Di Sipio[164], D. Di Valentino[33],
C. Diaconu[99], M. Diamond[164], F.A. Dias[39], T. Dias Do Vale[136a], M.A. Diaz[144a], J. Dickinson[18],
E.B. Diehl[103], J. Dietrich[19], S. Díez Cornell[44], A. Dimitrievska[18], J. Dingfelder[24], F. Dittus[35],
F. Djama[99], T. Djobava[156b], J.I. Djuvsland[59a], M.A.B. Do Vale[78c], M. Dobre[27b], D. Dodsworth[26],
C. Doglioni[94], J. Dolejsi[139], Z. Dolezal[139], M. Donadelli[78d], J. Donini[37], A. D'onofrio[90],
M. D'Onofrio[88], J. Dopke[141], A. Doria[67a], M.T. Dova[86], A.T. Doyle[55], E. Drechsler[51],
E. Dreyer[149], T. Dreyer[51], Y. Du[58b], J. Duarte-Campderros[158], F. Dubinin[108], M. Dubovsky[28a],
A. Dubreuil[52], E. Duchovni[177], G. Duckeck[112], A. Ducourthial[132], O.A. Ducu[107,v], D. Duda[113],
A. Dudarev[35], A.C. Dudder[97], E.M. Duffield[18], L. Duflot[128], M. Dührssen[35], C. Dülsen[179],
M. Dumancic[177], A.E. Dumitriu[27b,d], A.K. Duncan[55], M. Dunford[59a], A. Duperrin[99],
H. Duran Yildiz[4a], M. Düren[54], A. Durglishvili[156b], D. Duschinger[46], B. Dutta[44], D. Duvnjak[1],
M. Dyndal[44], S. Dysch[98], B.S. Dziedzic[82], C. Eckardt[44], K.M. Ecker[113], R.C. Edgar[103],
T. Eifert[35], G. Eigen[17], K. Einsweiler[18], T. Ekelof[169], M. El Kacimi[34c], R. El Kosseifi[99],
V. Ellajosyula[99], M. Ellert[169], F. Ellinghaus[179], A.A. Elliot[90], N. Ellis[35], J. Elmsheuser[29],
M. Elsing[35], D. Emeliyanov[141], Y. Enari[160], J.S. Ennis[175], M.B. Epland[47], J. Erdmann[45],
A. Ereditato[20], S. Errede[170], M. Escalier[128], C. Escobar[171], O. Estrada Pastor[171], A.I. Etienvre[142],
E. Etzion[158], H. Evans[63], A. Ezhilov[134], M. Ezzi[34e], F. Fabbri[55], L. Fabbri[23b,23a], V. Fabiani[117],
G. Facini[92], R.M. Faisca Rodrigues Pereira[136a], R.M. Fakhrutdinov[140], S. Falciano[70a], P.J. Falke[5],
S. Falke[5], J. Faltova[139], Y. Fang[15a], M. Fanti[66a,66b], A. Farbin[8], A. Farilla[72a], E.M. Farina[68a,68b],
T. Farooque[104], S. Farrell[18], S.M. Farrington[175], P. Farthouat[35], F. Fassi[34e], P. Fassnacht[35],
D. Fassouliotis[9], M. Faucci Giannelli[48], A. Favareto[53b,53a], W.J. Fawcett[31], L. Fayard[128],
O.L. Fedin[134,o], W. Fedorko[172], M. Feickert[41], S. Feigl[130], L. Feligioni[99], C. Feng[58b], E.J. Feng[35],
M. Feng[47], M.J. Fenton[55], A.B. Fenyuk[140], L. Feremenga[8], J. Ferrando[44], A. Ferrari[169],
P. Ferrari[118], R. Ferrari[68a], D.E. Ferreira de Lima[59b], A. Ferrer[171], D. Ferrere[52], C. Ferretti[103],
F. Fiedler[97], A. Filipčič[89], F. Filthaut[117], K.D. Finelli[25], M.C.N. Fiolhais[136a,136c,a], L. Fiorini[171],
C. Fischer[14], W.C. Fisher[104], N. Flaschel[44], I. Fleck[148], P. Fleischmann[103], R.R.M. Fletcher[133],
T. Flick[179], B.M. Flierl[112], L.M. Flores[133], L.R. Flores Castillo[61a], F.M. Follega[73a,73b],

N. Fomin[17], G.T. Forcolin[98], A. Formica[142], F.A. Förster[14], A.C. Forti[98], A.G. Foster[21],
D. Fournier[128], H. Fox[87], S. Fracchia[146], P. Francavilla[69a,69b], M. Franchini[23b,23a],
S. Franchino[59a], D. Francis[35], L. Franconi[130], M. Franklin[57], M. Frate[168], M. Fraternali[68a,68b],
D. Freeborn[92], S.M. Fressard-Batraneanu[35], B. Freund[107], W.S. Freund[78b], D.C. Frizzell[124],
D. Froidevaux[35], J.A. Frost[131], C. Fukunaga[161], E. Fullana Torregrosa[171], T. Fusayasu[114],
J. Fuster[171], O. Gabizon[157], A. Gabrielli[23b,23a], A. Gabrielli[18], G.P. Gach[81a], S. Gadatsch[52],
P. Gadow[113], G. Gagliardi[53b,53a], L.G. Gagnon[107], C. Galea[27b], B. Galhardo[136a,136c],
E.J. Gallas[131], B.J. Gallop[141], P. Gallus[138], G. Galster[39], R. Gamboa Goni[90], K.K. Gan[122],
S. Ganguly[177], J. Gao[58a], Y. Gao[88], Y.S. Gao[150,l], C. García[171], J.E. García Navarro[171],
J.A. García Pascual[15a], M. Garcia-Sciveres[18], R.W. Gardner[36], N. Garelli[150], V. Garonne[130],
K. Gasnikova[44], A. Gaudiello[53b,53a], G. Gaudio[68a], I.L. Gavrilenko[108], A. Gavrilyuk[109],
C. Gay[172], G. Gaycken[24], E.N. Gazis[10], C.N.P. Gee[141], J. Geisen[51], M. Geisen[97], M.P. Geisler[59a],
K. Gellerstedt[43a,43b], C. Gemme[53b], M.H. Genest[56], C. Geng[103], S. Gentile[70a,70b], S. George[91],
D. Gerbaudo[14], G. Gessner[45], S. Ghasemi[148], M. Ghasemi Bostanabad[173], M. Ghneimat[24],
B. Giacobbe[23b], S. Giagu[70a,70b], N. Giangiacomi[23b,23a], P. Giannetti[69a], A. Giannini[67a,67b],
S.M. Gibson[91], M. Gignac[143], D. Gillberg[33], G. Gilles[179], D.M. Gingrich[3,aq], M.P. Giordani[64a,64c],
F.M. Giorgi[23b], P.F. Giraud[142], P. Giromini[57], G. Giugliarelli[64a,64c], D. Giugni[66a], F. Giuli[131],
M. Giulini[59b], S. Gkaitatzis[159], I. Gkialas[9,i], E.L. Gkougkousis[14], P. Gkountoumis[10],
L.K. Gladilin[111], C. Glasman[96], J. Glatzer[14], P.C.F. Glaysher[44], A. Glazov[44],
M. Goblirsch-Kolb[26], J. Godlewski[82], S. Goldfarb[102], T. Golling[52], D. Golubkov[140],
A. Gomes[136a,136b,136d], R. Goncalves Gama[78a], R. Gonçalo[136a], G. Gonella[50], L. Gonella[21],
A. Gongadze[77], F. Gonnella[21], J.L. Gonski[57], S. González de la Hoz[171], S. Gonzalez-Sevilla[52],
L. Goossens[35], P.A. Gorbounov[109], H.A. Gordon[29], B. Gorini[35], E. Gorini[65a,65b], A. Gorišek[89],
A.T. Goshaw[47], C. Gössling[45], M.I. Gostkin[77], C.A. Gottardo[24], C.R. Goudet[128], D. Goujdami[34c],
A.G. Goussiou[145], N. Govender[32b,b], C. Goy[5], E. Gozani[157], I. Grabowska-Bold[81a],
P.O.J. Gradin[169], E.C. Graham[88], J. Gramling[168], E. Gramstad[130], S. Grancagnolo[19],
V. Gratchev[134], P.M. Gravila[27f], F.G. Gravili[65a,65b], C. Gray[55], H.M. Gray[18],
Z.D. Greenwood[93,ag], C. Grefe[24], K. Gregersen[94], I.M. Gregor[44], P. Grenier[150], K. Grevtsov[44],
N.A. Grieser[124], J. Griffiths[8], A.A. Grillo[143], K. Grimm[150], S. Grinstein[14,x], Ph. Gris[37],
J.-F. Grivaz[128], S. Groh[97], E. Gross[177], J. Grosse-Knetter[51], G.C. Grossi[93], Z.J. Grout[92],
C. Grud[103], A. Grummer[116], L. Guan[103], W. Guan[178], J. Guenther[35], A. Guerguichon[128],
F. Guescini[165a], D. Guest[168], R. Gugel[50], B. Gui[122], T. Guillemin[5], S. Guindon[35], U. Gul[55],
C. Gumpert[35], J. Guo[58c], W. Guo[103], Y. Guo[58a,q], Z. Guo[99], R. Gupta[41], S. Gurbuz[12c],
G. Gustavino[124], B.J. Gutelman[157], P. Gutierrez[124], C. Gutschow[92], C. Guyot[142], M.P. Guzik[81a],
C. Gwenlan[131], C.B. Gwilliam[88], A. Haas[121], C. Haber[18], H.K. Hadavand[8], N. Haddad[34e],
A. Hadef[58a], S. Hageböck[24], M. Hagihara[166], H. Hakobyan[181,*], M. Haleem[174], J. Haley[125],
G. Halladjian[104], G.D. Hallewell[99], K. Hamacher[179], P. Hamal[126], K. Hamano[173], A. Hamilton[32a],
G.N. Hamity[146], K. Han[58a,af], L. Han[58a], S. Han[15d], K. Hanagaki[79,t], M. Hance[143],
D.M. Handl[112], B. Haney[133], R. Hankache[132], P. Hanke[59a], E. Hansen[94], J.B. Hansen[39],
J.D. Hansen[39], M.C. Hansen[24], P.H. Hansen[39], K. Hara[166], A.S. Hard[178], T. Harenberg[179],
S. Harkusha[105], P.F. Harrison[175], N.M. Hartmann[112], Y. Hasegawa[147], A. Hasib[48], S. Hassani[142],
S. Haug[20], R. Hauser[104], L. Hauswald[46], L.B. Havener[38], M. Havranek[138], C.M. Hawkes[21],
R.J. Hawkings[35], D. Hayden[104], C. Hayes[152], C.P. Hays[131], J.M. Hays[90], H.S. Hayward[88],
S.J. Haywood[141], M.P. Heath[48], V. Hedberg[94], L. Heelan[8], S. Heer[24], K.K. Heidegger[50],
J. Heilman[33], S. Heim[44], T. Heim[18], B. Heinemann[44,al], J.J. Heinrich[112], L. Heinrich[121],
C. Heinz[54], J. Hejbal[137], L. Helary[35], A. Held[172], S. Hellesund[130], S. Hellman[43a,43b], C. Helsens[35],
R.C.W. Henderson[87], Y. Heng[178], S. Henkelmann[172], A.M. Henriques Correia[35], G.H. Herbert[19],
H. Herde[26], V. Herget[174], Y. Hernández Jiménez[32c], H. Herr[97], M.G. Herrmann[112], G. Herten[50],

JHEP09 (2018) 139

R. Hertenberger[112], L. Hervas[35], T.C. Herwig[133], G.G. Hesketh[92], N.P. Hessey[165a],
J.W. Hetherly[41], S. Higashino[79], E. Higón-Rodriguez[171], K. Hildebrand[36], E. Hill[173], J.C. Hill[31],
K.K. Hill[29], K.H. Hiller[44], S.J. Hillier[21], M. Hils[46], I. Hinchliffe[18], M. Hirose[129],
D. Hirschbuehl[179], B. Hiti[89], O. Hladik[137], D.R. Hlaluku[32c], X. Hoad[48], J. Hobbs[152], N. Hod[165a],
M.C. Hodgkinson[146], A. Hoecker[35], M.R. Hoeferkamp[116], F. Hoenig[112], D. Hohn[24], D. Hohov[128],
T.R. Holmes[36], M. Holzbock[112], M. Homann[45], S. Honda[166], T. Honda[79], T.M. Hong[135],
A. Hönle[113], B.H. Hooberman[170], W.H. Hopkins[127], Y. Horii[115], P. Horn[46], A.J. Horton[149],
L.A. Horyn[36], J-Y. Hostachy[56], A. Hostiuc[145], S. Hou[155], A. Hoummada[34a], J. Howarth[98],
J. Hoya[86], M. Hrabovsky[126], J. Hrdinka[35], I. Hristova[19], J. Hrivnac[128], A. Hrynevich[106],
T. Hryn'ova[5], P.J. Hsu[62], S.-C. Hsu[145], Q. Hu[29], S. Hu[58c], Y. Huang[15a], Z. Hubacek[138],
F. Hubaut[99], M. Huebner[24], F. Huegging[24], T.B. Huffman[131], E.W. Hughes[38], M. Huhtinen[35],
R.F.H. Hunter[33], P. Huo[152], A.M. Hupe[33], N. Huseynov[77,ad], J. Huston[104], J. Huth[57],
R. Hyneman[103], G. Iacobucci[52], G. Iakovidis[29], I. Ibragimov[148], L. Iconomidou-Fayard[128],
Z. Idrissi[34e], P. Iengo[35], R. Ignazzi[39], O. Igonkina[118,z], R. Iguchi[160], T. Iizawa[52], Y. Ikegami[79],
M. Ikeno[79], D. Iliadis[159], N. Ilic[150], F. Iltzsche[46], G. Introzzi[68a,68b], M. Iodice[72a], K. Iordanidou[38],
V. Ippolito[70a,70b], M.F. Isacson[169], N. Ishijima[129], M. Ishino[160], M. Ishitsuka[162], W. Islam[125],
C. Issever[131], S. Istin[12c,ak], F. Ito[166], J.M. Iturbe Ponce[61a], R. Iuppa[73a,73b], A. Ivina[177],
H. Iwasaki[79], J.M. Izen[42], V. Izzo[67a], P. Jacka[137], P. Jackson[1], R.M. Jacobs[24], V. Jain[2],
G. Jäkel[179], K.B. Jakobi[97], K. Jakobs[50], S. Jakobsen[74], T. Jakoubek[137], D.O. Jamin[125],
D.K. Jana[93], R. Jansky[52], J. Janssen[24], M. Janus[51], P.A. Janus[81a], G. Jarlskog[94], N. Javadov[77,ad],
T. Javůrek[35], M. Javurkova[50], F. Jeanneau[142], L. Jeanty[18], J. Jejelava[156a,ae], A. Jelinskas[175],
P. Jenni[50,c], J. Jeong[44], S. Jézéquel[5], H. Ji[178], J. Jia[152], H. Jiang[76], Y. Jiang[58a], Z. Jiang[150],
S. Jiggins[50], F.A. Jimenez Morales[37], J. Jimenez Pena[171], S. Jin[15c], A. Jinaru[27b], O. Jinnouchi[162],
H. Jivan[32c], P. Johansson[146], K.A. Johns[7], C.A. Johnson[63], W.J. Johnson[145], K. Jon-And[43a,43b],
R.W.L. Jones[87], S.D. Jones[153], S. Jones[7], T.J. Jones[88], J. Jongmanns[59a], P.M. Jorge[136a,136b],
J. Jovicevic[165a], X. Ju[18], J.J. Junggeburth[113], A. Juste Rozas[14,x], A. Kaczmarska[82], M. Kado[128],
H. Kagan[122], M. Kagan[150], T. Kaji[176], E. Kajomovitz[157], C.W. Kalderon[94], A. Kaluza[97],
S. Kama[41], A. Kamenshchikov[140], L. Kanjir[89], Y. Kano[160], V.A. Kantserov[110], J. Kanzaki[79],
B. Kaplan[121], L.S. Kaplan[178], D. Kar[32c], M.J. Kareem[165b], E. Karentzos[10], S.N. Karpov[77],
Z.M. Karpova[77], V. Kartvelishvili[87], A.N. Karyukhin[140], L. Kashif[178], R.D. Kass[122],
A. Kastanas[151], Y. Kataoka[160], C. Kato[58d,58c], J. Katzy[44], K. Kawade[80], K. Kawagoe[85],
T. Kawamoto[160], G. Kawamura[51], E.F. Kay[88], V.F. Kazanin[120b,120a], R. Keeler[173], R. Kehoe[41],
J.S. Keller[33], E. Kellermann[94], J.J. Kempster[21], J. Kendrick[21], O. Kepka[137], S. Kersten[179],
B.P. Kersevan[89], R.A. Keyes[101], M. Khader[170], F. Khalil-Zada[13], A. Khanov[125],
A.G. Kharlamov[120b,120a], T. Kharlamova[120b,120a], E.E. Khoda[172], A. Khodinov[163], T.J. Khoo[52],
E. Khramov[77], J. Khubua[156b], S. Kido[80], M. Kiehn[52], C.R. Kilby[91], Y.K. Kim[36],
N. Kimura[64a,64c], O.M. Kind[19], B.T. King[88], D. Kirchmeier[46], J. Kirk[141], A.E. Kiryunin[113],
T. Kishimoto[160], D. Kisielewska[81a], V. Kitali[44], O. Kivernyk[5], E. Kladiva[28b],
T. Klapdor-Kleingrothaus[50], M.H. Klein[103], M. Klein[88], U. Klein[88], K. Kleinknecht[97],
P. Klimek[119], A. Klimentov[29], R. Klingenberg[45,*], T. Klingl[24], T. Klioutchnikova[35],
F.F. Klitzner[112], P. Kluit[118], S. Kluth[113], E. Kneringer[74], E.B.F.G. Knoops[99], A. Knue[50],
A. Kobayashi[160], D. Kobayashi[85], T. Kobayashi[160], M. Kobel[46], M. Kocian[150], P. Kodys[139],
P.T. Koenig[24], T. Koffas[33], E. Koffeman[118], N.M. Köhler[113], T. Koi[150], M. Kolb[59b], I. Koletsou[5],
T. Kondo[79], N. Kondrashova[58c], K. Köneke[50], A.C. König[117], T. Kono[79], R. Konoplich[121,ah],
V. Konstantinides[92], N. Konstantinidis[92], B. Konya[94], R. Kopeliansky[63], S. Koperny[81a],
K. Korcyl[82], K. Kordas[159], G. Koren[158], A. Korn[92], I. Korolkov[14], E.V. Korolkova[146],
N. Korotkova[111], O. Kortner[113], S. Kortner[113], T. Kosek[139], V.V. Kostyukhin[24], A. Kotwal[47],
A. Koulouris[10], A. Kourkoumeli-Charalampidi[68a,68b], C. Kourkoumelis[9], E. Kourlitis[146],

V. Kouskoura[29], A.B. Kowalewska[82], R. Kowalewski[173], T.Z. Kowalski[81a], C. Kozakai[160],
W. Kozanecki[142], A.S. Kozhin[140], V.A. Kramarenko[111], G. Kramberger[89], D. Krasnopevtsev[58a],
M.W. Krasny[132], A. Krasznahorkay[35], D. Krauss[113], J.A. Kremer[81a], J. Kretzschmar[88],
P. Krieger[164], K. Krizka[18], K. Kroeninger[45], H. Kroha[113], J. Kroll[137], J. Kroll[133], J. Krstic[16],
U. Kruchonak[77], H. Krüger[24], N. Krumnack[76], M.C. Kruse[47], T. Kubota[102], S. Kuday[4b],
J.T. Kuechler[179], S. Kuehn[35], A. Kugel[59a], F. Kuger[174], T. Kuhl[44], V. Kukhtin[77], R. Kukla[99],
Y. Kulchitsky[105], S. Kuleshov[144b], Y.P. Kulinich[170], M. Kuna[56], T. Kunigo[83], A. Kupco[137],
T. Kupfer[45], O. Kuprash[158], H. Kurashige[80], L.L. Kurchaninov[165a], Y.A. Kurochkin[105],
M.G. Kurth[15d], E.S. Kuwertz[35], M. Kuze[162], J. Kvita[126], T. Kwan[101], A. La Rosa[113],
J.L. La Rosa Navarro[78d], L. La Rotonda[40b,40a], F. La Ruffa[40b,40a], C. Lacasta[171],
F. Lacava[70a,70b], J. Lacey[44], D.P.J. Lack[98], H. Lacker[19], D. Lacour[132], E. Ladygin[77], R. Lafaye[5],
B. Laforge[132], T. Lagouri[32c], S. Lai[51], S. Lammers[63], W. Lampl[7], E. Lançon[29], U. Landgraf[50],
M.P.J. Landon[90], M.C. Lanfermann[52], V.S. Lang[44], J.C. Lange[14], R.J. Langenberg[35],
A.J. Lankford[168], F. Lanni[29], K. Lantzsch[24], A. Lanza[68a], A. Lapertosa[53b,53a], S. Laplace[132],
J.F. Laporte[142], T. Lari[66a], F. Lasagni Manghi[23b,23a], M. Lassnig[35], T.S. Lau[61a], A. Laudrain[128],
M. Lavorgna[67a,67b], A.T. Law[143], P. Laycock[88], M. Lazzaroni[66a,66b], B. Le[102], O. Le Dortz[132],
E. Le Guirriec[99], E.P. Le Quilleuc[142], M. LeBlanc[7], T. LeCompte[6], F. Ledroit-Guillon[56],
C.A. Lee[29], G.R. Lee[144a], L. Lee[57], S.C. Lee[155], B. Lefebvre[101], M. Lefebvre[173], F. Legger[112],
C. Leggett[18], K. Lehmann[149], N. Lehmann[179], G. Lehmann Miotto[35], W.A. Leight[44],
A. Leisos[159,u], M.A.L. Leite[78d], R. Leitner[139], D. Lellouch[177], B. Lemmer[51], K.J.C. Leney[92],
T. Lenz[24], B. Lenzi[35], R. Leone[7], S. Leone[69a], C. Leonidopoulos[48], G. Lerner[153], C. Leroy[107],
R. Les[164], A.A.J. Lesage[142], C.G. Lester[31], M. Levchenko[134], J. Levêque[5], D. Levin[103],
L.J. Levinson[177], D. Lewis[90], B. Li[103], C-Q. Li[58a], H. Li[58b], L. Li[58c], Q. Li[15d], Q.Y. Li[58a],
S. Li[58d,58c], X. Li[58c], Y. Li[148], Z. Liang[15a], B. Liberti[71a], A. Liblong[164], K. Lie[61c], S. Liem[118],
A. Limosani[154], C.Y. Lin[31], K. Lin[104], T.H. Lin[97], R.A. Linck[63], J.H. Lindon[21],
B.E. Lindquist[152], A.L. Lionti[52], E. Lipeles[133], A. Lipniacka[17], M. Lisovyi[59b], T.M. Liss[170,an],
A. Lister[172], A.M. Litke[143], J.D. Little[8], B. Liu[76], B.L Liu[6], H.B. Liu[29], H. Liu[103], J.B. Liu[58a],
J.K.K. Liu[131], K. Liu[132], M. Liu[58a], P. Liu[18], Y. Liu[15a], Y.L. Liu[58a], Y.W. Liu[58a],
M. Livan[68a,68b], A. Lleres[56], J. Llorente Merino[15a], S.L. Lloyd[90], C.Y. Lo[61b], F. Lo Sterzo[41],
E.M. Lobodzinska[44], P. Loch[7], A. Loesle[50], T. Lohse[19], K. Lohwasser[146], M. Lokajicek[137],
B.A. Long[25], J.D. Long[170], R.E. Long[87], L. Longo[65a,65b], K.A. Looper[122], J.A. Lopez[144b],
I. Lopez Paz[14], A. Lopez Solis[146], J. Lorenz[112], N. Lorenzo Martinez[5], M. Losada[22], P.J. Lösel[112],
X. Lou[44], X. Lou[15a], A. Lounis[128], J. Love[6], P.A. Love[87], J.J. Lozano Bahilo[171], H. Lu[61a],
M. Lu[58a], N. Lu[103], Y.J. Lu[62], H.J. Lubatti[145], C. Luci[70a,70b], A. Lucotte[56], C. Luedtke[50],
F. Luehring[63], I. Luise[132], L. Luminari[70a], B. Lund-Jensen[151], M.S. Lutz[100], P.M. Luzi[132],
D. Lynn[29], R. Lysak[137], E. Lytken[94], F. Lyu[15a], V. Lyubushkin[77], H. Ma[29], L.L. Ma[58b],
Y. Ma[58b], G. Maccarrone[49], A. Macchiolo[113], C.M. Macdonald[146], J. Machado Miguens[133,136b],
D. Madaffari[171], R. Madar[37], W.F. Mader[46], A. Madsen[44], N. Madysa[46], J. Maeda[80],
K. Maekawa[160], S. Maeland[17], T. Maeno[29], A.S. Maevskiy[111], V. Magerl[50], C. Maidantchik[78b],
T. Maier[112], A. Maio[136a,136b,136d], O. Majersky[28a], S. Majewski[127], Y. Makida[79], N. Makovec[128],
B. Malaescu[132], Pa. Malecki[82], V.P. Maleev[134], F. Malek[56], U. Mallik[75], D. Malon[6], C. Malone[31],
S. Maltezos[10], S. Malyukov[35], J. Mamuzic[171], G. Mancini[49], I. Mandić[89], J. Maneira[136a],
L. Manhaes de Andrade Filho[78a], J. Manjarres Ramos[46], K.H. Mankinen[94], A. Mann[112],
A. Manousos[74], B. Mansoulie[142], J.D. Mansour[15a], M. Mantoani[51], S. Manzoni[66a,66b],
G. Marceca[30], L. March[52], L. Marchese[131], G. Marchiori[132], M. Marcisovsky[137],
C.A. Marin Tobon[35], M. Marjanovic[37], D.E. Marley[103], F. Marroquim[78b], Z. Marshall[18],
M.U.F Martensson[169], S. Marti-Garcia[171], C.B. Martin[122], T.A. Martin[175], V.J. Martin[48],
B. Martin dit Latour[17], M. Martinez[14,x], V.I. Martinez Outschoorn[100], S. Martin-Haugh[141],

V.S. Martoiu[27b], A.C. Martyniuk[92], A. Marzin[35], L. Masetti[97], T. Mashimo[160],
R. Mashinistov[108], J. Masik[98], A.L. Maslennikov[120b,120a], L.H. Mason[102], L. Massa[71a,71b],
P. Massarotti[67a,67b], P. Mastrandrea[5], A. Mastroberardino[40b,40a], T. Masubuchi[160], P. Mättig[179],
J. Maurer[27b], B. Maček[89], S.J. Maxfield[88], D.A. Maximov[120b,120a], R. Mazini[155], I. Maznas[159],
S.M. Mazza[143], N.C. Mc Fadden[116], G. Mc Goldrick[164], S.P. Mc Kee[103], A. McCarn[103],
T.G. McCarthy[113], L.I. McClymont[92], E.F. McDonald[102], J.A. Mcfayden[35], G. Mchedlidze[51],
M.A. McKay[41], K.D. McLean[173], S.J. McMahon[141], P.C. McNamara[102], C.J. McNicol[175],
R.A. McPherson[173,ab], J.E. Mdhluli[32c], Z.A. Meadows[100], S. Meehan[145], T. Megy[50],
S. Mehlhase[112], A. Mehta[88], T. Meideck[56], B. Meirose[42], D. Melini[171,g], B.R. Mellado Garcia[32c],
J.D. Mellenthin[51], M. Melo[28a], F. Meloni[44], A. Melzer[24], S.B. Menary[98],
E.D. Mendes Gouveia[136a], L. Meng[88], X.T. Meng[103], A. Mengarelli[23b,23a], S. Menke[113],
E. Meoni[40b,40a], S. Mergelmeyer[19], C. Merlassino[20], P. Mermod[52], L. Merola[67a,67b], C. Meroni[66a],
F.S. Merritt[36], A. Messina[70a,70b], J. Metcalfe[6], A.S. Mete[168], C. Meyer[133], J. Meyer[157],
J-P. Meyer[142], H. Meyer Zu Theenhausen[59a], F. Miano[153], R.P. Middleton[141], L. Mijović[48],
G. Mikenberg[177], M. Mikestikova[137], M. Mikuž[89], M. Milesi[102], A. Milic[164], D.A. Millar[90],
D.W. Miller[36], A. Milov[177], D.A. Milstead[43a,43b], A.A. Minaenko[140], M. Miñano Moya[171],
I.A. Minashvili[156b], A.I. Mincer[121], B. Mindur[81a], M. Mineev[77], Y. Minegishi[160], Y. Ming[178],
L.M. Mir[14], A. Mirto[65a,65b], K.P. Mistry[133], T. Mitani[176], J. Mitrevski[112], V.A. Mitsou[171],
A. Miucci[20], P.S. Miyagawa[146], A. Mizukami[79], J.U. Mjörnmark[94], T. Mkrtchyan[181],
M. Mlynarikova[139], T. Moa[43a,43b], K. Mochizuki[107], P. Mogg[50], S. Mohapatra[38],
S. Molander[43a,43b], R. Moles-Valls[24], M.C. Mondragon[104], K. Mönig[44], J. Monk[39], E. Monnier[99],
A. Montalbano[149], J. Montejo Berlingen[35], F. Monticelli[86], S. Monzani[66a], N. Morange[128],
D. Moreno[22], M. Moreno Llácer[35], P. Morettini[53b], M. Morgenstern[118], S. Morgenstern[46],
D. Mori[149], M. Morii[57], M. Morinaga[176], V. Morisbak[130], A.K. Morley[35], G. Mornacchi[35],
A.P. Morris[92], J.D. Morris[90], L. Morvaj[152], P. Moschovakos[10], M. Mosidze[156b], H.J. Moss[146],
J. Moss[150,m], K. Motohashi[162], R. Mount[150], E. Mountricha[35], E.J.W. Moyse[100], S. Muanza[99],
F. Mueller[113], J. Mueller[135], R.S.P. Mueller[112], D. Muenstermann[87], G.A. Mullier[20],
F.J. Munoz Sanchez[98], P. Murin[28b], W.J. Murray[175,141], A. Murrone[66a,66b], M. Muškinja[89],
C. Mwewa[32a], A.G. Myagkov[140,ai], J. Myers[127], M. Myska[138], B.P. Nachman[18], O. Nackenhorst[45],
K. Nagai[131], K. Nagano[79], Y. Nagasaka[60], M. Nagel[50], E. Nagy[99], A.M. Nairz[35], Y. Nakahama[115],
K. Nakamura[79], T. Nakamura[160], I. Nakano[123], H. Nanjo[129], F. Napolitano[59a],
R.F. Naranjo Garcia[44], R. Narayan[11], D.I. Narrias Villar[59a], I. Naryshkin[134], T. Naumann[44],
G. Navarro[22], R. Nayyar[7], H.A. Neal[103], P.Y. Nechaeva[108], T.J. Neep[142], A. Negri[68a,68b],
M. Negrini[23b], S. Nektarijevic[117], C. Nellist[51], M.E. Nelson[131], S. Nemecek[137], P. Nemethy[121],
M. Nessi[35,e], M.S. Neubauer[170], M. Neumann[179], P.R. Newman[21], T.Y. Ng[61c], Y.S. Ng[19],
H.D.N. Nguyen[99], T. Nguyen Manh[107], E. Nibigira[37], R.B. Nickerson[131], R. Nicolaidou[142],
J. Nielsen[143], N. Nikiforou[11], V. Nikolaenko[140,ai], I. Nikolic-Audit[132], K. Nikolopoulos[21],
P. Nilsson[29], Y. Ninomiya[79], A. Nisati[70a], N. Nishu[58c], R. Nisius[113], I. Nitsche[45], T. Nitta[176],
T. Nobe[160], Y. Noguchi[83], M. Nomachi[129], I. Nomidis[132], M.A. Nomura[29], T. Nooney[90],
M. Nordberg[35], N. Norjoharuddeen[131], T. Novak[89], O. Novgorodova[46], R. Novotny[138],
L. Nozka[126], K. Ntekas[168], E. Nurse[92], F. Nuti[102], F.G. Oakham[33,aq], H. Oberlack[113],
T. Obermann[24], J. Ocariz[132], A. Ochi[80], I. Ochoa[38], J.P. Ochoa-Ricoux[144a], K. O'Connor[26],
S. Oda[85], S. Odaka[79], S. Oerdek[51], A. Oh[98], S.H. Oh[47], C.C. Ohm[151], H. Oide[53b,53a],
M.L. Ojeda[164], H. Okawa[166], Y. Okazaki[83], Y. Okumura[160], T. Okuyama[79], A. Olariu[27b],
L.F. Oleiro Seabra[136a], S.A. Olivares Pino[144a], D. Oliveira Damazio[29], J.L. Oliver[1],
M.J.R. Olsson[36], A. Olszewski[82], J. Olszowska[82], D.C. O'Neil[149], A. Onofre[136a,136e], K. Onogi[115],
P.U.E. Onyisi[11], H. Oppen[130], M.J. Oreglia[36], Y. Oren[158], D. Orestano[72a,72b], E.C. Orgill[98],
N. Orlando[61b], A.A. O'Rourke[44], R.S. Orr[164], B. Osculati[53b,53a,*], V. O'Shea[55], R. Ospanov[58a],

G. Otero y Garzon[30], H. Otono[85], M. Ouchrif[34d], F. Ould-Saada[130], A. Ouraou[142], Q. Ouyang[15a],
M. Owen[55], R.E. Owen[21], V.E. Ozcan[12c], N. Ozturk[8], J. Pacalt[126], H.A. Pacey[31], K. Pachal[149],
A. Pacheco Pages[14], L. Pacheco Rodriguez[142], C. Padilla Aranda[14], S. Pagan Griso[18],
M. Paganini[180], G. Palacino[63], S. Palazzo[40b,40a], S. Palestini[35], M. Palka[81b], D. Pallin[37],
I. Panagoulias[10], C.E. Pandini[35], J.G. Panduro Vazquez[91], P. Pani[35], G. Panizzo[64a,64c],
L. Paolozzi[52], T.D. Papadopoulou[10], K. Papageorgiou[9,i], A. Paramonov[6],
D. Paredes Hernandez[61b], S.R. Paredes Saenz[131], B. Parida[58c], A.J. Parker[87], K.A. Parker[44],
M.A. Parker[31], F. Parodi[53b,53a], J.A. Parsons[38], U. Parzefall[50], V.R. Pascuzzi[164],
J.M.P. Pasner[143], E. Pasqualucci[70a], S. Passaggio[53b], F. Pastore[91], P. Pasuwan[43a,43b],
S. Pataraia[97], J.R. Pater[98], A. Pathak[178,j], T. Pauly[35], B. Pearson[113], M. Pedersen[130],
L. Pedraza Diaz[117], R. Pedro[136a,136b], S.V. Peleganchuk[120b,120a], O. Penc[137], C. Peng[15d],
H. Peng[58a], B.S. Peralva[78a], M.M. Perego[142], A.P. Pereira Peixoto[136a], D.V. Perepelitsa[29],
F. Peri[19], L. Perini[66a,66b], H. Pernegger[35], S. Perrella[67a,67b], V.D. Peshekhonov[77,*], K. Peters[44],
R.F.Y. Peters[98], B.A. Petersen[35], T.C. Petersen[39], E. Petit[56], A. Petridis[1], C. Petridou[159],
P. Petroff[128], M. Petrov[131], F. Petrucci[72a,72b], M. Pettee[180], N.E. Pettersson[100], A. Peyaud[142],
R. Pezoa[144b], T. Pham[102], F.H. Phillips[104], P.W. Phillips[141], G. Piacquadio[152], E. Pianori[18],
A. Picazio[100], M.A. Pickering[131], R.H. Pickles[98], R. Piegaia[30], J.E. Pilcher[36], A.D. Pilkington[98],
M. Pinamonti[71a,71b], J.L. Pinfold[3], M. Pitt[177], M-A. Pleier[29], V. Pleskot[139], E. Plotnikova[77],
D. Pluth[76], P. Podberezko[120b,120a], R. Poettgen[94], R. Poggi[52], L. Poggioli[128], I. Pogrebnyak[104],
D. Pohl[24], I. Pokharel[51], G. Polesello[68a], A. Poley[18], A. Policicchio[70a,70b], R. Polifka[35],
A. Polini[23b], C.S. Pollard[44], V. Polychronakos[29], D. Ponomarenko[110], L. Pontecorvo[70a],
G.A. Popeneciu[27d], D.M. Portillo Quintero[132], S. Pospisil[138], K. Potamianos[44], I.N. Potrap[77],
C.J. Potter[31], H. Potti[11], T. Poulsen[94], J. Poveda[35], T.D. Powell[146], M.E. Pozo Astigarraga[35],
P. Pralavorio[99], S. Prell[76], D. Price[98], M. Primavera[65a], S. Prince[101], N. Proklova[110],
K. Prokofiev[61c], F. Prokoshin[144b], S. Protopopescu[29], J. Proudfoot[6], M. Przybycien[81a],
A. Puri[170], P. Puzo[128], J. Qian[103], Y. Qin[98], A. Quadt[51], M. Queitsch-Maitland[44], A. Qureshi[1],
P. Rados[102], F. Ragusa[66a,66b], G. Rahal[95], J.A. Raine[52], S. Rajagopalan[29], A. Ramirez Morales[90],
T. Rashid[128], S. Raspopov[5], M.G. Ratti[66a,66b], D.M. Rauch[44], F. Rauscher[112], S. Rave[97],
B. Ravina[146], I. Ravinovich[177], J.H. Rawling[98], M. Raymond[35], A.L. Read[130], N.P. Readioff[56],
M. Reale[65a,65b], D.M. Rebuzzi[68a,68b], A. Redelbach[174], G. Redlinger[29], R. Reece[143], R.G. Reed[32c],
K. Reeves[42], L. Rehnisch[19], J. Reichert[133], A. Reiss[97], C. Rembser[35], H. Ren[15d], M. Rescigno[70a],
S. Resconi[66a], E.D. Resseguie[133], S. Rettie[172], E. Reynolds[21], O.L. Rezanova[120b,120a],
P. Reznicek[139], E. Ricci[73a,73b], R. Richter[113], S. Richter[92], E. Richter-Was[81b], O. Ricken[24],
M. Ridel[132], P. Rieck[113], C.J. Riegel[179], O. Rifki[44], M. Rijssenbeek[152], A. Rimoldi[68a,68b],
M. Rimoldi[20], L. Rinaldi[23b], G. Ripellino[151], B. Ristić[87], E. Ritsch[35], I. Riu[14],
J.C. Rivera Vergara[144a], F. Rizatdinova[125], E. Rizvi[90], C. Rizzi[14], R.T. Roberts[98],
S.H. Robertson[101,ab], D. Robinson[31], J.E.M. Robinson[44], A. Robson[55], E. Rocco[97],
C. Roda[69a,69b], Y. Rodina[99], S. Rodriguez Bosca[171], A. Rodriguez Perez[14],
D. Rodriguez Rodriguez[171], A.M. Rodríguez Vera[165b], S. Roe[35], C.S. Rogan[57], O. Røhne[130],
R. Röhrig[113], C.P.A. Roland[63], J. Roloff[57], A. Romaniouk[110], M. Romano[23b,23a], N. Rompotis[88],
M. Ronzani[121], L. Roos[132], S. Rosati[70a], K. Rosbach[50], P. Rose[143], N-A. Rosien[51], E. Rossi[44],
E. Rossi[67a,67b], L.P. Rossi[53b], L. Rossini[66a,66b], J.H.N. Rosten[31], R. Rosten[14], M. Rotaru[27b],
J. Rothberg[145], D. Rousseau[128], D. Roy[32c], A. Rozanov[99], Y. Rozen[157], X. Ruan[32c], F. Rubbo[150],
F. Rühr[50], A. Ruiz-Martinez[171], Z. Rurikova[50], N.A. Rusakovich[77], H.L. Russell[101],
J.P. Rutherfoord[7], E.M. Rüttinger[44,k], Y.F. Ryabov[134], M. Rybar[170], G. Rybkin[128], S. Ryu[6],
A. Ryzhov[140], G.F. Rzehorz[51], P. Sabatini[51], G. Sabato[118], S. Sacerdoti[128],
H.F-W. Sadrozinski[143], R. Sadykov[77], F. Safai Tehrani[70a], P. Saha[119], M. Sahinsoy[59a], A. Sahu[179],
M. Saimpert[44], M. Saito[160], T. Saito[160], H. Sakamoto[160], A. Sakharov[121,ah], D. Salamani[52],

G. Salamanna[72a,72b], J.E. Salazar Loyola[144b], D. Salek[118], P.H. Sales De Bruin[169], D. Salihagic[113],
A. Salnikov[150], J. Salt[171], D. Salvatore[40b,40a], F. Salvatore[153], A. Salvucci[61a,61b,61c],
A. Salzburger[35], J. Samarati[35], D. Sammel[50], D. Sampsonidis[159], D. Sampsonidou[159],
J. Sánchez[171], A. Sanchez Pineda[64a,64c], H. Sandaker[130], C.O. Sander[44], M. Sandhoff[179],
C. Sandoval[22], D.P.C. Sankey[141], M. Sannino[53b,53a], Y. Sano[115], A. Sansoni[49], C. Santoni[37],
H. Santos[136a], I. Santoyo Castillo[153], A. Santra[171], A. Sapronov[77], J.G. Saraiva[136a,136d],
O. Sasaki[79], K. Sato[166], E. Sauvan[5], P. Savard[164,aq], N. Savic[113], R. Sawada[160], C. Sawyer[141],
L. Sawyer[93,ag], C. Sbarra[23b], A. Sbrizzi[23b,23a], T. Scanlon[92], J. Schaarschmidt[145], P. Schacht[113],
B.M. Schachtner[112], D. Schaefer[36], L. Schaefer[133], J. Schaeffer[97], S. Schaepe[35], U. Schäfer[97],
A.C. Schaffer[128], D. Schaile[112], R.D. Schamberger[152], N. Scharmberg[98], V.A. Schegelsky[134],
D. Scheirich[139], F. Schenck[19], M. Schernau[168], C. Schiavi[53b,53a], S. Schier[143], L.K. Schildgen[24],
Z.M. Schillaci[26], E.J. Schioppa[35], M. Schioppa[40b,40a], K.E. Schleicher[50], S. Schlenker[35],
K.R. Schmidt-Sommerfeld[113], K. Schmieden[35], C. Schmitt[97], S. Schmitt[44], S. Schmitz[97],
J.C. Schmoeckel[44], U. Schnoor[50], L. Schoeffel[142], A. Schoening[59b], E. Schopf[24], M. Schott[97],
J.F.P. Schouwenberg[117], J. Schovancova[35], S. Schramm[52], A. Schulte[97], H-C. Schultz-Coulon[59a],
M. Schumacher[50], B.A. Schumm[143], Ph. Schune[142], A. Schwartzman[150], T.A. Schwarz[103],
H. Schweiger[98], Ph. Schwemling[142], R. Schwienhorst[104], A. Sciandra[24], G. Sciolla[26],
M. Scornajenghi[40b,40a], F. Scuri[69a], F. Scutti[102], L.M. Scyboz[113], J. Searcy[103],
C.D. Sebastiani[70a,70b], P. Seema[24], S.C. Seidel[116], A. Seiden[143], T. Seiss[36], J.M. Seixas[78b],
G. Sekhniaidze[67a], K. Sekhon[103], S.J. Sekula[41], N. Semprini-Cesari[23b,23a], S. Sen[47], S. Senkin[37],
C. Serfon[130], L. Serin[128], L. Serkin[64a,64b], M. Sessa[72a,72b], H. Severini[124], F. Sforza[167],
A. Sfyrla[52], E. Shabalina[51], J.D. Shahinian[143], N.W. Shaikh[43a,43b], L.Y. Shan[15a], R. Shang[170],
J.T. Shank[25], M. Shapiro[18], A.S. Sharma[1], A. Sharma[131], P.B. Shatalov[109], K. Shaw[153],
S.M. Shaw[98], A. Shcherbakova[134], Y. Shen[124], N. Sherafati[33], A.D. Sherman[25], P. Sherwood[92],
L. Shi[155,am], S. Shimizu[79], C.O. Shimmin[180], M. Shimojima[114], I.P.J. Shipsey[131], S. Shirabe[85],
M. Shiyakova[77], J. Shlomi[177], A. Shmeleva[108], D. Shoaleh Saadi[107], M.J. Shochet[36], S. Shojaii[102],
D.R. Shope[124], S. Shrestha[122], E. Shulga[110], P. Sicho[137], A.M. Sickles[170], P.E. Sidebo[151],
E. Sideras Haddad[32c], O. Sidiropoulou[35], A. Sidoti[23b,23a], F. Siegert[46], Dj. Sijacki[16], J. Silva[136a],
M. Silva Jr.[178], M.V. Silva Oliveira[78a], S.B. Silverstein[43a], L. Simic[77], S. Simion[128], E. Simioni[97],
M. Simon[97], R. Simoniello[97], P. Sinervo[164], N.B. Sinev[127], M. Sioli[23b,23a], G. Siragusa[174],
I. Siral[103], S.Yu. Sivoklokov[111], J. Sjölin[43a,43b], P. Skubic[124], M. Slater[21], T. Slavicek[138],
M. Slawinska[82], K. Sliwa[167], R. Slovak[139], V. Smakhtin[177], B.H. Smart[5], J. Smiesko[28a],
N. Smirnov[110], S.Yu. Smirnov[110], Y. Smirnov[110], L.N. Smirnova[111], O. Smirnova[94], J.W. Smith[51],
M.N.K. Smith[38], M. Smizanska[87], K. Smolek[138], A. Smykiewicz[82], A.A. Snesarev[108],
I.M. Snyder[127], S. Snyder[29], R. Sobie[173,ab], A.M. Soffa[168], A. Soffer[158], A. Søgaard[48],
D.A. Soh[155], G. Sokhrannyi[89], C.A. Solans Sanchez[35], M. Solar[138], E.Yu. Soldatov[110],
U. Soldevila[171], A.A. Solodkov[140], A. Soloshenko[77], O.V. Solovyanov[140], V. Solovyev[134],
P. Sommer[146], H. Son[167], W. Song[141], W.Y. Song[165b], A. Sopczak[138], F. Sopkova[28b], D. Sosa[59b],
C.L. Sotiropoulou[69a,69b], S. Sottocornola[68a,68b], R. Soualah[64a,64c,h], A.M. Soukharev[120b,120a],
D. South[44], B.C. Sowden[91], S. Spagnolo[65a,65b], M. Spalla[113], M. Spangenberg[175], F. Spanò[91],
D. Sperlich[19], F. Spettel[113], T.M. Spieker[59a], R. Spighi[23b], G. Spigo[35], L.A. Spiller[102],
D.P. Spiteri[55], M. Spousta[139], A. Stabile[66a,66b], R. Stamen[59a], S. Stamm[19], E. Stanecka[82],
R.W. Stanek[6], C. Stanescu[72a], B. Stanislaus[131], M.M. Stanitzki[44], B.S. Stapf[118], S. Stapnes[130],
E.A. Starchenko[140], G.H. Stark[36], J. Stark[56], S.H Stark[39], P. Staroba[137], P. Starovoitov[59a],
S. Stärz[35], R. Staszewski[82], M. Stegler[44], P. Steinberg[29], B. Stelzer[149], H.J. Stelzer[35],
O. Stelzer-Chilton[165a], H. Stenzel[54], T.J. Stevenson[90], G.A. Stewart[55], M.C. Stockton[127],
G. Stoicea[27b], P. Stolte[51], S. Stonjek[113], A. Straessner[46], J. Strandberg[151], S. Strandberg[43a,43b],
M. Strauss[124], P. Strizenec[28b], R. Ströhmer[174], D.M. Strom[127], R. Stroynowski[41], A. Strubig[48],

S.A. Stucci[29], B. Stugu[17], J. Stupak[124], N.A. Styles[44], D. Su[150], J. Su[135], S. Suchek[59a],
Y. Sugaya[129], M. Suk[138], V.V. Sulin[108], D.M.S. Sultan[52], S. Sultansoy[4c], T. Sumida[83], S. Sun[103],
X. Sun[3], K. Suruliz[153], C.J.E. Suster[154], M.R. Sutton[153], S. Suzuki[79], M. Svatos[137],
M. Swiatlowski[36], S.P. Swift[2], A. Sydorenko[97], I. Sykora[28a], T. Sykora[139], D. Ta[97],
K. Tackmann[44,y], J. Taenzer[158], A. Taffard[168], R. Tafirout[165a], E. Tahirovic[90], N. Taiblum[158],
H. Takai[29], R. Takashima[84], E.H. Takasugi[113], K. Takeda[80], T. Takeshita[147], Y. Takubo[79],
M. Talby[99], A.A. Talyshev[120b,120a], J. Tanaka[160], M. Tanaka[162], R. Tanaka[128],
B.B. Tannenwald[122], S. Tapia Araya[144b], S. Tapprogge[97], A. Tarek Abouelfadl Mohamed[132],
S. Tarem[157], G. Tarna[27b,d], G.F. Tartarelli[66a], P. Tas[139], M. Tasevsky[137], T. Tashiro[83],
E. Tassi[40b,40a], A. Tavares Delgado[136a,136b], Y. Tayalati[34e], A.C. Taylor[116], A.J. Taylor[48],
G.N. Taylor[102], P.T.E. Taylor[102], W. Taylor[165b], A.S. Tee[87], P. Teixeira-Dias[91], H. Ten Kate[35],
P.K. Teng[155], J.J. Teoh[118], F. Tepel[179], S. Terada[79], K. Terashi[160], J. Terron[96], S. Terzo[14],
M. Testa[49], R.J. Teuscher[164,ab], S.J. Thais[180], T. Theveneaux-Pelzer[44], F. Thiele[39],
D.W. Thomas[91], J.P. Thomas[21], A.S. Thompson[55], P.D. Thompson[21], L.A. Thomsen[180],
E. Thomson[133], Y. Tian[38], R.E. Ticse Torres[51], V.O. Tikhomirov[108,aj], Yu.A. Tikhonov[120b,120a],
S. Timoshenko[110], P. Tipton[180], S. Tisserant[99], K. Todome[162], S. Todorova-Nova[5], S. Todt[46],
J. Tojo[85], S. Tokár[28a], K. Tokushuku[79], E. Tolley[122], K.G. Tomiwa[32c], M. Tomoto[115],
L. Tompkins[150], K. Toms[116], B. Tong[57], P. Tornambe[50], E. Torrence[127], H. Torres[46],
E. Torró Pastor[145], C. Tosciri[131], J. Toth[99,aa], F. Touchard[99], D.R. Tovey[146], C.J. Treado[121],
T. Trefzger[174], F. Tresoldi[153], A. Tricoli[29], I.M. Trigger[165a], S. Trincaz-Duvoid[132],
M.F. Tripiana[14], W. Trischuk[164], B. Trocmé[56], A. Trofymov[128], C. Troncon[66a], M. Trovatelli[173],
F. Trovato[153], L. Truong[32b], M. Trzebinski[82], A. Trzupek[82], F. Tsai[44], J.C-L. Tseng[131],
P.V. Tsiareshka[105], A. Tsirigotis[159], N. Tsirintanis[9], V. Tsiskaridze[152], E.G. Tskhadadze[156a],
I.I. Tsukerman[109], V. Tsulaia[18], S. Tsuno[79], D. Tsybychev[152], Y. Tu[61b], A. Tudorache[27b],
V. Tudorache[27b], T.T. Tulbure[27a], A.N. Tuna[57], S. Turchikhin[77], D. Turgeman[177],
I. Turk Cakir[4b,s], R. Turra[66a], P.M. Tuts[38], E. Tzovara[97], G. Ucchielli[23b,23a], I. Ueda[79],
M. Ughetto[43a,43b], F. Ukegawa[166], G. Unal[35], A. Undrus[29], G. Unel[168], F.C. Ungaro[102],
Y. Unno[79], K. Uno[160], J. Urban[28b], P. Urquijo[102], P. Urrejola[97], G. Usai[8], J. Usui[79],
L. Vacavant[99], V. Vacek[138], B. Vachon[101], K.O.H. Vadla[130], A. Vaidya[92], C. Valderanis[112],
E. Valdes Santurio[43a,43b], M. Valente[52], S. Valentinetti[23b,23a], A. Valero[171], L. Valéry[44],
R.A. Vallance[21], A. Vallier[5], J.A. Valls Ferrer[171], T.R. Van Daalen[14], H. Van der Graaf[118],
P. Van Gemmeren[6], J. Van Nieuwkoop[149], I. Van Vulpen[118], M. Vanadia[71a,71b], W. Vandelli[35],
A. Vaniachine[163], P. Vankov[118], R. Vari[70a], E.W. Varnes[7], C. Varni[53b,53a], T. Varol[41],
D. Varouchas[128], K.E. Varvell[154], G.A. Vasquez[144b], J.G. Vasquez[180], F. Vazeille[37],
D. Vazquez Furelos[14], T. Vazquez Schroeder[101], J. Veatch[51], V. Vecchio[72a,72b], L.M. Veloce[164],
F. Veloso[136a,136c], S. Veneziano[70a], A. Ventura[65a,65b], M. Venturi[173], N. Venturi[35], V. Vercesi[68a],
M. Verducci[72a,72b], C.M. Vergel Infante[76], C. Vergis[24], W. Verkerke[118], A.T. Vermeulen[118],
J.C. Vermeulen[118], M.C. Vetterli[149,aq], N. Viaux Maira[144b], M. Vicente Barreto Pinto[52],
I. Vichou[170,*], T. Vickey[146], O.E. Vickey Boeriu[146], G.H.A. Viehhauser[131], S. Viel[18], L. Vigani[131],
M. Villa[23b,23a], M. Villaplana Perez[66a,66b], E. Vilucchi[49], M.G. Vincter[33], V.B. Vinogradov[77],
A. Vishwakarma[44], C. Vittori[23b,23a], I. Vivarelli[153], S. Vlachos[10], M. Vogel[179], P. Vokac[138],
G. Volpi[14], S.E. Von Buddenbrock[32c], E. Von Toerne[24], V. Vorobel[139], K. Vorobev[110], M. Vos[171],
J.H. Vossebeld[88], N. Vranjes[16], M. Vranjes Milosavljevic[16], V. Vrba[138], M. Vreeswijk[118],
T. Šfiligoj[89], R. Vuillermet[35], I. Vukotic[36], T. Ženiš[28a], L. Živković[16], P. Wagner[24], W. Wagner[179],
J. Wagner-Kuhr[112], H. Wahlberg[86], S. Wahrmund[46], K. Wakamiya[80], V.M. Walbrecht[113],
J. Walder[87], R. Walker[112], S.D. Walker[91], W. Walkowiak[148], V. Wallangen[43a,43b], A.M. Wang[57],
C. Wang[58b,d], F. Wang[178], H. Wang[18], H. Wang[3], J. Wang[154], J. Wang[59b], P. Wang[41],
Q. Wang[124], R.-J. Wang[132], R. Wang[58a], R. Wang[6], S.M. Wang[155], W.T. Wang[58a],

W. Wang[15c,ac], W.X. Wang[58a,ac], Y. Wang[58a], Z. Wang[58c], C. Wanotayaroj[44], A. Warburton[101], C.P. Ward[31], D.R. Wardrope[92], A. Washbrook[48], P.M. Watkins[21], A.T. Watson[21], M.F. Watson[21], G. Watts[145], S. Watts[98], B.M. Waugh[92], A.F. Webb[11], S. Webb[97], C. Weber[180], M.S. Weber[20], S.A. Weber[33], S.M. Weber[59a], A.R. Weidberg[131], B. Weinert[63], J. Weingarten[51], M. Weirich[97], C. Weiser[50], P.S. Wells[35], T. Wenaus[29], T. Wengler[35], S. Wenig[35], N. Wermes[24], M.D. Werner[76], P. Werner[35], M. Wessels[59a], T.D. Weston[20], K. Whalen[127], N.L. Whallon[145], A.M. Wharton[87], A.S. White[103], A. White[8], M.J. White[1], R. White[144b], D. Whiteson[168], B.W. Whitmore[87], F.J. Wickens[141], W. Wiedenmann[178], M. Wielers[141], C. Wiglesworth[39], L.A.M. Wiik-Fuchs[50], A. Wildauer[113], F. Wilk[98], H.G. Wilkens[35], L.J. Wilkins[91], H.H. Williams[133], S. Williams[31], C. Willis[104], S. Willocq[100], J.A. Wilson[21], I. Wingerter-Seez[5], E. Winkels[153], F. Winklmeier[127], O.J. Winston[153], B.T. Winter[24], M. Wittgen[150], M. Wobisch[93], A. Wolf[97], T.M.H. Wolf[118], R. Wolff[99], M.W. Wolter[82], H. Wolters[136a,136c], V.W.S. Wong[172], N.L. Woods[143], S.D. Worm[21], B.K. Wosiek[82], K.W. Woźniak[82], K. Wraight[55], M. Wu[36], S.L. Wu[178], X. Wu[52], Y. Wu[58a], T.R. Wyatt[98], B.M. Wynne[48], S. Xella[39], Z. Xi[103], L. Xia[175], D. Xu[15a], H. Xu[58a], L. Xu[29], T. Xu[142], W. Xu[103], B. Yabsley[154], S. Yacoob[32a], K. Yajima[129], D.P. Yallup[92], D. Yamaguchi[162], Y. Yamaguchi[162], A. Yamamoto[79], T. Yamanaka[160], F. Yamane[80], M. Yamatani[160], T. Yamazaki[160], Y. Yamazaki[80], Z. Yan[25], H.J. Yang[58c,58d], H.T. Yang[18], S. Yang[75], Y. Yang[160], Z. Yang[17], W-M. Yao[18], Y.C. Yap[44], Y. Yasu[79], E. Yatsenko[58c,58d], J. Ye[41], S. Ye[29], I. Yeletskikh[77], E. Yigitbasi[25], E. Yildirim[97], K. Yorita[176], K. Yoshihara[133], C.J.S. Young[35], C. Young[150], J. Yu[8], J. Yu[76], X. Yue[59a], S.P.Y. Yuen[24], B. Zabinski[82], G. Zacharis[10], E. Zaffaroni[52], R. Zaidan[14], A.M. Zaitsev[140,ai], T. Zakareishvili[156b], N. Zakharchuk[44], J. Zalieckas[17], S. Zambito[57], D. Zanzi[35], D.R. Zaripovas[55], S.V. Zeißner[45], C. Zeitnitz[179], G. Zemaityte[131], J.C. Zeng[170], Q. Zeng[150], O. Zenin[140], D. Zerwas[128], M. Zgubič[131], D.F. Zhang[58b], D. Zhang[103], F. Zhang[178], G. Zhang[58a], H. Zhang[15c], J. Zhang[6], L. Zhang[15c], L. Zhang[58a], M. Zhang[170], P. Zhang[15c], R. Zhang[58a], R. Zhang[24], X. Zhang[58b], Y. Zhang[15d], Z. Zhang[128], X. Zhao[41], Y. Zhao[58b,128,af], Z. Zhao[58a], A. Zhemchugov[77], B. Zhou[103], C. Zhou[178], L. Zhou[41], M.S. Zhou[15d], M. Zhou[152], N. Zhou[58c], Y. Zhou[7], C.G. Zhu[58b], H.L. Zhu[58a], H. Zhu[15a], J. Zhu[103], Y. Zhu[58a], X. Zhuang[15a], K. Zhukov[108], V. Zhulanov[120b,120a], A. Zibell[174], D. Zieminska[63], N.I. Zimine[77], S. Zimmermann[50], Z. Zinonos[113], M. Zinser[97], M. Ziolkowski[148], G. Zobernig[178], A. Zoccoli[23b,23a], K. Zoch[51], T.G. Zorbas[146], R. Zou[36], M. Zur Nedden[19] and L. Zwalinski[35]

1   *Department of Physics, University of Adelaide, Adelaide; Australia*

2   *Physics Department, SUNY Albany, Albany NY; United States of America*

3   *Department of Physics, University of Alberta, Edmonton AB; Canada*

4   *(a) Department of Physics, Ankara University, Ankara;(b) Istanbul Aydin University, Istanbul;(c) Division of Physics, TOBB University of Economics and Technology, Ankara; Turkey*

5   *LAPP, Université Grenoble Alpes, Université Savoie Mont Blanc, CNRS/IN2P3, Annecy; France*

6   *High Energy Physics Division, Argonne National Laboratory, Argonne IL; United States of America*

7   *Department of Physics, University of Arizona, Tucson AZ; United States of America*

8   *Department of Physics, University of Texas at Arlington, Arlington TX; United States of America*

9   *Physics Department, National and Kapodistrian University of Athens, Athens; Greece*

10  *Physics Department, National Technical University of Athens, Zografou; Greece*

11  *Department of Physics, University of Texas at Austin, Austin TX; United States of America*

12  *(a) Bahcesehir University, Faculty of Engineering and Natural Sciences, Istanbul;(b) Istanbul Bilgi University, Faculty of Engineering and Natural Sciences, Istanbul;(c) Department of Physics, Bogazici University, Istanbul;(d) Department of Physics Engineering, Gaziantep University, Gaziantep; Turkey*

13  *Institute of Physics, Azerbaijan Academy of Sciences, Baku; Azerbaijan*

14 *Institut de Física d'Altes Energies (IFAE), Barcelona Institute of Science and Technology, Barcelona; Spain*

15 [a]*Institute of High Energy Physics, Chinese Academy of Sciences, Beijing;*[b]*Physics Department, Tsinghua University, Beijing;*[c]*Department of Physics, Nanjing University, Nanjing;*[d]*University of Chinese Academy of Science (UCAS), Beijing; China*

16 *Institute of Physics, University of Belgrade, Belgrade; Serbia*

17 *Department for Physics and Technology, University of Bergen, Bergen; Norway*

18 *Physics Division, Lawrence Berkeley National Laboratory and University of California, Berkeley CA; United States of America*

19 *Institut für Physik, Humboldt Universität zu Berlin, Berlin; Germany*

20 *Albert Einstein Center for Fundamental Physics and Laboratory for High Energy Physics, University of Bern, Bern; Switzerland*

21 *School of Physics and Astronomy, University of Birmingham, Birmingham; United Kingdom*

22 *Centro de Investigaciónes, Universidad Antonio Nariño, Bogota; Colombia*

23 [a]*Dipartimento di Fisica e Astronomia, Università di Bologna, Bologna;*[b]*INFN Sezione di Bologna; Italy*

24 *Physikalisches Institut, Universität Bonn, Bonn; Germany*

25 *Department of Physics, Boston University, Boston MA; United States of America*

26 *Department of Physics, Brandeis University, Waltham MA; United States of America*

27 [a]*Transilvania University of Brasov, Brasov;*[b]*Horia Hulubei National Institute of Physics and Nuclear Engineering, Bucharest;*[c]*Department of Physics, Alexandru Ioan Cuza University of Iasi, Iasi;*[d]*National Institute for Research and Development of Isotopic and Molecular Technologies, Physics Department, Cluj-Napoca;*[e]*University Politehnica Bucharest, Bucharest;*[f]*West University in Timisoara, Timisoara; Romania*

28 [a]*Faculty of Mathematics, Physics and Informatics, Comenius University, Bratislava;*[b]*Department of Subnuclear Physics, Institute of Experimental Physics of the Slovak Academy of Sciences, Kosice; Slovak Republic*

29 *Physics Department, Brookhaven National Laboratory, Upton NY; United States of America*

30 *Departamento de Física, Universidad de Buenos Aires, Buenos Aires; Argentina*

31 *Cavendish Laboratory, University of Cambridge, Cambridge; United Kingdom*

32 [a]*Department of Physics, University of Cape Town, Cape Town;*[b]*Department of Mechanical Engineering Science, University of Johannesburg, Johannesburg;*[c]*School of Physics, University of the Witwatersrand, Johannesburg; South Africa*

33 *Department of Physics, Carleton University, Ottawa ON; Canada*

34 [a]*Faculté des Sciences Ain Chock, Réseau Universitaire de Physique des Hautes Energies — Université Hassan II, Casablanca;*[b]*Centre National de l'Energie des Sciences Techniques Nucleaires (CNESTEN), Rabat;*[c]*Faculté des Sciences Semlalia, Université Cadi Ayyad, LPHEA-Marrakech;*[d]*Faculté des Sciences, Université Mohamed Premier and LPTPM, Oujda;*[e]*Faculté des sciences, Université Mohammed V, Rabat; Morocco*

35 *CERN, Geneva; Switzerland*

36 *Enrico Fermi Institute, University of Chicago, Chicago IL; United States of America*

37 *LPC, Université Clermont Auvergne, CNRS/IN2P3, Clermont-Ferrand; France*

38 *Nevis Laboratory, Columbia University, Irvington NY; United States of America*

39 *Niels Bohr Institute, University of Copenhagen, Copenhagen; Denmark*

40 [a]*Dipartimento di Fisica, Università della Calabria, Rende;*[b]*INFN Gruppo Collegato di Cosenza, Laboratori Nazionali di Frascati; Italy*

41 *Physics Department, Southern Methodist University, Dallas TX; United States of America*

42 *Physics Department, University of Texas at Dallas, Richardson TX; United States of America*

43 [a]*Department of Physics, Stockholm University;*[b]*Oskar Klein Centre, Stockholm; Sweden*

44 *Deutsches Elektronen-Synchrotron DESY, Hamburg and Zeuthen; Germany*

45 *Lehrstuhl für Experimentelle Physik IV, Technische Universität Dortmund, Dortmund; Germany*

46 *Institut für Kern- und Teilchenphysik, Technische Universität Dresden, Dresden; Germany*

47  Department of Physics, Duke University, Durham NC; United States of America

48  SUPA — School of Physics and Astronomy, University of Edinburgh, Edinburgh; United Kingdom

49  INFN e Laboratori Nazionali di Frascati, Frascati; Italy

50  Physikalisches Institut, Albert-Ludwigs-Universität Freiburg, Freiburg; Germany

51  II. Physikalisches Institut, Georg-August-Universität Göttingen, Göttingen; Germany

52  Département de Physique Nucléaire et Corpusculaire, Université de Genève, Genève; Switzerland

53  [a] Dipartimento di Fisica, Università di Genova, Genova;[b] INFN Sezione di Genova; Italy

54  II. Physikalisches Institut, Justus-Liebig-Universität Giessen, Giessen; Germany

55  SUPA — School of Physics and Astronomy, University of Glasgow, Glasgow; United Kingdom

56  LPSC, Université Grenoble Alpes, CNRS/IN2P3, Grenoble INP, Grenoble; France

57  Laboratory for Particle Physics and Cosmology, Harvard University, Cambridge MA; United States of America

58  [a] Department of Modern Physics and State Key Laboratory of Particle Detection and Electronics, University of Science and Technology of China, Hefei;[b] Institute of Frontier and Interdisciplinary Science and Key Laboratory of Particle Physics and Particle Irradiation (MOE), Shandong University, Qingdao;[c] School of Physics and Astronomy, Shanghai Jiao Tong University, KLPPAC-MoE, SKLPPC, Shanghai;[d] Tsung-Dao Lee Institute, Shanghai; China

59  [a] Kirchhoff-Institut für Physik, Ruprecht-Karls-Universität Heidelberg, Heidelberg;[b] Physikalisches Institut, Ruprecht-Karls-Universität Heidelberg, Heidelberg; Germany

60  Faculty of Applied Information Science, Hiroshima Institute of Technology, Hiroshima; Japan

61  [a] Department of Physics, Chinese University of Hong Kong, Shatin, N.T., Hong Kong;[b] Department of Physics, University of Hong Kong, Hong Kong;[c] Department of Physics and Institute for Advanced Study, Hong Kong University of Science and Technology, Clear Water Bay, Kowloon, Hong Kong; China

62  Department of Physics, National Tsing Hua University, Hsinchu; Taiwan

63  Department of Physics, Indiana University, Bloomington IN; United States of America

64  [a] INFN Gruppo Collegato di Udine, Sezione di Trieste, Udine;[b] ICTP, Trieste;[c] Dipartimento di Chimica, Fisica e Ambiente, Università di Udine, Udine; Italy

65  [a] INFN Sezione di Lecce;[b] Dipartimento di Matematica e Fisica, Università del Salento, Lecce; Italy

66  [a] INFN Sezione di Milano;[b] Dipartimento di Fisica, Università di Milano, Milano; Italy

67  [a] INFN Sezione di Napoli;[b] Dipartimento di Fisica, Università di Napoli, Napoli; Italy

68  [a] INFN Sezione di Pavia;[b] Dipartimento di Fisica, Università di Pavia, Pavia; Italy

69  [a] INFN Sezione di Pisa;[b] Dipartimento di Fisica E. Fermi, Università di Pisa, Pisa; Italy

70  [a] INFN Sezione di Roma;[b] Dipartimento di Fisica, Sapienza Università di Roma, Roma; Italy

71  [a] INFN Sezione di Roma Tor Vergata;[b] Dipartimento di Fisica, Università di Roma Tor Vergata, Roma; Italy

72  [a] INFN Sezione di Roma Tre;[b] Dipartimento di Matematica e Fisica, Università Roma Tre, Roma; Italy

73  [a] INFN-TIFPA;[b] Università degli Studi di Trento, Trento; Italy

74  Institut für Astro- und Teilchenphysik, Leopold-Franzens-Universität, Innsbruck; Austria

75  University of Iowa, Iowa City IA; United States of America

76  Department of Physics and Astronomy, Iowa State University, Ames IA; United States of America

77  Joint Institute for Nuclear Research, Dubna; Russia

78  [a] Departamento de Engenharia Elétrica, Universidade Federal de Juiz de Fora (UFJF), Juiz de Fora;[b] Universidade Federal do Rio De Janeiro COPPE/EE/IF, Rio de Janeiro;[c] Universidade Federal de São João del Rei (UFSJ), São João del Rei;[d] Instituto de Física, Universidade de São Paulo, São Paulo; Brazil

79  KEK, High Energy Accelerator Research Organization, Tsukuba; Japan

80  Graduate School of Science, Kobe University, Kobe; Japan

81  [a] AGH University of Science and Technology, Faculty of Physics and Applied Computer Science, Krakow;[b] Marian Smoluchowski Institute of Physics, Jagiellonian University, Krakow; Poland

[82] Institute of Nuclear Physics Polish Academy of Sciences, Krakow; Poland

[83] Faculty of Science, Kyoto University, Kyoto; Japan

[84] Kyoto University of Education, Kyoto; Japan

[85] Research Center for Advanced Particle Physics and Department of Physics, Kyushu University, Fukuoka ; Japan

[86] Instituto de Física La Plata, Universidad Nacional de La Plata and CONICET, La Plata; Argentina

[87] Physics Department, Lancaster University, Lancaster; United Kingdom

[88] Oliver Lodge Laboratory, University of Liverpool, Liverpool; United Kingdom

[89] Department of Experimental Particle Physics, Jožef Stefan Institute and Department of Physics, University of Ljubljana, Ljubljana; Slovenia

[90] School of Physics and Astronomy, Queen Mary University of London, London; United Kingdom

[91] Department of Physics, Royal Holloway University of London, Egham; United Kingdom

[92] Department of Physics and Astronomy, University College London, London; United Kingdom

[93] Louisiana Tech University, Ruston LA; United States of America

[94] Fysiska institutionen, Lunds universitet, Lund; Sweden

[95] Centre de Calcul de l'Institut National de Physique Nucléaire et de Physique des Particules (IN2P3), Villeurbanne; France

[96] Departamento de Física Teorica C-15 and CIAFF, Universidad Autónoma de Madrid, Madrid; Spain

[97] Institut für Physik, Universität Mainz, Mainz; Germany

[98] School of Physics and Astronomy, University of Manchester, Manchester; United Kingdom

[99] CPPM, Aix-Marseille Université, CNRS/IN2P3, Marseille; France

[100] Department of Physics, University of Massachusetts, Amherst MA; United States of America

[101] Department of Physics, McGill University, Montreal QC; Canada

[102] School of Physics, University of Melbourne, Victoria; Australia

[103] Department of Physics, University of Michigan, Ann Arbor MI; United States of America

[104] Department of Physics and Astronomy, Michigan State University, East Lansing MI; United States of America

[105] B.I. Stepanov Institute of Physics, National Academy of Sciences of Belarus, Minsk; Belarus

[106] Research Institute for Nuclear Problems of Byelorussian State University, Minsk; Belarus

[107] Group of Particle Physics, University of Montreal, Montreal QC; Canada

[108] P.N. Lebedev Physical Institute of the Russian Academy of Sciences, Moscow; Russia

[109] Institute for Theoretical and Experimental Physics (ITEP), Moscow; Russia

[110] National Research Nuclear University MEPhI, Moscow; Russia

[111] D.V. Skobeltsyn Institute of Nuclear Physics, M.V. Lomonosov Moscow State University, Moscow; Russia

[112] Fakultät für Physik, Ludwig-Maximilians-Universität München, München; Germany

[113] Max-Planck-Institut für Physik (Werner-Heisenberg-Institut), München; Germany

[114] Nagasaki Institute of Applied Science, Nagasaki; Japan

[115] Graduate School of Science and Kobayashi-Maskawa Institute, Nagoya University, Nagoya; Japan

[116] Department of Physics and Astronomy, University of New Mexico, Albuquerque NM; United States of America

[117] Institute for Mathematics, Astrophysics and Particle Physics, Radboud University Nijmegen/Nikhef, Nijmegen; Netherlands

[118] Nikhef National Institute for Subatomic Physics and University of Amsterdam, Amsterdam; Netherlands

[119] Department of Physics, Northern Illinois University, DeKalb IL; United States of America

[120] [a]Budker Institute of Nuclear Physics, SB RAS, Novosibirsk;[b]Novosibirsk State University Novosibirsk; Russia

[121] Department of Physics, New York University, New York NY; United States of America

[122] Ohio State University, Columbus OH; United States of America

[123] Faculty of Science, Okayama University, Okayama; Japan

124    *Homer L. Dodge Department of Physics and Astronomy, University of Oklahoma, Norman OK; United States of America*

125    *Department of Physics, Oklahoma State University, Stillwater OK; United States of America*

126    *Palacký University, RCPTM, Joint Laboratory of Optics, Olomouc; Czech Republic*

127    *Center for High Energy Physics, University of Oregon, Eugene OR; United States of America*

128    *LAL, Université Paris-Sud, CNRS/IN2P3, Université Paris-Saclay, Orsay; France*

129    *Graduate School of Science, Osaka University, Osaka; Japan*

130    *Department of Physics, University of Oslo, Oslo; Norway*

131    *Department of Physics, Oxford University, Oxford; United Kingdom*

132    *LPNHE, Sorbonne Université, Paris Diderot Sorbonne Paris Cité, CNRS/IN2P3, Paris; France*

133    *Department of Physics, University of Pennsylvania, Philadelphia PA; United States of America*

134    *Konstantinov Nuclear Physics Institute of National Research Centre "Kurchatov Institute", PNPI, St. Petersburg; Russia*

135    *Department of Physics and Astronomy, University of Pittsburgh, Pittsburgh PA; United States of America*

136    $^{(a)}$*Laboratório de Instrumentação e Física Experimental de Partículas — LIP;*$^{(b)}$*Departamento de Física, Faculdade de Ciências, Universidade de Lisboa, Lisboa;*$^{(c)}$*Departamento de Física, Universidade de Coimbra, Coimbra;*$^{(d)}$*Centro de Física Nuclear da Universidade de Lisboa, Lisboa;*$^{(e)}$*Departamento de Física, Universidade do Minho, Braga;*$^{(f)}$*Departamento de Física Teorica y del Cosmos, Universidad de Granada, Granada (Spain);*$^{(g)}$*Dep Física and CEFITEC of Faculdade de Ciências e Tecnologia, Universidade Nova de Lisboa, Caparica; Portugal*

137    *Institute of Physics, Academy of Sciences of the Czech Republic, Prague; Czech Republic*

138    *Czech Technical University in Prague, Prague; Czech Republic*

139    *Charles University, Faculty of Mathematics and Physics, Prague; Czech Republic*

140    *State Research Center Institute for High Energy Physics, NRC KI, Protvino; Russia*

141    *Particle Physics Department, Rutherford Appleton Laboratory, Didcot; United Kingdom*

142    *IRFU, CEA, Université Paris-Saclay, Gif-sur-Yvette; France*

143    *Santa Cruz Institute for Particle Physics, University of California Santa Cruz, Santa Cruz CA; United States of America*

144    $^{(a)}$*Departamento de Física, Pontificia Universidad Católica de Chile, Santiago;*$^{(b)}$*Departamento de Física, Universidad Técnica Federico Santa María, Valparaíso; Chile*

145    *Department of Physics, University of Washington, Seattle WA; United States of America*

146    *Department of Physics and Astronomy, University of Sheffield, Sheffield; United Kingdom*

147    *Department of Physics, Shinshu University, Nagano; Japan*

148    *Department Physik, Universität Siegen, Siegen; Germany*

149    *Department of Physics, Simon Fraser University, Burnaby BC; Canada*

150    *SLAC National Accelerator Laboratory, Stanford CA; United States of America*

151    *Physics Department, Royal Institute of Technology, Stockholm; Sweden*

152    *Departments of Physics and Astronomy, Stony Brook University, Stony Brook NY; United States of America*

153    *Department of Physics and Astronomy, University of Sussex, Brighton; United Kingdom*

154    *School of Physics, University of Sydney, Sydney; Australia*

155    *Institute of Physics, Academia Sinica, Taipei; Taiwan*

156    $^{(a)}$*E. Andronikashvili Institute of Physics, Iv. Javakhishvili Tbilisi State University, Tbilisi;*$^{(b)}$*High Energy Physics Institute, Tbilisi State University, Tbilisi; Georgia*

157    *Department of Physics, Technion, Israel Institute of Technology, Haifa; Israel*

158    *Raymond and Beverly Sackler School of Physics and Astronomy, Tel Aviv University, Tel Aviv; Israel*

159    *Department of Physics, Aristotle University of Thessaloniki, Thessaloniki; Greece*

160    *International Center for Elementary Particle Physics and Department of Physics, University of Tokyo, Tokyo; Japan*

161    *Graduate School of Science and Technology, Tokyo Metropolitan University, Tokyo; Japan*

162 *Department of Physics, Tokyo Institute of Technology, Tokyo; Japan*

163 *Tomsk State University, Tomsk; Russia*

164 *Department of Physics, University of Toronto, Toronto ON; Canada*

165 *(a) TRIUMF, Vancouver BC;(b) Department of Physics and Astronomy, York University, Toronto ON; Canada*

166 *Division of Physics and Tomonaga Center for the History of the Universe, Faculty of Pure and Applied Sciences, University of Tsukuba, Tsukuba; Japan*

167 *Department of Physics and Astronomy, Tufts University, Medford MA; United States of America*

168 *Department of Physics and Astronomy, University of California Irvine, Irvine CA; United States of America*

169 *Department of Physics and Astronomy, University of Uppsala, Uppsala; Sweden*

170 *Department of Physics, University of Illinois, Urbana IL; United States of America*

171 *Instituto de Física Corpuscular (IFIC), Centro Mixto Universidad de Valencia — CSIC, Valencia; Spain*

172 *Department of Physics, University of British Columbia, Vancouver BC; Canada*

173 *Department of Physics and Astronomy, University of Victoria, Victoria BC; Canada*

174 *Fakultät für Physik und Astronomie, Julius-Maximilians-Universität Würzburg, Würzburg; Germany*

175 *Department of Physics, University of Warwick, Coventry; United Kingdom*

176 *Waseda University, Tokyo; Japan*

177 *Department of Particle Physics, Weizmann Institute of Science, Rehovot; Israel*

178 *Department of Physics, University of Wisconsin, Madison WI; United States of America*

179 *Fakultät für Mathematik und Naturwissenschaften, Fachgruppe Physik, Bergische Universität Wuppertal, Wuppertal; Germany*

180 *Department of Physics, Yale University, New Haven CT; United States of America*

181 *Yerevan Physics Institute, Yerevan; Armenia*

[a] *Also at Borough of Manhattan Community College, City University of New York, NY; United States of America*

[b] *Also at Centre for High Performance Computing, CSIR Campus, Rosebank, Cape Town; South Africa*

[c] *Also at CERN, Geneva; Switzerland*

[d] *Also at CPPM, Aix-Marseille Université, CNRS/IN2P3, Marseille; France*

[e] *Also at Département de Physique Nucléaire et Corpusculaire, Université de Genève, Genève; Switzerland*

[f] *Also at Departament de Fisica de la Universitat Autonoma de Barcelona, Barcelona; Spain*

[g] *Also at Departamento de Física Teorica y del Cosmos, Universidad de Granada, Granada (Spain); Spain*

[h] *Also at Department of Applied Physics and Astronomy, University of Sharjah, Sharjah; United Arab Emirates*

[i] *Also at Department of Financial and Management Engineering, University of the Aegean, Chios; Greece*

[j] *Also at Department of Physics and Astronomy, University of Louisville, Louisville, KY; United States of America*

[k] *Also at Department of Physics and Astronomy, University of Sheffield, Sheffield; United Kingdom*

[l] *Also at Department of Physics, California State University, Fresno CA; United States of America*

[m] *Also at Department of Physics, California State University, Sacramento CA; United States of America*

[n] *Also at Department of Physics, King's College London, London; United Kingdom*

[o] *Also at Department of Physics, St. Petersburg State Polytechnical University, St. Petersburg; Russia*

[p] *Also at Department of Physics, University of Fribourg, Fribourg; Switzerland*

[q] *Also at Department of Physics, University of Michigan, Ann Arbor MI; United States of America*

[r] *Also at Dipartimento di Fisica E. Fermi, Università di Pisa, Pisa; Italy*

[s] *Also at Giresun University, Faculty of Engineering, Giresun; Turkey*

[t] *Also at Graduate School of Science, Osaka University, Osaka; Japan*

[u] *Also at Hellenic Open University, Patras; Greece*

[v] *Also at Horia Hulubei National Institute of Physics and Nuclear Engineering, Bucharest; Romania*

[w] *Also at II. Physikalisches Institut, Georg-August-Universität Göttingen, Göttingen; Germany*

[x] *Also at Institucio Catalana de Recerca i Estudis Avancats, ICREA, Barcelona; Spain*

[y] *Also at Institut für Experimentalphysik, Universität Hamburg, Hamburg; Germany*

[z] *Also at Institute for Mathematics, Astrophysics and Particle Physics, Radboud University Nijmegen/Nikhef, Nijmegen; Netherlands*

[aa] *Also at Institute for Particle and Nuclear Physics, Wigner Research Centre for Physics, Budapest; Hungary*

[ab] *Also at Institute of Particle Physics (IPP); Canada*

[ac] *Also at Institute of Physics, Academia Sinica, Taipei; Taiwan*

[ad] *Also at Institute of Physics, Azerbaijan Academy of Sciences, Baku; Azerbaijan*

[ae] *Also at Institute of Theoretical Physics, Ilia State University, Tbilisi; Georgia*

[af] *Also at LAL, Université Paris-Sud, CNRS/IN2P3, Université Paris-Saclay, Orsay; France*

[ag] *Also at Louisiana Tech University, Ruston LA; United States of America*

[ah] *Also at Manhattan College, New York NY; United States of America*

[ai] *Also at Moscow Institute of Physics and Technology State University, Dolgoprudny; Russia*

[aj] *Also at National Research Nuclear University MEPhI, Moscow; Russia*

[ak] *Also at Near East University, Nicosia, North Cyprus, Mersin; Turkey*

[al] *Also at Physikalisches Institut, Albert-Ludwigs-Universität Freiburg, Freiburg; Germany*

[am] *Also at School of Physics, Sun Yat-sen University, Guangzhou; China*

[an] *Also at The City College of New York, New York NY; United States of America*

[ao] *Also at The Collaborative Innovation Center of Quantum Matter (CICQM), Beijing; China*

[ap] *Also at Tomsk State University, Tomsk, and Moscow Institute of Physics and Technology State University, Dolgoprudny; Russia*

[aq] *Also at TRIUMF, Vancouver BC; Canada*

[ar] *Also at Universita di Napoli Parthenope, Napoli; Italy*

[*] *Deceased*